

Joana Sócrates Dantas

**Priority Realloc: A threefold
mechanism for route and resources
allocation in EONs**

Tese apresentada à Escola Politécnica da
Universidade de São Paulo e Universitat
Politécnica de Catalunya para obtenção
da dupla Titulação de Doutor em
Engenharia Elétrica.

Joana Sócrates Dantas

**Priority Realloc: A threefold
mechanism for route and resources
allocation in EONs**

Tese apresentada à Escola Politécnica da
Universidade de São Paulo e Universitat
Politécnica de Catalunya para obtenção
da dupla Titulação de Doutor em
Engenharia Elétrica.

Área:
Engenharia de Computação

Orientadores:
Prof. Dra. Regina Melo Silveira
e Prof. Dr. Davide Careglio

Co-orientador:
Prof. Dr. Josep Solè-Pareta

Ficha Catalográfica

Dantas, Joana Sócrates

Priority Realloc: A threefold mechanism for route and resources allocation in EONs. São Paulo, 2015. 151 p.

(Doutorado) Tese — Escola Politécnica da Universidade de São Paulo. Laboratório de Arquitetura e Redes de Computadores.

1. Telecomunicações. 2. Redes de computadores. 3. Redes ópticas. I. Universidade de São Paulo. Escola Politécnica. Laboratório de Arquitetura e Redes de Computadores. II. t.

Abstract

Backbone networks are responsible for long-haul data transport serving many clients with a large volume of data. Since long-haul data transport service must rely on a robust high capacity network the current technology broadly adopted by the industry is Wavelength Division Multiplexing (WDM). WDM networks enable one single fiber to operate with multiple high capacity channels, drastically increasing the fiber capacity. In WDM networks each channel is associated with an individual wavelength. Therefore a whole wavelength capacity is assigned to a connection, causing waste of bandwidth in case the connection bandwidth requirement is less than the channel total capacity.

In the last half decade, Elastic Optical Networks (EON) have been proposed and developed based on the flexible use of the optical spectrum known as the flexigrid. EONs are adaptable to clients requirements and may enhance optical networks performance. For these reasons, research community and data transport providers have been demonstrating increasingly high interest in EONs which are likely to replace WDM as the universally adopted technology in backbone networks in the near future.

EONs have two characteristics that may limit its efficient resources use. The spectrum fragmentation, inherent to the dynamic EON operation, decrease the network capacity to assign resources to connection requests increasing network blocking probability. The spectrum fragmentation also intensifies the denial of service to higher rate request inducing service unfairness.

Due to the fact EONs were just recently developed and proposed, the aforementioned issues were not yet extensively studied and solutions are still being proposed. Furthermore, EONs do not yet provide specific features as differentiated service mechanisms. Differentiated service strategies are important in backbone networks to guarantee client's diverse requirements in case of a network failure or the natural congestion and resources contention that may occur at some periods of time in a network.

Impelled by the foregoing facts, this thesis objective is three-fold. By means of developing and proposing a mechanism for routing and resources assignment in EONs, we intend to provide differentiated service while decreasing fragmentation level and increasing service fairness.

The mechanism proposed and explained in this thesis was tested in a EON simulation environment and performance results indicated that it promotes beneficial performance enhancements when compared to benchmark algorithms.

Resumo

Redes *backbone* são responsáveis pelo transporte de dados à longa distância que atendem a uma grande quantidade de clientes com um grande volume de dados. Como redes *backbone* devem basear-se em uma rede robusta e de alta capacidade, a tecnologia atual amplamente adotada pela indústria é *Wavelength Division Multiplexing* (WDM). Redes WDM permitem que uma única fibra opere com múltiplos canais de alta largura de banda, aumentando drasticamente a capacidade da fibra. Em redes WDM cada canal está associado a um comprimento de onda particular. Por conseguinte, toda capacidade do comprimento de onda é atribuída a uma única conexão, fazendo com que parte da largura de banda seja desperdiçada no caso em que a requisição de largura de banda da conexão seja menor do que a capacidade total do canal.

A partir da metade da última década, as Redes Ópticas Elásticas (*Elastic Optical Networks* - EON) têm sido propostas e desenvolvidas com base no uso flexível do espectro óptico conhecido como *flexigrid*. EONs são adaptáveis às requisições por banda dos clientes e podem, portanto, melhorar o desempenho das redes ópticas. Por estas razões, EONs têm recebido cada vez mais interesse dos meios de pesquisa e provedores de serviço e provavelmente substituirão WDM como a tecnologia universalmente adotada pela indústria em redes *backbone*.

EONs têm duas características que podem limitar a utilização eficiente de recursos. A fragmentação do espectro, inerente à operação dinâmica das EONs, pode diminuir a capacidade da rede em distribuir recursos ao atender às solicitações por conexões aumentando a probabilidade de bloqueio na rede. A fragmentação do espectro também intensifica a negação de serviço a solicitações por taxa de transmissão mais elevada, gerando injustiça no serviço prestado.

Como EONs foram desenvolvidas recentemente, respostas às questões acima mencionadas ainda estão sob estudo e soluções continuam sendo propostas na literatura. Além disso, EONs ainda não fornecem funções específicas como um mecanismo que proveja diferenciação de serviço. Estratégias de diferenciação de serviço são importantes em redes *backbone* para garantir os diversos requisitos dos clientes em caso de uma falha na rede ou do congestionamento e disputa por recursos que podem ocorrer em alguns períodos em uma rede.

Impulsionada pelos fatos anteriormente mencionados, esta tese possui três objetivos. Através do desenvolvimento e proposta de um mecanismo de roteamento e atribuição de recursos para EONs, temos a intenção de disponibilizar diferenciação de serviço, diminuir o nível de fragmentação de espectro e aumentar a justiça na distribuição de serviços.

O mecanismo proposto nesta tese foi testado em simulações de EONs. Resultados indicaram que o mecanismo proposto promove benefícios através do aprimoramento da performance de uma rede EON quando comparado com algoritmos de referência.

Content

List of Figures

List of Tables

1	Introduction	1
1.1	Problem Definition	1
1.2	Motivations	3
1.3	Objectives	4
1.3.1	Additional contributions	4
1.4	Scope	5
1.4.1	Out of scope	6
1.5	Methodology	8
1.6	Thesis outline	9
2	Theoretical background	11
2.1	WDM Networks	11
2.1.1	Routing and Wavelength Assignment (RWA)	12
2.2	Elastic Optical Networks	14
2.2.1	Technical advances that enable flexigrids	16
2.2.2	Routing and Spectrum Assignment	17
2.2.3	Modulation Level and Spectrum Assignment	20
2.2.4	Spectrum fragmentation problem	21
2.2.5	Service fairness in EONs	26
3	Related Work	29

3.1	Differentiated service strategies based on constrained distribution of resources	29
3.1.1	Differentiated service strategies in MPLS networks	30
3.1.2	Differentiated service strategies for WSONs	31
3.1.3	Differentiated service strategies for EONs	32
3.2	Fragmentation-aware RSA for EONs	32
3.3	Defragmentation techniques	38
3.4	Fairness issue in EONs	40
4	Precedent contributions	42
4.1	Priority of connection request processing	42
4.1.1	Results and analysis	43
4.2	Proposed RDM mechanism	44
4.3	Offline differentiated service for WDM networks	47
4.3.1	Results and analysis	48
4.4	Dynamic differentiated service for WDM networks	50
4.4.1	Proposed algorithm	51
4.4.2	Algorithm's complexity	54
4.4.3	Performance study and analysis of results	58
5	Priority Realloc: a threefold RSA mechanism for EONs	69
5.1	Priority Realloc first part: Exact Gap Size with fragmentation level	71
5.2	Priority Realloc second part: FSs reallocation	73
5.3	Analysis and explanation of proposed algorithms	77
5.3.1	Algorithms procedure alternatives	79
5.3.2	Algorithm's computational complexity	82
6	DSEON-Jsim: an ad-hoc event driven Java based simulator for EONs	85
6.1	Operation description	86

6.2	Validation process	89
7	Simulation Results	96
7.1	EON simulations performance results and analysis	98
7.1.1	Comparison between EON and WDM network with grooming performances	98
7.1.2	EON performance with diverse BW requirement scenario .	101
7.2	Simulation results for Priority Realloc mechanism performance in EONs	109
7.2.1	ESG-FL algorithm results	110
7.2.2	Priority Realloc mechanism results	113
8	Conclusion and future works	131
	References	135
	Appendix A – RDM mechanism for WDM networks economic impact analysis	143

List of Figures

2.1	a) traditional fixed grid in a WDM network; b) flexigrid used in EON	14
2.2	FSs and respective indexes	15
2.3	Spectrum of (a) WDM or FDM signals (b) OFDM signal [1] . . .	16
2.4	Spectrum assignment in: a) WDM networks and b) EONs [2] . . .	17
2.5	A connection X is allocated in the same indexed FSs in all links through the assigned route	18
2.6	The diagram shows a) connections with contiguous allocated FSs and b) one connection has non-contiguous allocated FSs, this is not possible in an EON	18
2.7	The diagram shows a) the original link state before connections termination, b) the link state after connections termination	21
2.8	A selected route comprises a given number of links. Each link may be serving different connection from the other. The vertical fragmentation represents the spectrum fragmentation experienced by each link, the horizontal fragmentation represents the misalignment of FSs gaps so that the resulting route fragmentation is more prejudicial than the individual link fragmentation	22
2.9	The diagram shows a) an EON only contains 4 FSs connections, whenever any connection is terminated the gap left will always fit an incoming demand and b) the network connection rate is heterogeneous and when a 2 FSs connection is terminated the gap left cannot accommodate the incoming demand.	23

2.10	The diagram presents a scenario where bandwidth requirements have a common denominator. In a) initial link state with active connections, in b) four connections with 2 FSs and one with 4 FSs are terminated leaving a gap of 8 contiguous available FSs and a gap of 4 FSs and in c) one gap may accommodate one 8 FSs connection and the other may accommodate one 2 FSs connection and the gap left may still accommodate another 2 FSs connection leaving no gap of available FS and therefore diminishing the link spectrum fragmentation	23
2.11	The diagram shows a scenario of bandwidth requirements without common denominator. In a) initial link state with active connections, b) a connection with 8 FSs is terminated leaving a gap of 8 contiguous available FSs, c) one connection with 3 FSs and two connections with 2 FSs are accommodated leaving a gap of one available FS that can not accommodate any incoming connection requests and therefore increase the links spectrum fragmentation.	24
2.12	The diagram shows a) five connection of 2 FSs each, are accommodated in the spectrum band and there is still contiguous FSs available and b) two connections of 8 FSs each are accommodated in the spectrum band leaving no available FSs	26
2.13	The diagrams shows a) original link condition with active connections, b) a connection with 8 FSs is terminate leaving a gap of 8 contiguous available FSs. c) four connections of 2 FSs are accommodated in the gap, d) two connections of 4 FSs are accommodated in the gap and e) one connection of 8 FSs is accommodated in the gap . . .	28
3.1	The diagram shows a) link state, b) connection accommodation following SF and c) connection accommodation following EF . . .	34
3.2	The diagram shows a) Dedicated Partition (DP) and b) Shared Partition (SP) [3]	36
3.3	Multi-fiber algorithm proposals [3]	37
3.4	Example FISH network and the spectral assignment status on the links, (b) number of cuts to all the candidate solution to connection request A-E, and (c) alignment factor increase if choosing path ADE with slot 8 [4]	38

3.5	The diagram shows a) original link state before connections termination, b) spectrum fragmented link after connections termination and c) link state after defragmentation	39
4.1	The Russian Dolls Model	45
4.2	RDM with constant difference between BC values	46
4.3	RDM with increasing difference between BC values	46
4.4	Number of connections established per CT values and total	49
4.5	Amount of bandwidth assigned per CT values and total	49
4.6	Variations on RDM bandwidth constraint use. a) depicts original RDM where a BC value is shared among all connections with same CT. b) depicts adapted RDM where each connection is assigned resources up to its own BC value.	50
4.7	Connections and/or demands are represented by rectangles. The bandwidth required or assigned is represented by the rectangles lengths, the number in the rectangles represent both the demand's id and its CT value, being 1 the highest priority and 4 the lowest priority. Demands arrive in the order illustrated being the first the one from the far left and the last the one from the far right in the demand arrivals figures a) and b). In a) the last demand to arrive has a low CT value. In b) the last demand to arrive has the highest CT value.	53
4.8	RDM connections per total number of connections for different scenarios with varied combinations of number of wavelengths and source and destination nodes for a network with offered traffic load of 1000 Erlang.	59
4.9	RDM connections per number of times RDM mechanism was triggered for different scenarios with varied combinations of number of wavelengths and source and destination nodes for a network with offered traffic load of 1000 Erlang.	60
4.10	Proportion of RDM connections per total number of connections for scenarios with different offered traffic load.	61
4.11	Constraint values for BC model A	62
4.12	Constraint values for BC model B	62

4.13	Constraint values for BC model C	62
4.14	Constraint values for BC model D	63
4.15	Blocking probability for RDM-less and grooming scenarios for total number of demands	64
4.16	Blocking probability for RDM-full and grooming scenarios for total number of demands	64
4.17	Blocking probability for RDM-less and grooming scenarios according to different CT values	64
4.18	Blocking probability for RDM-full and grooming scenarios according to different CT values	65
4.19	Proportion of total requested resources by total allocated resources for RDM-less and grooming scenarios.	66
4.20	Proportion of total requested resources by total allocated resources for RDM-full and grooming scenarios.	66
4.21	Resources allocation for RDM-less and grooming scenarios according to different CT values.	67
4.22	Resources allocation for RDM-full and grooming scenarios according to different CT values.	67
5.1	Links comprised by a selected route with busy FSs, the intersection of FSs in all the route's links results on the available FSs in the route	70
5.2	Gap availability map: gap index and respective gap size in number of FSs	71
5.3	The diagram shows two different situations, in a) there are two gaps that can accommodate the demand, the algorithm selects the exact size one, and in b) there are two gaps that can accommodate the demand, the algorithm selects the smallest one	72
5.4	The diagram shows two situations, in a) the selected largest gap's index is 4 and therefore there are FSs on the left of the selected gap to be inspected and in b) the selected largest gap is 0 and therefore there is no FSs to the left of the selected largest gap to be inspected	73

5.5	From the selected route's resulting gap availability map, the route's largest gap is selected. The FSs on the left of the selected gap are inspected for reallocation	74
5.6	The diagram shows a) link state when connection request arrives, there is not enough number of available continuous FSs to accommodate the incoming demand, all connections on the left of the largest gap have CT value 0 and b) the necessary number of FSs are reallocated to the incoming demand	75
5.7	The diagram shows a) link state before Priority Realloc: connection X is accommodated in a different route from the selected route but both routes have one link in common and b) link state after Priority Realloc: connection X have all its FSs preempted. In the common link the preempted FSs are reallocated to the incoming demand, in the other links from connection X's route the FSs remain available	75
6.1	DSEON-Jsim software architecture diagram	86
6.2	DSEON-Jsim operation flowchart	89
6.3	Plotted results generated by Matlab code and Java code used in the simulator	90
6.4	Plotted results generated by Matlab code and Java code used in the simulator	90
6.5	BP results achieved by simulation described in [4] and by DSEON-Jsim simulation	93
6.6	BP results achieved by simulation described in [5] and by DSEON-Jsim simulation	94
6.7	BBP results achieved by simulation described in [6] and by DSEON-Jsim simulation	94
6.8	Comparison between BP and fairness ratio results obtained by DSEON-Jsim and those presented in [7]	94
7.1	NSFNET reference network topology	97
7.2	Nobel German reference network topology	97
7.3	BP results for WDM and EON scenarios 1, 2 and 5 using KSP-FF algorithm	100

7.4	BBP results for WDM and EON bandwidth requirement scenarios 1, 2 and 5 using KSP-FF algorithm	101
7.5	BP for various BW requirement scenarios in Nobel German network topology	102
7.6	BP for various BW requirement scenarios in NSFNET network topology	103
7.7	Ratio between highest and lowest BW requirement demands BP in Nobel German network topology	104
7.8	Ratio between highest and lowest BW requirement demands BP in NSFNET network topology	104
7.9	Difference between highest and lowest BW requirement demands BP results in Nobel German network topology	105
7.10	Difference between highest and lowest BW requirement demands BP results in NSFNET network topology	105
7.11	BP for lowest bandwidth requirement connections in Nobel German network topology	106
7.12	BP for lowest bandwidth requirement connections in NSFNET network topology	106
7.13	Spectrum fragmentation level in NSFNET network topology . . .	108
7.14	Spectrum fragmentation level in NSFNET network topology . . .	108
7.15	BP results of tested RSA algorithms	110
7.16	BP reduction gain of tested algorithms over KSP-FF	111
7.17	BBP results for tested algorithms	111
7.18	BBP reduction gain of tested algorithms over KSP-FF	112
7.19	Spectrum fragmentation level for tested algorithms and KSP-FF	113
7.20	Proportion of times mechanism was triggered compared to the total number of demands	116
7.21	Proportion of times mechanism was triggered compared to the number of highest BW requirement demands for Priority Realloc HB and compared to the number of CT2 and highest BW requirement demands for Priority Realloc HBCT	117

7.22	BP results for KSP-FF, EGS-FL and Priority Realloc HB mechanisms	117
7.23	BP decrease gain of Priority Realloc HB and EGS-FL mechanisms when compared to KSP-FF mechanism	118
7.24	BBP results for KSP-FF, EGS-FL and Priority Realloc HB mechanisms	119
7.25	BBP decrease gain of EGS-FL and Priority Realloc HB mechanisms when compared to KSP-FF mechanism	119
7.26	Ratio between highest and lowest BW requirement demands BP results	120
7.27	BP results for highest BW requirement demands	121
7.28	BP results for lowest BW requirement demands	121
7.29	Ratio between highest and lowest BW requirement demands BBP results	122
7.30	BBP results for highest BW requirement demands	123
7.31	BBP results for lowest BW requirement demands	123
7.32	For each simulated offered traffic load in Erlang, dots represent the resulting fairness ratio and respective BP for Priority Realloc HB and TRR [7] algorithms	124
7.33	Average external fragmentation of routes	125
7.34	BP results per CT value for load 1,100 Erlang	126
7.35	BBP results per CT value connections for load 1,100 Erlang . . .	126
7.36	Average external fragmentation of routes for scenarios 3 and 4 . .	127
7.37	Proportion of times mechanism was triggered compared to the total number of demands for scenarios 3 and 4	128
7.38	BP results for scenarios 3 and 4	128
7.39	BBP results for scenarios 3 and 4	129
7.40	Ratio between highest and lowest BW requirement demands BP for scenarios 3 and 4	130
7.41	Ratio between highest and lowest BW requirement demands BBP for scenarios 3 and 4	130

A.1	Proportional net-revenue for each RDM scenario minus the proportional net-revenue for grooming according to fee per connection assigned	146
A.2	Proportional revenue for each RDM scenario minus the proportional revenue for grooming according to fee per BW served	148
A.3	Proportional net-revenue for each RDM scenario minus the proportional net-revenue for grooming according to fee per established connection for different CT distributions	149
A.4	Proportional revenue for each RDM scenario minus the proportional revenue for grooming according to fee per BW served for different CT distributions	150
A.5	Proportional revenue for RDM-less scenario minus the proportional revenue for grooming according to fee per BW served for different CT distributions and BC models adopted	151

List of Tables

2.1	Contiguous slots required per connection request considering 12.5 GHz FS width	20
2.2	Fragmentation level % according to equations 1 and 2	26
4.1	BW requested and BW assigned following BC model	43
4.2	BW requested and BW assigned following BC model	46
4.3	BC values per CT values for the two tested scenarios	48
4.4	BW requested values distribution	58
4.5	CT values distribution	61
4.6	BC Model A	61
4.7	BC Model B	61
4.8	BC Model C	61
4.9	BC Model D	62
6.1	Statistical metrics for simulations results implementing KSP-FF bandwidth requirement scenario 4 with load equivalent to 1,000 Erlang	92
7.1	Distribution of bandwidth requirements	100
7.2	Bandwidth requirement scenarios (in number of FSs)	102
7.3	BW requirement and CT value probabilities for BW requirement scenario 4	109
A.1	Nominal service fee values and corresponding proportional values	144
A.2	Nominal penalty values and corresponding proportional values . .	145
A.3	CT value distributions	148
A.4	Mechanism configurations in order of level of benefit for a pricing policy based on established connection	150

A.5 Mechanism configurations in order of level of benefit for a pricing policy based on resources allocation	151
---	-----

ACRONYMS

AFFF *Ahead Fiber First Fit Assignment*

ATM *Asynchronous Transfer Mode*

BFF *Bandwidth based First Fit assignment*

bps *Bits per second*

BP *Blocking probability*

BBP *Bandwidth blocking probability*

CS *Complete Sharing*

CT *class-type*

DP *Dedicated Partition*

DiffServ *Differentiated services*

DWDM *Dense WDM*

EGS-FL *Exact Gap Size with fragmentation level*

Gbps *Gigabits per second*

GMPLS *Generalized Multi-Protocol Label Switching*

IETF *Internet Engineering Task Force*

ILP *Integer Linear Programming*

IP *Internet Protocol*

ISP *Internet Service Provider*

ITU-T *International Telecommunications Union - Telecommunications Standardization Sector*

KSP-FF *K shortest path - first fit*

Mbps *Megabits per second*

MPLS *Multi-protocol Label Switching*

MILP *Mixed Integer Linear Programming*

MSFF *Minimum Spectrum First Fit Assignment*

O-E-O *Optical-Electronic-Optical*

OFDM *Orthogonal Frequency Division Multiplexing*

OXC *Optical Crossconnects*

PCE *Path Computation Element*

PCEP *Path Computation Element Protocol*

PCC *Path Computation Client*

QAM *Quadrature amplitude modulation*

QoS *Quality of Service*

OSNR *Optical Signal-to-Noise Ratio*

OTN *Optical Transport Network*

OSPF-TE *Open Shortest Path First with Traffic Engineering*

PP *Pseudo-Partition*

PSK *Phase-Shift Keying*

RSA *Routing and Spectrum Assignment*

RDM *Russian Dolls Model*

RMLSA *Routing Modulation Level and Spectrum Assignment*

RSVP *Resource Reservation Protocol*

RSVP-TE *Resource Reservation Protocol with Traffic Engineering*

RWA *Routing and Wavelength Assignment*

SP *Shared Partition*

TED *Traffic Engineering Database*

TRR *Two Rate Reservation*

WDM *Wavelength Division Multiplexing*

WSO *Wavelength Switched Optical Network*

1 Introduction

This introductory chapter presents the general problems dealt with in this doctoral thesis research. In order to do so, Section 1.1 describes backbone network current conditions and requirements that justify the study in this thesis. We also explain the specific characteristics inherent to Elastic Optical Networks (EON), which is the reference technology of this work.

The problems defined in Section 1.1 impelled the motivations described in Section 1.2 which prompted the development of the mechanism here proposed. Section 1.3 describes the main and the specific objectives of this thesis.

In Section 1.4 we delineate the subjects and specify the sub-areas that are out of scope of this study. In Section 1.5 we explain the methodology steps we adopted. Finally, in Section 1.6 we present the thesis outline.

1.1 Problem Definition

Long-haul data transport is a crucial task performed by backbone networks, where a large amount of data is carried. Backbone networks rely on optical data communication which large resource capacity cannot be currently provided by any other physical-layer technology [8].

The resource capacity of a single fiber has been increasing over the past years due to the continuing research and development of multiplexing technologies. The main technology adopted, nowadays, in optical networks is Wavelength Division Multiplexing (WDM). The large bandwidth availability and high speed of data forwarding characteristic of WDM networks make them extremely suitable for backbone networks where this type of technology is mostly implemented.

Recent advances in signal processing and modulation techniques have enabled the flexible use of the optical spectrum [9]. The resulting flexible grid optical network is the basis for the Elastic Optical Network (EON) foundation. This new technology provides communication channels with variable resource capacity.

Even though EONs may provide large and flexible resources capacity, it is hard to predict whether technology advances will be able to cope with the intense growth of resource requirements [10]. Recent studies show a continuous growth of data traffic demand as a trend in the Internet evolution. Core network data traffic has been doubling in value almost every two years and is likely to continue growing exponentially [11], [12].

Moreover, optical networks are susceptible to physical failures. When a failure happens in an optical network element, a data is rerouted to a new path and share the path's resources capacity with other connections. In this case active links may become congested, there is contention for resources and some connections may be disrupted. Due to the large amount of resources offered by backbone networks, a connection disruption has a heavy impact on the service provided to a client.

Backbone network clients may be served with different service levels previously defined by Service Level Agreements. The different service levels may refer to different lighthpath availability or protection schemes [13], a service minimum bandwidth guaranteed [14], or connection holding time [15]. In order to be able to provide this differentiated level of services, network manager has to be able to adopt differentiated service mechanisms and strategies [16].

Even though differentiated service strategies may be important for backbone network managers, currently there is no proposal for differentiated resources allocation according to service priority levels for WDM networks. EONs are currently under research and development and specific features are neither broadly studied nor proposed. In particular, proposals for the provisioning of different service levels for EONs have not yet been published.

Furthermore, EONs hold characteristics intrinsic to its operation which are presented as obstacles to network efficient performance. One of the characteristics is the spectrum fragmentation. Spectrum fragmentation jeopardizes resources distribution and therefore increases service denial to connection requests [17]. A second characteristic is the unfairness of service to different rate connections. Both EON issues represent a limitation to the amount of resources and level of service this new paradigm may provide [7].

Due to EONs novelty simulation tools to assess this type of network performance are scarce in the literature.

1.2 Motivations

As explained in the previous section, backbone networks usually require differentiated service strategies. Current differentiated service strategies designed for WDM networks do not focus on the differentiated distribution of resources.

Due to its large increased resources capacity and its flexibility in resources allocation [18], EONs are likely to become the definite and broadly adopted technology for backbone network service providers. However, differentiated service strategies have not yet been proposed for EONs. Although mechanisms originally developed for virtual circuit networks could be adapted to EON, the adaptation would carry natural restrains and should be carefully planned and tested. In this work, we intend to develop a differentiated service mechanism that is efficient and properly designed for EONs.

As another shortcoming, spectrum fragmentation is unconditionally present in EON dynamic service provision [19]. The spectrum fragmentation jeopardizes efficient resources distribution [17]. Therefore algorithms that prevent or reduce spectrum fragmentation when assigning resources are commonly found in the literature [20]. Both strategies have drawbacks. Algorithms that intend to prevent spectrum fragmentation provide a slight improvement in the spectrum use and minimal benefit on the network's blocking probability. Procedures that reduce existing spectrum fragmentation usually promote network instability due to constant connections disruption and re-establishment [17].

Finally, EON's traffic matrix characteristic has a direct impact on the spectrum fragmentation. Studies and performance analysis of network simulations regarding this assumption are not available and theoretical studies are limited. However having a good knowledge of spectrum use in relation to bandwidth requirement values could permit the development of an efficient strategy on resources allocation policies.

In EONs a particular phenomenon occurs regarding highest bandwidth requirement demands. In any network systems higher rate demands are more likely to be denied service due to the lack of resources availability. However, in an EON the spectrum fragmentation tremendously increases the probability of higher rate demands being blocked [7]. Even if there are enough resources available in the network, due to spectrum fragmentation, highest bandwidth requirement connections are more likely to be blocked than lower rate ones. Studies regarding the EON's service unfairness are seldom available in the

literature and proposals to reduce the unfairness level are extremely limited.

1.3 Objectives

Due to the research area current state, the main objective of this thesis is:

MO: Develop a mechanism for routing and resources assignment to be implemented in an EON dynamic service establishment scenario.

The proposed mechanism will promote specific performance optimization and new features in an EON. This proposed mechanism is named Priority Realloc. The aim of the mechanism extends into the specific objectives of this thesis proposal and are detailed as follows.

O1: Promote differentiated service for traffic with different priority of service.

O2: Decrease spectrum fragmentation in network links and routes.

O3: Increase service fairness between different rate connections.

The **O1** procedure considers alternative policies to prioritize and classify traffic. This objective promotes provisioning of different service levels by differentiated resources assignment and blocking probability for the different service classes. It also intends to guarantee a minimum level of service to lower priority traffic.

To accomplish **O2** the proposed algorithms focus on preventing spectrum fragmentation and reducing established spectrum fragmentation in EON links. In both cases we intend to increase the benefit already promoted by available mechanisms by further decreasing overall blocking probability and increasing resources assignment.

O3 will be achieved via the service prioritization of specific traffic types and an efficient resources allocation strategy. This objective aims at promoting service fairness and avoid an unbalanced service towards originally deprived demands.

1.3.1 Additional contributions

Before focusing on EONs, we have studied differentiated service for WDM networks. During this research phase we have analyzed the impact on service levels and network performance derived from the order of processing of connections requests. We have also developed and proposed a differentiated

service mechanism based on the differentiated distribution of resources according to classes of service. We developed two versions of the mechanism one to be implemented on an offline scenario, and another to be implemented on a dynamic scenario.

In order to study EONs performance under different network configurations and to assess Priority Realloc promoted benefit we have developed an EON simulator with differentiated service capabilities, named DSEON-Jsim. DSEON-Jsim represents a contribution to EON research area since, currently, there are few EON simulators available.

In the course of our research development, we have studied EONs operational characteristics. Most of the studies were performed under network simulations of dynamic service establishment. The EONs simulation have produced valuable performance results that portray EONs behavior under certain scenarios.

Some simulation results indicated the level of performance advancement of EONs over WDM networks. Other simulations concern a practical observation of the impact of traffic matrix characteristics on efficient resources assignment and blocking probability in EONs. The aforementioned results are unique in the literature and studies of dynamic scenarios regarding this subject have never been published before.

1.4 Scope

The EONs research area is extremely broad and comprises many sub areas of study. The different features an EON may provide and the diverse type of issues relating to the service it offers may derive into a vast selection of research topics. For this reason, in this section, we delineate the specific sub-areas and topics on which this doctoral thesis will focus. This thesis regards the following topics:

- Dynamic service operation. The resources allocation debated in this thesis concentrates on EON operational phase, in which clients' demands arrives randomly with arbitrary lifetime (i.e. traffic matrix is not known in advance). In such a scenario, as a connection request arrives the system attempts to serve it according to the current network state.
- Differentiated service provisioning. The provisioning of different levels of service regarded in this work focus on the distribution of resources, resources preemption and connection establishment or disruption. We consider

that traffic service classes are either previously determined by network management, or defined according to connection bandwidth requirement.

- Spectrum fragmentation. In this work we study the traffic matrix characteristics and network conditions that may increase spectrum fragmentation. We explain and enumerate mechanisms for spectrum fragmentation prevention and reduction.
- Fair allocation. In this thesis we debate service fairness related to diverse rate demands. We analyze service denial to highest bandwidth requirement connections, study and propose solutions to improve resources allocation to this type of request. In order to account for network fairness level we separately simulate and analyze the service provided to highest and lowest bandwidth requirement connections.
- Network performance. In this work, we analyze network performance improvement regarding the network's blocking probability, bandwidth assignment, spectrum fragmentation level, and service fairness level. In order to assess the proposed mechanism benefit we also consider and measure the mechanism's algorithms computational complexity.

1.4.1 Out of scope

Some specific sub-areas are closely related to the subjects we debate and study in this thesis proposal. However we will not discuss the following subjects:

- Enabling technologies. In this work we do not explain EON's hardware including transponders, optical switchers etc. We do not explain, nor debate, optical signal modulation formats and spectral efficiency.
- Routing and resources assignment (RSA). We do not study the offline allocation of routes and resources. We do not consider optimized distribution of resources in a network planning phase. In the dynamic scenario we consider, we do not consider adaptive routing schemes, where routes are calculated during network operation and according to updated network state. We do not offer an exhaustive review of RSA algorithms. RSA algorithm proposals in the literature are abundant and we have selected to review the algorithms that are most influential or that have inspired our mechanism design. We do not consider, in the proposed mechanism, modulation format as a routing and spectrum assignment variable.

- Control plane. Even though our proposal is focused on centralized routing and resources assignment computation, in this thesis, we do not study or consider EONs control plane or protocols. We do not analyze the current proposals on this topic and do not propose protocol extensions for the implementation of the proposed mechanism.
- Re-routing and connection reallocation. The mechanism we propose promotes either connection disruption or resources preemption. We do not propose re-routing solutions for reallocation of disrupted connections. In fact, many solutions are available in the literature and we would particularly recommend the adoption of re-tuning proposed in [21]. Regarding preemption strategies we do not present an extensive study regarding preemption consequences on network instability and control messages exchange in EONs.
- Time varying traffic. Time varying traffic is a current topic in EON's research field. Time varying traffic may require anticipated reservation of spectrum band in case the connection has its bandwidth requirement increased or decreased. We did not consider this type of traffic in the proposed mechanism development.
- Differentiation of service and quality of service. Differentiated service strategy based on restoration or protection schemes is out-of-scope of this research. So is the differentiation of service based on signal quality or deterioration. Quality of service regarding physical impairments and bit-error rate is not studied in this thesis. We do not discuss traffic's service classification criteria. We assume network management determines traffic service class based on Service Level Agreement and network revenue which are out of scope of this study.
- Fairness allocation. The fairness issue we study regards the system demands diversity bandwidth requirements and not the assigned path's number of hops. Considering the different rate connections, we exclusively analyze the performance metrics of the lowest and highest bandwidth requirement demands. We neither measure nor analyze intermediary rate connections level of received service. In the scenario we consider there is only one intermediate connection rate and therefore it is straightforward to infer performance results for this type of connection based on service offered to lowest and highest rate connections.

- CapEx, OpEx and network revenue. Due to service fee and differentiated service fee according to service class, the network performance benefit and differentiated service promoted by our mechanism indicate a possible increase in service provider profit. However we do not provide a specialized study or analysis on the economic impact promoted by our proposed mechanism. Even though we analyze the mechanism computational complexity, we do not evaluate the increase in CapEx or OpEx resulted from its implementation.

1.5 Methodology

The work in this research belongs to the field of optical communications in the Telecommunications area. The methodology adopted in this engineering research is described in [22] and comprises the following four phases:

1) Information phase. In this first step we have gathered information on the current characteristics of the subject area and the problem definition. This step aims at clearly defining and delineating the subject under research. This phase usually consists on the revision of the literature. In this phase we have studied the network, routing and resources assignment's basic concepts and current state. We have reviewed IETF technical reports on all current standardization proposals related to the topic of our research. Finally we have extensively reviewed work related to our proposal available in the literature. Moreover we identify documented practical studies and experiments on the subject.

2) Definition phase. From the information gathered in the previous phase we have understood the state of the art in the subject area and identified problems that have not already been solved and published. We have, then, developed a solution proposal that overcomes limitations on the current network conditions and that have not yet been proposed by the available alternatives.

3) Implementation phase. In this phase we have delineated the network condition and scenario at which the mechanism would be implemented. We have developed the procedural architecture of the proposed mechanism. We have produced the algorithms contained by the mechanism, and we have also elaborated and described the tasks that the mechanism would perform.

4) Validation phase. The last step of the applied methodology is the definition and deployment of network simulations that evaluate the proposed mechanism performance and compare it to benchmark solutions performance.

These simulations were performed in DSEON-Jsim, an ad-hoc Java base discreet event simulator described and validated in Chapter 5.3.2. Performance results are evaluated and analyzed and served as proof to the beneficial impact of our proposed mechanism in an EON.

1.6 Thesis outline

The remainder of this thesis is as follows.

Chapter 2 briefly introduces WDM networks deployed in current operators' infrastructures. Then, it explains concepts, characteristics, operational phases, issues and open problems of the new EON paradigm.

Chapter 3 reviews related works available in the literature. The reviewed work includes proposals regarding fragmentation-aware RSA algorithms, defragmentation mechanisms, allocation of resources criteria to increase service fairness level and provisioning of different service levels.

Chapter 4 explains our previous work on differentiated service for WDM networks. This research work and the mechanism we proposed are important contributions to the research area of optical network, but, most importantly, have served as a background research to inspire the creation and development of Priority Realloc mechanism.

Chapter 5 addresses Priority Realloc objectives: provisioning of different service levels, decreasing the spectrum fragmentation in the network and increasing fair allocation of resources. The chapter also explains the mechanism operation guidelines, describes its algorithms and analyzes its computational complexity.

Chapter 5.3.2 presents DSEON-Jsim, an ad-hoc Java based EON simulator we have developed in order to assess Priority Realloc performance results. Besides explaining the simulator operation, Chapter 5.3.2 also describes the validation process of DSEON-Jsim.

Chapter 7 presents network simulation results regarding: EON performance compared to a WDM network with grooming, EONs with different traffic matrix characteristics and, most importantly, Priority Realloc performance results. We compare the mechanism's performance to benchmark algorithms and proposals from related work. We also assess the mechanism's impact depending on the network traffic matrix characteristics.

Finally, in Chapter 8 we analyze the benefit promoted by the proposed mechanism and how we achieved the thesis objectives. We also comment on the originality of the mechanism proposed and its contributions to the research community. We then expose future works derived from this thesis including operational variations of the proposed mechanism, adaptation to other network conditions and control plane enhancements to support the mechanism implementation in an EON.

2 Theoretical background

Optical networks, have, in the last decades, been the most relied upon technology for transmission of a vast amount of data. For this reason optical network are the de-facto technology implemented for data communication in backbone networks. In this chapter we introduce a brief overview on basic concepts related to WDM networks and then, in consecutive sections, we explain the main characteristics and issues in EONs that have impelled the studies and proposals of this thesis.

The WDM technology is currently adopted by the industry to enable a multiplication of optical channels in optical networks and is explained in Section 2.1. EONs are still under research but, due to their promising benefits and network performance optimization, they are likely to be the next technology broadly adopted supplementing WDM networks as the industry's choice. EON is explained in section 2.2.

2.1 WDM Networks

With WDM technology many channels, each of them an optical carrier signal, are multiplexed into one optical fiber. Each non-overlapping wavelength band supports a single communication channel [23], enabling the original fiber capacity multiplication.

With the advances in hardware and modulation technology Dense WDM enables one single fiber to operate with multiple channels of up to 100 Gbps. Currently with the available technologies on receivers and transponders it is operational to transmit up to 160 wavelengths in one single fiber [24].

In a WDM network data can be switched exclusively in the optical domain without the need of optical-electronic-optical conversion, these are known as transparent WDM networks. With the automatic operation, promoted by a robust control plane, transparent WDM networks are also known as Wavelength Switched Optical Networks (WSO). A route assigned in tandem with a

wavelength is known as a lightpath. When a lightpath is set, a single electronic hop channel is available between any two nodes, even if these nodes are geographically far apart and by-pass many optical nodes in the physical network [25].

In WSONs the optical signal is switched at the wavelength granularity. A lightpath is established by the assignment of the physical route and an available wavelength. The Routing and Wavelength Assignment (RSA) problem plays a crucial role in the dynamic network operation [26].

In WDM network, usually, a connection's bandwidth requirement is much lower than the capacity provided by a wavelength. Grooming low-speed connections onto high-capacity lightpaths improves the network throughput and reduces resources waste. When a grooming technique is implemented on a WDM network, two or more connections share the same wavelength capacity. Grooming is performed electronically and therefore, in a transparent network, it is solely executed at a route's end nodes [27].

2.1.1 Routing and Wavelength Assignment (RWA)

The RWA problem may aid in connections establishment online or offline. In an online RWA scenario, demands arrive in different moments while the network is already fully operational, hence connections are established and tear down dynamically. In an offline scenario the network topology is free of use, all links have their full capacity available and demand matrix is known in advance, the task consists in distributing the available resources and paths to the demands at once on what is called the planning phase.

The RWA problem may be resolved in tandem or separately. When resolved in tandem the problem's computational complexity becomes extremely high, and, for this reason, it is conventional to separate the RWA problem into two sub-problems, the routing and the wavelength assignment. Diverse routing solutions can be found in the literature [26]. In the next paragraphs we explain the main adopted ones, which are, also, the ones that inspire routing decisions in EONs.

- **Fixed Routing** is the most straightforward approach. It consists of always choosing the same fixed route for each source-destination pair. One example of such an approach is fixed shortest-path routing. The shortest-path route for each source-destination pair is calculated off-line using standard

shortest-path algorithms, such as Dijkstra's algorithm or the Bellman-Ford algorithm. The disadvantage of such an approach is that, if resources along the path are tied up, the connection is not established. This approach can potentially lead to high blocking probabilities in the dynamic case, or may result in a large number of wavelengths being used in the static case. Also, fixed routing may be unable to handle fault situations in which one or more links in the network fail [26].

- In **Fixed-Alternate Routing**, each node in the network has a routing table that contains an ordered list of a number of fixed routes to each source and destination node pairs. The selection of routes follows the list order. This approach is also known as K shortest paths (KSP). When there is no available route into the list of alternate routes the connection request is blocked. In most cases, the routing tables are ordered by the number of hops of each route. Fixed-alternate routing provides simplicity of control for setting up and tearing down lightpaths, and it may also be used to provide some degree of fault tolerance upon link failures. It can significantly reduce the connection blocking probability compared to fixed routing [26].
- In **Adaptive Routing** routes are chosen dynamically according to current updated topology information of the network. Adaptive routing requires extensive support from the control layers to continuously update the routing tables, but as a result lower connection blocking occurs when compared to fixed and fixed-alternate routing [26].
- **Least-Congested-Path** (LCP) routing is similar to alternate routing, for each source-destination pair, a sequence of routes is pre-selected. Upon the arrival of a connection request, the least-congested path among the pre-determined routes is chosen. The congestion on a link is measured by the number of wavelengths available on the link. The congestion on a path is indicated by the congestion on the most congested link in the path. If there is a tie, then shortest-path routing may be used to break the tie. An alternate implementation is to always give priority to shortest paths, and to use LCP only for breaking ties. A disadvantage of LCP is its computational complexity. In choosing the least-congested path, all links on all candidate paths have to be examined [26].

Regarding the wavelength assignment many algorithms have been proposed in the literature. However only one of them is broadly adopted and mentioned in most articles. In the next paragraphs we review this algorithm and another

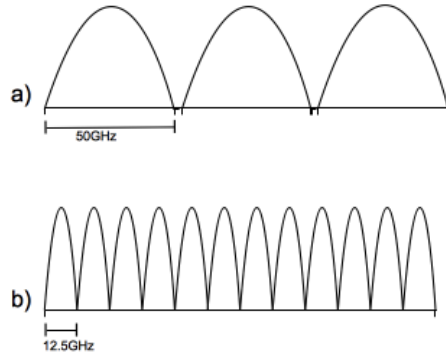


Figure 2.1: a) traditional fixed grid in a WDM network; b) flexigrid used in EON

straightforward one which similarities are found in the resources assignment for EONS. Due to the different paradigm in resources assignment for EONS, other wavelength assignment algorithms are hard to directly relate to resources assignment in EONS. For this reason we will not review these algorithms here.

In **random wavelength assignment** all wavelengths in the route are analyzed for availability. Among the available wavelength on the required route, one is assigned randomly [28]. **First Fit** (FF) is the most adopted algorithm. In FF all wavelengths are numbered, a lower number wavelength is inspected for availability in the given route, in case it can not accommodate the demand the next wavelength is inspected. FF promotes lower computation cost than the previous model, no global knowledge is required and it presents good performance results [28].

2.2 Elastic Optical Networks

In the traditional ITU-T DWDM rigid frequency grid [29], spectrum bands are spaced by 50 or 100 GHz. Each spectrum band is able to accommodated one wavelength. A flexigrid described in [30], divides the available optical spectrum into spectrum bands of fixed finer spectral width. The currently proposed spectral widths are 25 GHz, 12.5 GHz and 6.25 GHz and as low as [18]. 12.5 GHz or 6.25 GHz are most commonly found in the literature and the potential bandwidth granularity that will be adopted by the industry. Each of these spectrum band in the flexigrid is denominated a Frequency Slot (FS). Figure 2.1 depicts the traditional frequency grid in WDM and the flexigrid used in EONs.

Diverse number of FSs can be jointly allocated to a connection in order to better adapt to a connection requirement. An EON is based on this flexible use of the optical spectrum enabled by the concatenation of FSs constituting one optical

channel. The flexible allocation of spectrum presents an improvement in relation to the fixed grid used in WSONs because the resulting channels are able to serve a bandwidth requirement that is smaller than a wavelength capacity without the waste of resources.

Alternatively, if a demand requires more bandwidth than the wavelength capacity, FSs may be allocated composing an optical channel able to accommodate this demand. When a large amount of spectrum slots are jointly allocated, the resulting channel may reach as high bit rate as 400 Gbps or 1 Tbps [31], [32]. Authors in [33] describe the transmission of a non-guard interval 1.12 Tbps super-channel. These high capacity channels are called super-channels and are able to meet core networks bandwidth requirement growth [34].

An EON is also known as a Spectrum Switched Optical Network (SSON) [31] where channels are formed by bands of spectrum and this is the element switched over the optical network. The new concept of SSON is defined as an extension of WSON with flexible capabilities, a data plane connection is switched based on an optical spectrum frequency slot of a variable slot width, rather than based on a single wavelength within a fixed grid and with a fixed channel spacing as is the case for WSON. Thus, the distribution of resources in an EON is more efficient than in a WSON.

In an optical channel composed by a FS assemblage, the central frequency determines where the assigned spectrum is located in the spectrum grid. A slot granularity refers to the number of FSs in a fiber link, which relates to the FS width. The optical channel is identified by its central frequency, the number of slots and the slot width. Each FSs has an index that works as an identifier for the FS as illustrated in Figure 2.2

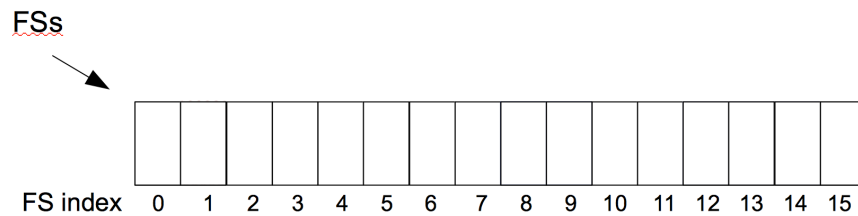


Figure 2.2: FSs and respective indexes

In the future, when EON technology start to be implemented in the currently established optical networks, it will have to, in a first step, co-exist with legacy WDM technology. Currently, it is not yet clear how this hybrid architecture will operate, one possible solution being considered is a condition where different

spectrum blocks are assigned to channels with different bit rates [35].

2.2.1 Technical advances that enable flexigrids

The finer spectrum division in flexigrid is enabled by recent advances in signal processing and modulation techniques that enable high-speed data stream using multiple lower-speed subcarriers with overlapped spectral positioning. Most common modulation techniques are Optical Orthogonal Frequency Division Multiplexing (OFDM) [1] and Nyquist WDM (N-WDM) [36], both offering the same spectral efficiency and enabling flexible grid optical networks deployment [9].

In [1] and [37] authors explain the physical aspects of the OFDM as a class of multi-carrier modulation scheme that transmits a high bit rate data stream by dividing it into a number of orthogonal channels. In either a WDM network or in an OFDM network information is transmitted in different frequencies simultaneously, however, in OFDM, the frequencies selected to be used by the sub-carriers have their signals mathematically orthogonal over one OFDM symbol period [1].

Modulation and multiplexing are achieved digitally using Inverse Fast Fourier Transform (IFFT) generating precise and computational efficient orthogonal signals. Consequently in OFDM there is no need for frequency guard bands between sub-carriers as there is in conventional FDM, in fact, in OFDM the spectra of individual sub-carriers overlap but they can be demodulated without interference and without the need of analogue filtering to separate the sub-carriers (Figure 2.3).

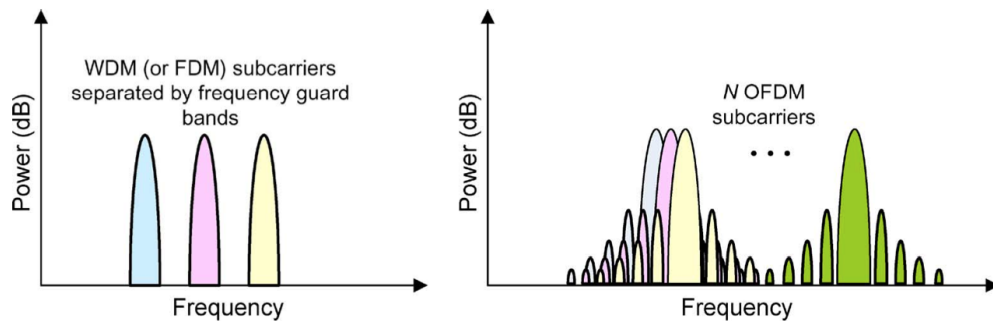


Figure 2.3: Spectrum of (a) WDM or FDM signals (b) OFDM signal [1]

Authors in [36], [9], [38], [39] and [40] explain the physical aspects of the N-WDM, where subcarriers spectra are shaped in order to occupy a

bandwidth close or equal to the Nyquist limit for inter-symbol-interference-free and cross-talk-free transmission.

The implementation of OFDM or N-WDM modulated signals enabling an EON requires the use of specific hardware. Some of the fundamental network elements are bandwidth variable transponders (BVTs), bandwidth variable optical cross-connects (BV-OXCs) and reconfigurable bandwidth variable optical add/drop multiplexers (ROADMs) that promotes, for instance, cross-connection of optical paths with arbitrary bandwidth and nominal center frequency [41]. Information on hardware requirements can be found in [32], [41] and [42]. The implementation of these hardware have passed through many tests and experiments which demonstrated the feasibility of EONs [43], [44], [34].

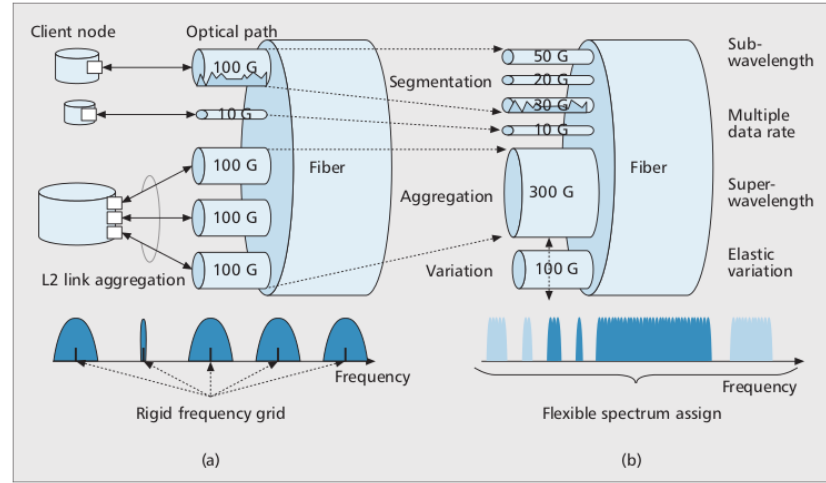


Figure 2.4: Spectrum assignment in: a) WDM networks and b) EONs [2]

2.2.2 Routing and Spectrum Assignment

In an EON the resources assignment refers to the allocation of spectrum resources, i.e. number of FSs. Therefore, the WSON's RWA problem becomes, in an EON, the routing and spectrum assignment (RSA) problem [45]. An RSA algorithm computes an end-to-end physical route and allocates a set of FSs around a central frequency.

In absence of wavelength converters, RSA is subject to the spectrum continuity constraint meaning that the same FSs (and the same FS index) in the optical signal must be assigned along all the links in the path [46] as illustrated in Figure 2.5. If the spectrum continuity is not observed, nodes must convert the central frequency along the path [31], an action that increases functionality cost and should, ideally, be avoided.

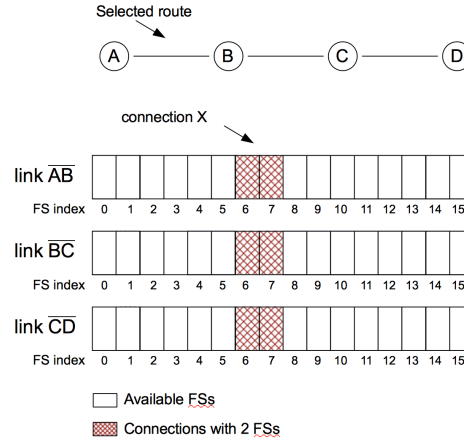


Figure 2.5: A connection X is allocated in the same indexed FSs in all links through the assigned route

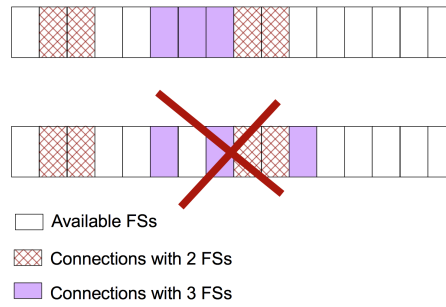


Figure 2.6: The diagram shows a) connections with contiguous allocated FSs and b) one connection has non-contiguous allocated FSs, this is not possible in an EON

The RSA problem must also regard the spectrum contiguity constraint which determines that if more than one FS is assigned to a connection the FSs must be contiguous to each other as illustrated in Figure 2.6.

The RSA problem may be implemented in a static or in a dynamic scenario. In a static scenario the RSA algorithms are implemented in the network planning phase when the set of connection requests is known in advance. In a static scenario the RSA algorithms are known as offline RSA algorithms. In the dynamic scenario dynamic RSA algorithms are implemented to provision connections at request arrivals.

In a dynamic traffic environment, due to the real-time nature of the problem, RSA algorithms must be straight forward and agile. Online RSA algorithms can tackle the routing and spectrum assignment jointly (i.e., in one step) or separately (i.e., in two steps) [17].

In one step algorithms, routing and spectrum assignment are solved simultaneously. The drawback of one step RSA algorithms is that the problem becomes highly complicated, thus highly computational complex and time consuming.

In two step algorithms, the RSA problem is decomposed into two subproblems, the routing subproblem and the spectrum assignment subproblem. The routing and the spectrum assignment are then solved separately and sequentially. The two step RSA algorithm will first compute a number of physical routes (a sequence of fiber links) for each source-destination node pair and arrange them following a specific policy, for instance shortest path on top of the list. The routing algorithm can be either static, where alternative routes are computed offline, or adaptive, where a route is computed online according to the network state [17].

Then, starting with the first route in the list, the spectrum assignment step selects the required number of contiguous available FSs. The selection of one and not other group of contiguous available FSs follows a previously defined spectrum allocation policy. The spectrum allocation policy is crucial to the performance of an online RSA algorithm.

Similar to WSONs, the most adopted routing method in the RSA problem is the offline computation of a given number of shortest routes. As in RWA, this method is known as K- shortest path (KSP), where K determines the number of alternative routes to be calculated. Usually in KSP the routes are ordered in a list according to their number of hops, so that the shortest route is the first in the route [47].

Different spectrum allocation policies have been proposed and tested before. A first-fit (FF) policy [47], [18] selects the lowest index set of available contiguous FSs. In Random policy one of the available sets of contiguous FSs is selected randomly [48] [35].

When implemented in tandem, the KSP routing and the FF result in the KSP-FF where the route with the lowest index set of available contiguous FSs will be selected and so will this set of FSs [47]. This algorithm has presented better results than the random FS assignment, and, due to its computational simplicity became the benchmark algorithm in most of the studies available in the literature [17].

The protocols that will be adopted as a control plane for an automatic RSA operation are still being enhanced from current WDM control plane standards as described in [49].

Table 2.1: Contiguous slots required per connection request considering 12.5 GHz FS width

Modulation format	Requested bit rate			
	10 Gbps	40 Gbps	100 Gbps	400 Gbps
BPSK	1	3	8	32
QPSK1	1	2	4	16
16-QAM	1	1	2	8

2.2.3 Modulation Level and Spectrum Assignment

In an EON each channel signal may be modulated with a different modulation format. Each modulation format enables a given number of bits per symbol, and, depending on the baud rate, a resulting ratio of bits per second per Hertz (b/s/Hz). When modulation format x permits a higher number of bps per Hertz than a modulation format y , the same spectrum band would transmit more bps if modulated with x than if modulated with y . This relation is known as spectrum efficiency. A modulation format that enables a higher number of bits per symbol can also be understood as a higher level modulation format. A relation between modulation formats and FS requirement for and FS width of 12.5 GHz may be observed in Table 2.1.

The modulation level is limited by the distance (in kilometers) the optical signal has to travel in the optical fiber. When passing through the optical fiber the optical signal starts to deteriorate due to physical impairments reaching a deterioration level at which the signal's bit error rate becomes unacceptable. The higher the modulation level the shorter the distance the signal can travel respecting a deterioration level threshold.

In order to increase spectral efficiency higher modulation levels can be selected for channels crossing a smaller distance while large distance connections may be modulated with a format with lower level. For instance, a modulation format such as 16-QAM can be selected for short paths (usually less than 500 km) and a more robust one, such as QPSK, can be selected for longer paths [50]. A short length elastic optical path is bound to undergo reduced signal impairment and, therefore, its signal may be modulated using a format occupying less optical spectrum and it might still reach destination with acceptable signal quality level [18]. The selection of the modulation format may also be considered in the path computation, extending the RSA problem into the Routing, Modulation Level

and Spectrum Allocation (RMLSA).

2.2.4 Spectrum fragmentation problem

In a dynamic network scenario, the constant setup and release of connections can create gaps of contiguous available FSs in the optical spectrum which size in number of FSs may limit the number of FSs requirements in a demand it can accommodate. Gaps in the optical spectrum throughout the network links result in the spectrum fragmentation problem. Figure 2.7 illustrates a link before and after connections termination, where we can see that the link spectrum becomes fragmented. The spectrum fragmentation problem may lead to inefficient resources use and thus high blocking probability.

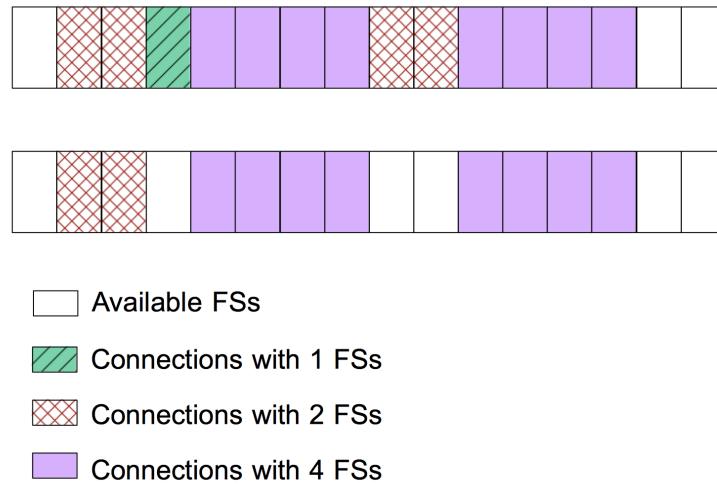


Figure 2.7: The diagram shows a) the original link state before connections termination, b) the link state after connections termination

Authors in [17] classify the fragmentation issue according to the constraint they jeopardize. The *vertical fragmentation* affects the spectral contiguity constraint. It occurs when the spectral resources in a link are fragmented into various small size gaps of available contiguous FSs. The smaller the number of contiguous available FSs, the less likely these groups of available FSs would be able to serve a connection request.

The *horizontal fragmentation* impairs the continuity constraint and occurs when a gap of available FSs in one link does not have the same correspondent FS availability along the successive links in the path. In this case available FSs in a link may not be assigned to a connection request even though each individual link may have enough contiguous FSs to attend demand's spectrum requirement. This fragmentation problem is also known as the misalignment of available FSs in a path's links [4]. In this fragmentation problem the smaller the number of

links in a selected path the less likely the misalignment of FS availability will occur between selected links and neighboring links. An example of vertical and horizontal fragmentation may be observed in Figure 2.8.

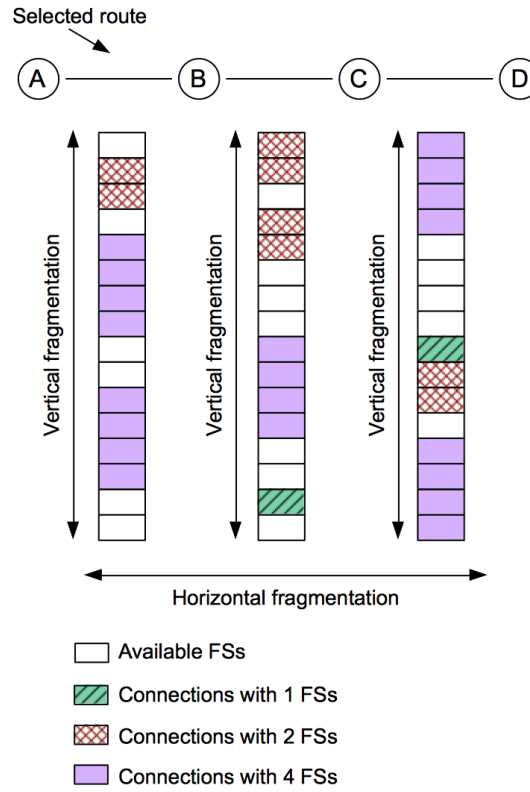


Figure 2.8: A selected route comprises a given number of links. Each link may be serving different connection from the other. The vertical fragmentation represents the spectrum fragmentation experienced by each link, the horizontal fragmentation represents the misalignment of FSs gaps so that the resulting route fragmentation is more prejudicial than the individual link fragmentation

The EON bandwidth requirement characteristics interferes on the spectrum fragmentation level. Clearly, on a network where all bandwidth requirements are the same, spectrum fragmentation is hardly a problem. When a connection is terminated the number of contiguous FSs it releases would accommodate any incoming connection request. However, as the diversity of bandwidth requirements increases, the size of gaps of contiguous available FSs become more varied and smaller gaps cannot accommodate demands with higher FS requirement as illustrated by Figure 2.9.

In case the EON connection rate is heterogeneous the relation between the possible BW requirements influence the spectrum fragmentation level. If the bandwidth requirements values have a common denominator, and therefore the values are multiples of one another, the aggregation of gaps from different terminated connections may accommodated a higher number of connection rates as depicted in Figure 2.10. In the scenario exemplified, all bandwidth

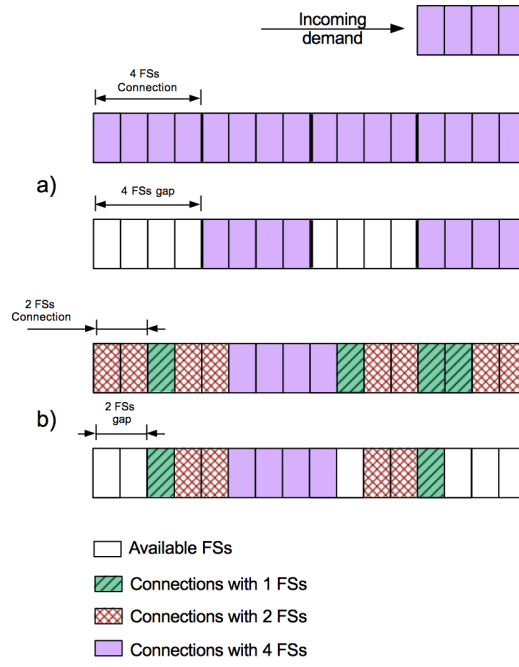


Figure 2.9: The diagram shows a) an EON only contains 4 FSs connections, whenever any connection is terminated the gap left will always fit an incoming demand and b) the network connection rate is heterogeneous and when a 2 FSs connection is terminated the gap left cannot accommodate the incoming demand.

requirements have a common denominator, the bandwidth requirements in the scenario illustrated are in the group (2,4,8) FSs. Under the described condition the fragmentation level has a lower detrimental effect on the network performance.

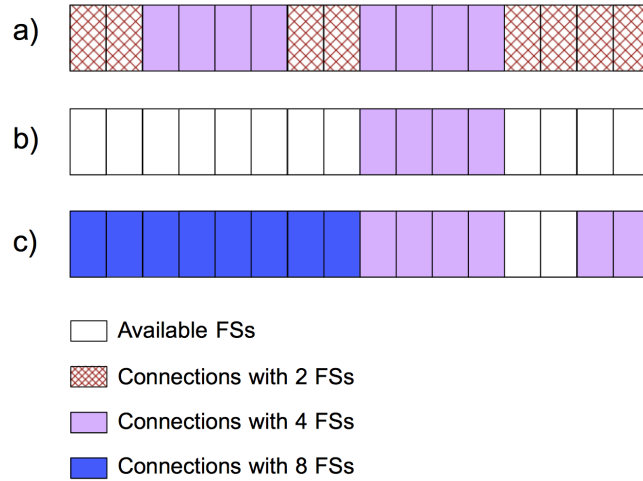


Figure 2.10: The diagram presents a scenario where bandwidth requirements have a common denominator. In a) initial link state with active connections, in b) four connections with 2 FSs and one with 4 FSs are terminated leaving a gap of 8 contiguous available FSs and a gap of 4 FSs and in c) one gap may accommodate one 8 FSs connection and the other may accommodate one 2 FSs connection and the gap left may still accommodate another 2 FSs connection leaving no gap of available FS and therefore diminishing the link spectrum fragmentation

On the other hand, if the bandwidth requirements do not share the same common denominator, then the spectrum fragmentation created from

the dynamic establishment and release of connections tend to result in gaps that would accommodate a fewer number of connection rates consequently increasing the blocking probability issue. Figure 2.11 presents a condition where the bandwidth requirements of connection requests do not have a common denominator.

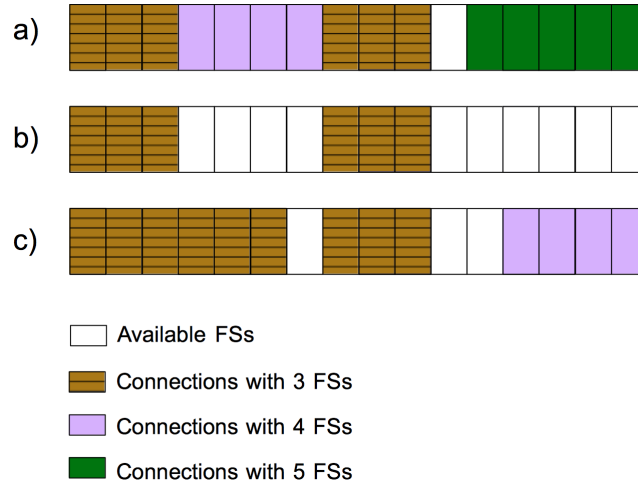


Figure 2.11: The diagram shows a scenario of bandwidth requirements without common denominator. In a) initial link state with active connections, b) a connection with 8 FSs is terminated leaving a gap of 8 contiguous available FSs, c) one connection with 3 FSs and two connections with 2 FSs are accommodated leaving a gap of one available FS that can not accommodate any incoming connection requests and therefore increase the links spectrum fragmentation.

Our contribution to the dynamic analysis on demand BW requirement characteristics can be observed in Chapter 7. In simulations performed, results proved that bandwidth requirement values profile do interfere on demand's blocking probability.

2.2.4.1 Spectrum fragmentation metrics

In the literature it is possible to find different measurements of spectrum fragmentation. Since the spectrum fragmentation problem may be related to the memory fragmentation problem in computer architecture, some authors propose implementing fragmentation evaluation techniques used to asses memory fragmentation in the spectrum fragmentation problem. Authors in [19] propose adapting models described in [51] to be used in the analysis of the spectrum fragmentation level. In what is called the external fragmentation, fragmentation is quantified as the relation between the largest gap and the total amount of free FSs and is given by:

$$F_{ext} = 1 - \frac{\text{largest gap}}{\text{total number available FS}} \quad (2.1)$$

An alternative fragmentation measure, also described in [19], considers a demand's bandwidth requirement and, therefore, a path's spectrum fragmentation is more severe when a larger number of FSs is required to satisfy a demand. The spectrum fragmentation in this case is a function of the number of FSs required and is expressed by:

$$F_c = 1 - \frac{c * \text{Free}(c)}{\text{total number available FS}} \quad (2.2)$$

In Equation 2.2, c represents the number of FSs required by a given demand and $\text{Free}(c)$ represents the number of simultaneous requests with requirement c FSs that can be satisfied in the analyzed path. Equation 2.2 is valid when there is at least 1 FS available in the analyzed path. Observe that following this equation each connection request would have its own fragmentation level for the same analyzed path according to the number or required FSs.

Consider the below 30 FSs spectrum range S_i and S_j and their respective FS states as cited in [19] :

$$S_i = (100110011010101110011000010101)$$

$$S_j = (11111111111110101000000000000000)$$

By inspection S_i is highly fragmented and S_j is less fragmented. Hence S_j can accommodate a wider variety of incoming connection bandwidth requirements (up to 13 FSs) than S_i that can accept connections with bandwidth requirements up to 4 FSs. Therefore S_i may undergo higher blocking probability than S_j . When analyzing the fragmentation level of each spectrum range by implementing Equation 2.1 each range has its own fragmentation level value, while if Equation 2.2 is implemented each spectrum range's resulting fragmentation level depends on a demand's number of FSs requirement. As an application example of both measuring techniques, the fragmented level of both spectrum ranges are quantified using Equation 2.1 named F_{ext} and Equation 2.2 named F_{dem} , where the number in brackets represent the number of FSs required. The resulting fragmented level in percentage can be observed in Table 2.2.

Table 2.2: Fragmentation level % according to equations 1 and 2

	F_{ext}	$F_{dem}(1)$	$F_{dem}(2)$	$F_{dem}(3)$
S_i	73.33	0.00	23.07	76.92
S_j	13.33	0.00	7.69	7.69

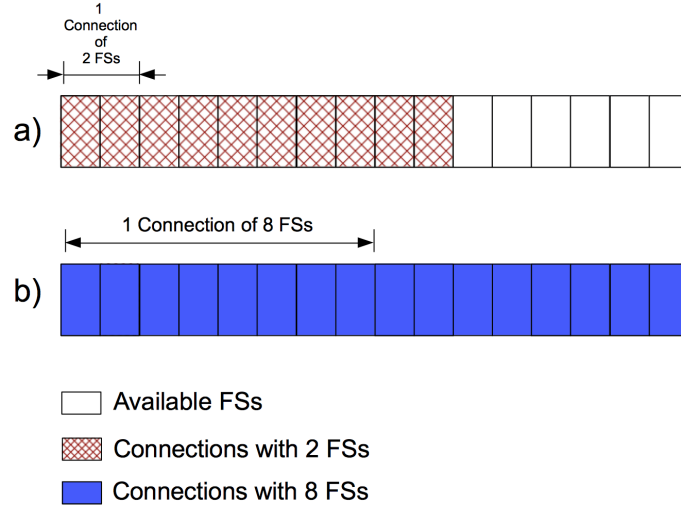


Figure 2.12: The diagram shows a) five connection of 2 FSs each, are accommodated in the spectrum band and there is still contiguous FSs available and b) two connections of 8 FSs each are accommodated in the spectrum band leaving no available FSs

2.2.5 Service fairness in EONs

Service fairness issue has been debated regarding the establishment of connection requiring route with many hops in WSONs [52]. The higher the number of hops, the less probable that all links in the route have the same wavelength available. In EONs, the same issue occurs as a route with many hops is less probable to have in all its links the same FSs available. Connection requests which may only be served by paths with a higher number of hops are more likely to be blocked due to FS availability misalignment than connection requests that require shorter paths [17].

However EONs also present another fairness problem that depends on the amount of resources a demand requires. First of all, highest BW requirement demands are mainly blocked because a spectrum band can accommodate a smaller number of them. Consider five demands requiring 2 FSs and also five demands requiring 8 FSs, with the conditions depicted in Figure 2.12, all 2 FSs connections are established resulting in 0 blocking probability, while in the same spectrum band only two 8 FSs connections are established resulting in 2/5, i.e. 0.4, blocking probability.

Highest bandwidth requirement requests are even more deprived of resources when the other bandwidth requirements requests are higher than a minimum value. For instance consider a spectrum band with 10 FSs and two networks with two bandwidth requirement values. Network A has bandwidth requirements 1 and 8 FSs and network B has 2 and 8 FSs. Consider that, in a given interval of time, in both networks there are two incoming connection requests for the lowest bandwidth requirement (1 FS in network A and 2 FSs in network B) and 1 connection request of highest bandwidth requirement (8 FSs in both networks). In network 1 all connections would be established, while in network 2 if connection request with 8 FSs arrives later it would be blocked.

Furthermore, with the spectrum fragmentation in many links throughout the network, a demand requiring many FSs is less likely to be established because it would be harder to find a gap with required number of contiguous available FS in a link and to find a route in which the same contiguous FSs are available in all its links [19]. For this reason, higher BW requirement demands are more likely to be blocked [7]. Indeed for a spectrum requirement that is small enough, as for instance 1 FS, even in a highly fragmented spectrum it is certain that a 1 FS connection will be established.

Consider, for example, a network where incoming connection requests may require 2, 4 or 8 FSs uniformly distributed, so that in a given interval of time the same number of connections requiring each of the possible number of FSs may arrive. Figure 2.13 a) illustrates a condition where part of a link spectrum is completely used by active connections with those bandwidth requirements, and there are ten connections requests for each bandwidth requirement. In Figure 2.13 b) a connection with 8 FSs is released leaving a gap of 8 contiguous FSs available, Figure 2.13 c) show a condition where four connections with 2 FSs are accommodated in the gap and therefore the blocking probability of this condition is $6/10 = 0.6$. Figure 2.13 d) describes a situation where the gap accommodates two connections of 4 FSs resulting in a blocking probability for this BW requirement of $8/10 = 0.8$ and finally Figure 2.13 e) describes a condition where the gap accommodates one connection of 8 FSs resulting in a blocking probability of $9/10 = 0.9$.

In order to measure the service fairness, in [7] a fairness level metric is defined as the ratio of the blocking probability of the highest BW requirement demands to the lowest BW requirement demands as given by Equation 2.3.

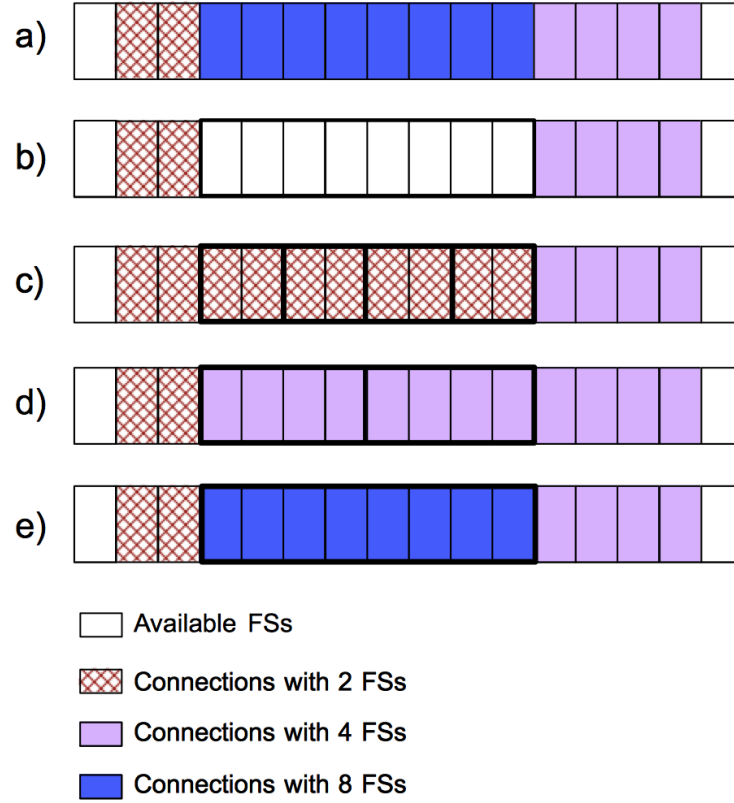


Figure 2.13: The diagrams shows a) original link condition with active connections, b) a connection with 8 FSs is terminate leaving a gap of 8 contiguous available FSs. c) four connections of 2 FSs are accommodated in the gap, d) two connections of 4 FSs are accommodated in the gap and e) one connection of 8 FSs is accommodated in the gap

$$\text{fairness ratio} = \frac{BP_{\text{highest BW requirement demands}}}{BP_{\text{lowest BW requirement demands}}} \quad (2.3)$$

In the scenarios and conditions described in [7] network simulations resulted in approximately 400 fairness ratio indicating that highest BW requirement demands suffered 400 times more blocking probability than lowest BW requirement demands.

3 Related Work

This chapter reviews related work in order to highlight shortcomings and opportunities that motivate the objectives of this thesis. Besides, some of this related work have served as basis to the development of the mechanism proposed here.

Section 3.1 reviews works related to differentiated service for different types of networks but all based on differentiated distribution of resources. The other Sections debate each of the EONs aspects we deal with in our work. Section 3.2 presents works that intend to prevent spectrum fragmentation in EONs, while Section 3.3 revises work that decrease spectrum fragmentation after it already has occurred. To conclude, Section 3.4 presents works that try to reduce the unfairness level in EONs.

3.1 Differentiated service strategies based on constrained distribution of resources

In this Section we review works that promote differentiated service in various types of networks and are somehow related to the mechanism we propose in this thesis. Our proposed mechanism promotes differentiation of service by prioritizing resource assignment according to traffic type by reallocating resources from lower priority connections. Such resources preemption and constrained resources allocation strategies were originally developed for virtual circuit networks. In Subsection 3.1.1 we revise preemption strategies in Multi-Protocol Label Switching (MPLS) [?].

In Subsection 3.1.2 we explain two service differentiation strategies that we have proposed for WDM networks adapting procedures from MPLS networks to WDM networks. The studies we have performed with the mechanisms we proposed were the basis for the development of Priority Realloc.

Finally, in Section 3.1.3, we present a recovery scheme for EONs that rely on

different priority of service when implementing a policy of resources allocation.

3.1.1 Differentiated service strategies in MPLS networks

MPLS based on Internet Protocol (IP) networks are circuit switched networks where necessary resources are reserved before data transport begins. As such, preemption or differentiated distribution of resources policies may be implemented in MPLS networks in a similar fashion as in optical networks. Therefore the resources preemption and priority of service paradigm originally developed for MPLS networks is the same as the one adopted in optical networks, more specifically WSONs.

When differentiated service is implemented in MPLS networks, traffic is classified according to its priority over service. In a dynamic connection establishment scenario, the traffic pattern is not known in advance. When a connection request with higher priority arrives, the necessary resources to its establishment may be already assigned to other connections. In case there is not enough resources available to accommodate a higher priority connection, lower priority connections are preempted from their resources to avail resources to the incoming demand.

In order to determine which demands would have priority over resources and which connections would have its resources preempt to accommodate incoming connection requests, priority levels are determined by a set-up and a holding priority values [53]. A set-up value determines the priority of a connection request to use resources originally assigned to an active connection, while a holding priority value determines the priority of an active connection to maintain its originally assigned resources .

When lower holding priority value connections have their resources preempted they are either disrupted or re-allocated into alternative paths. To avoid continuous preemption and oscillations, a connection's holding priority should never be lower than its setup priority [54]. The priority service levels and the preemption strategy are proposed and described in [53] and in [55].

The constant connection disruption and reallocation promoted by preemption strategies may lead to network instability, due to excessive re-routing decisions, and excessive control message exchange [56]. Therefore works in [56], [57] and [58] propose preemption optimization strategies aiming at reducing network instability and control message exchange.

In [57] and [56] authors propose under-provisioning for lower priority connections. With under-provisioning only a partial amount of resources that would satisfy a higher priority demand would be preempted from lower priority connections. Another alternative is to block low priority connection requests in case network load reaches a previously determined threshold [58].

In MPLS architecture differentiated service may also be implemented via differentiated distribution of resources. In [53] connections are established with a given bandwidth limit and a bandwidth guarantee. The amount of bandwidth that can be reserved varies according to different service priority levels defined by a class-type (CT) and follows a bandwidth distribution constraint model.

Constraint models determine how a link's capacity will be shared between the different CT value connections. The capacity may be partitioned and reserved to each CT value as in Maximum Allocation Model (MAM) or shared among CT values as in the Russian Dolls Model (RDM) [59]. In the next Section we explain a differentiated service mechanism for WDM networks that relies on the RDM for the distribution of resources to different CT connections.

3.1.2 Differentiated service strategies for WSONs

Data transport networks based on optical communications are susceptible to several types of failure, as accidental or intentional fiber cuts, power outages, equipment defects and operational mistakes. Current optical network design comprises efficient recovery techniques to overcome possible failures and maintain service continuity [60].

In backbone WDM networks, most differentiated service strategies rely on link availability or resilience mechanisms. An availability-aware routing scheme examines different availability profiles of network links when performing routing and grooming decisions [61]. The availability profile of a link is determined by the amount of time the link is working without failure. When differentiated service is implemented, links with higher availability profile are assigned to higher priority connections.

The differentiated resilience service concerns the provisioning of different protection schemes to customers' paths such as dedicated path, shared path protection or restoration/no protection scheme [62] [63], a scheme providing higher resilience being applied on lighthpaths assigned to higher priority connections.

In [64] we have studied and analyzed the priority field described in [65] for the Path Computation Element (PCE) [66]. The PCE centralizes the route and resource assignment tasks in a network. When the priority field is enabled in the network the PCE will first compute lightpaths for higher priority requests and then to lower priority requests. In [64] we tested priority fields with values relating to the set up and holding priority values described by [53] and explained in Subsection 3.1.1. We observed, via network simulations results, that some priority field values tend to favor service to higher priority connections and other values tend to increase the total number of connections established. Chapter 4 fully explain this study.

The differentiated distribution of resources offline mechanism proposed in [67] and explained in Chapter 4, and the dynamic mechanism explained in Chapter 4 are based on the under-provisioning proposed in [57] and [56] and on the constrained distribution of resources described in [53]. However both mechanism are adapted to be implemented in WSONs. These works are fully described in Chapter 4.

3.1.3 Differentiated service strategies for EONs

EONs are still under research and development and thus differentiated service proposals for EONs are scarce. The only work found in the literature that proposes a differentiated service strategy for EONs is focused on recovery strategies. A temporary under provisioning is proposed in [68] as a recovery scheme for EONs. In the proposed strategy traffic is classified into mission critic and best-effort.

In case of a failure, the network capacity is decreased in the links affected by the failed element. In this case, best effort connections are switched to backup paths and have their bandwidth reduced to the client's required minimum amount, a committed rate. The spared resources are assigned to mission critic traffic. With this policy a higher number of connections survive a failure situation by sharing the same backup path. The network also manages to serve a higher number of requests than conventional restoration policies.

3.2 Fragmentation-aware RSA for EONs

The spectrum fragmentation problem is characteristic to EONs. It can decrease network performance by increasing demands blocking probability as discussed

in Chapter 2. For this reason many fragmentation-aware RSA algorithms are available in the literature. A fragmentation-aware RSA algorithm tries to decrease future spectrum fragmentation resulted by allocating results in an optimum manner.

Different approaches of fragmentation-aware RSA may be found in the literature, but most of them consider K shortest paths computed offline as explained in Chapter 2. Some solutions focus solely in path selection between the K shortest paths when dealing with spectrum fragmentation. This is the case of the algorithm proposals in [69] and [70] in which the algorithms select the route with lower spectrum fragmentation level according to the metric proposed in [19] and explained in Chapter 2. In [70], however, the algorithm also considers the modulation format most adequate for the selected route, achieving, with this step, better blocking probability results.

In a different proposal in [69] the algorithm selects the route that can accommodate a larger variety of bandwidth requirements. For instance, if a route has 5 available contiguous FSs that means this route may accommodate 5 different FSs requirements, 1, 2, 3, 4 and 5 FSs. Once a route is selected, in both algorithms, the contiguous available FSs are selected in a first-fit basis. Simulation results indicated that the proposed mechanisms presented better results regarding blocking probability when compared to algorithms where the selected route is either the shortest or the cheapest.

Since the spectrum fragmentation is a consequence of spectrum assignment, most algorithm proposals focus on the available FSs selection criteria. In Smallest Fit (SF) a connection is assigned a gap containing the minimum number of FSs available as long as the number of contiguous available FSs is at least the same as the number of required FSs [17], [19]. The SF policy aims on filling smaller gaps first consequently sparing larger gaps to other incoming connection requests.

In Exact Fit (EF), proposed in [19], a connection is assigned a gap with the exact amount of FSs as required if there is no gap with this characteristic, the largest sized gap is assigned. Results from analysis described in [19] indicate that the EF policy promoted better results regarding blocking probability when compared to SF, having a higher effect on performance increase over First Fit algorithm (refer to Chapter 2). Figure 3.1 illustrates SF and EF resources allocation criteria.

In [35] authors propose a RSA algorithm called shortest path with maximum number of free frequency slot units (SPMFF). The proposed algorithm considers

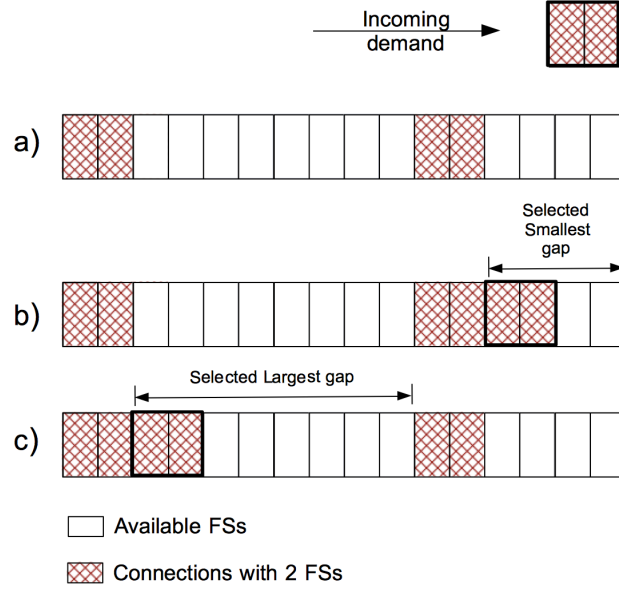


Figure 3.1: The diagram shows a) link state, b) connection accommodation following SF and c) connection accommodation following EF

the ordered shortest path from K-shortest paths and searches for a gap with maximum number of contiguous available FSs that can accommodate the demand resources requirement. Simulation results indicate that SPMFF resulted in lower blocking probability than First Fit when greater values of offered traffic loads are considered.

Spectrum fragmentation in EONs is primarily affected by the diversity of bandwidth sharing the same spectrum range, as discussed in Chapter 2. Authors in [71] propose algorithms where the spectrum is partitioned to accommodate connections according to their bandwidth requirement. In this way each part of the spectrum is reserved to connections with same bandwidth. In fact the proposed algorithm also tends to decreased service fairness issue as discussed in Chapter 2. Other works intending to tackle the fairness issue are presented in Section 3.4.

In the algorithm called Complete Sharing (CS) [71] connections are assigned FSs in a first fit basis and therefore connections with diverse bandwidth assignment share the same spectrum range; there is no spectrum partition. In this scenario smaller bandwidth requirement compete for resources with connections with higher bandwidth requirement. This algorithm is used as a baseline to access partitioning algorithms performance.

In the algorithm called Pseudo-Partition (PP) [71] higher bandwidth connections and lower bandwidth connections are bifurcated to the two ends of the spectrum. Connections with higher bandwidth requirements are assigned

spectrum in a first-fit basis while connections with lower bandwidth requirements are assigned spectrum in a last-fit basis. This solution is very straight-forward but if there are more than two values of bandwidth requirements in the network, connections with different bandwidth requirements will eventually share the same spectrum range even though the sharing is minimized. A statistical demarcation is necessary to determine which bandwidth value connections should be allocated to one end of the spectrum and which bandwidth value connections should be allocated to the other end.

In the solution called Dedicated Partition (DP) [71] the spectrum's partitions are dedicated to each bandwidth connections. In this solution each spectrum partition accommodates connections with same bandwidth, and spectrum fragmentation caused by mismatch of different bandwidths is eliminated. An optimized partition should be calculated based on information of traffic characteristic of each group of bandwidth requirement intensity arrivals. Authors propose a linear optimization solution to achieve the best result regarding the spectrum partition.

In Shared Partition (SP) [71] the authors propose a solution as a hybrid between shared and dedicated partition. In this algorithm, each spectrum partition can be either uniquely reserved to one bandwidth value or shared among a set of different bandwidth values. Since higher bandwidth connections suffer more blocking probability they have larger shares of the spectrum reserved to them. Lower bandwidth connections share their partition with other connections bandwidths and their reserved partition is smaller. DP and SP algorithms are depicted in Figure 3.2.

In [71] results from network simulations indicate that any of the algorithms proposing a spectrum partition presented better results regarding bandwidth blocking probability than CS. Bandwidth blocking probability accounts for the ratio of blocked bandwidth to the served bandwidth. DP and SP offered best bandwidth blocking probability than PP.

Authors in [72], propose a RSA algorithm where traffic is classified according to the number of FSs required. Each class of demand has a respective position in the network link's spectrum. When a demand arrives the algorithm will try to accommodate it in a gap of contiguous available FSs closer to its class position in the spectrum. The aim of this algorithm is to group connections with same number of assigned FSs to approximate location in the spectrum, thus reducing spectrum fragmentation negative impact.

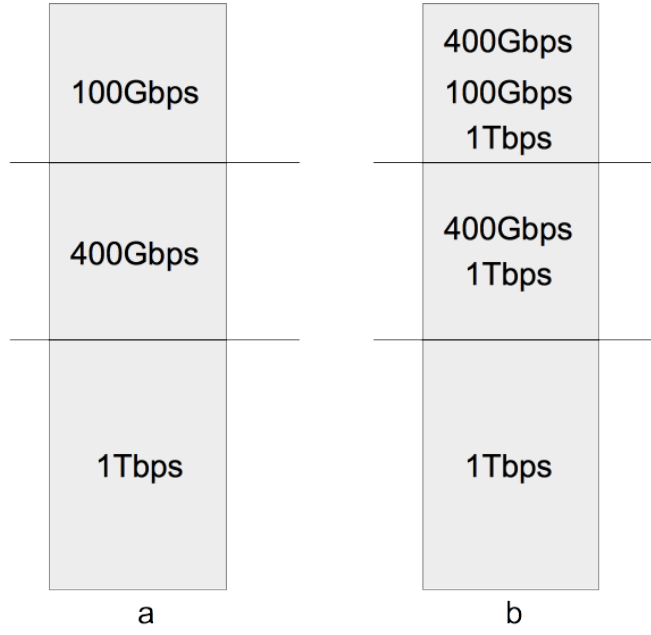


Figure 3.2: The diagram shows a) Dedicated Partition (DP) and b) Shared Partition (SP) [3]

A similar alternative is to reserve groups of FSs to each source-destination pair connections [73]. In this proposal a given number of contiguous FSs, named sub-carriers, are reserved while others are used for best effort traffic or when a connection requires extra bandwidth. With this reservation scheme, links present in the same route have the same band of spectrum assigned or released tending to decrease the horizontal fragmentation, explained in Chapter 2. To calculate the number of FSs to be reserved to a source destination node pair, the authors formulated a function of the average rate required, an upper bound bandwidth value, a burst value and the number of hops of the shortest path between source and destination nodes. The mechanism is simulated for different numbers of FSs reserved and it was observed that as the rate required grows the higher number of reserved FSs had a higher impact on the blocking probability decrease. The drawback of this strategy is that in case there are many pairs of sources-destination nodes, and the reservation of spectrum is exclusive, there might not be enough spectrum band to properly serve each of the source-destination pair connections resulting in an increased blocking probability.

In [3] authors present RSA solutions for a multi-fiber network scenario. They propose three RSA algorithms, the third of them effectively aiming at minimizing spectrum fragmentation. In Ahead Fiber First Fit Assignment (AFFF), there is no fragmentation awareness as in fact the selection of fiber and contiguous available FSs follow a first-fit policy, this algorithm serves as a benchmark for performance comparisons. In Minimum Spectrum First Fit

Assignment (MSFF) in each fiber link the first group of available sufficient FSs are computed. Among the considered group of available contiguous FSs the algorithm selects the FS group whose starting frequency is the lowest and its respective fiber. In Bandwidth based First Fit Assignment (BFF) spectrum use optimization is considered and each fiber has a bandwidth range and spectrum allocation are prioritized for the fiber which bandwidth corresponds to the request's requirement. The resulting resources allocation for a connection request served according to each of the three proposed algorithm is depicted in Fig. 3.3. As expected, when comparing the performance of the three proposed algorithms, BFF presented best blocking probability.

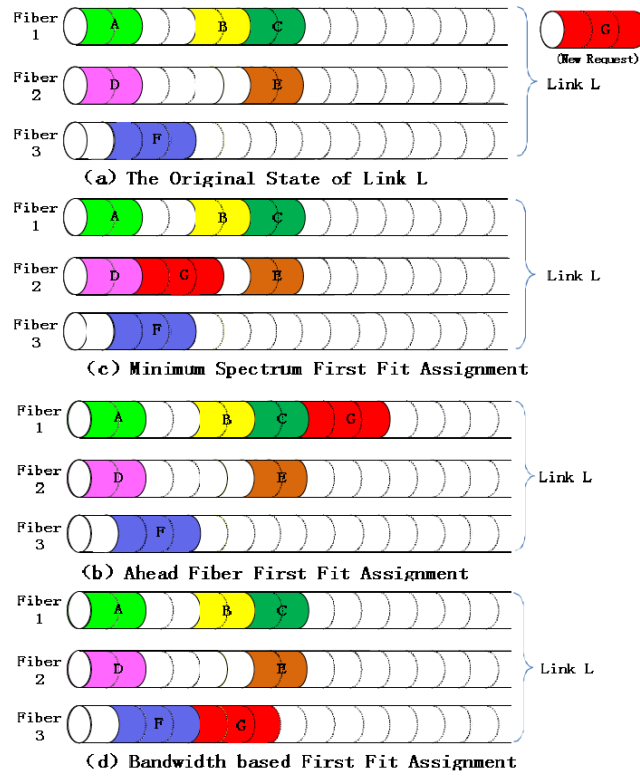


Figure 3.3: Multi-fiber algorithm proposals [3]

The available FSs in a path result from the intersection of available FSs in all links belonging to that path. In [4] authors propose a spectrum assignment policy in which the impact of selecting an FS on individual links in the path is considered in the spectrum assignment decision. Their algorithm analyses if the candidate FS would disrupt a group of contiguous available FSs in all links belonging to the candidate path. Their proposal also considers if selecting a given FS would result in a new misalignment or correct an existing misalignment in neighboring links that do not belong to the candidate path. Their proposal aims at mitigating both horizontal and vertical fragmentation. Figure 3.4, extracted from [4], illustrates the algorithm decision policy.

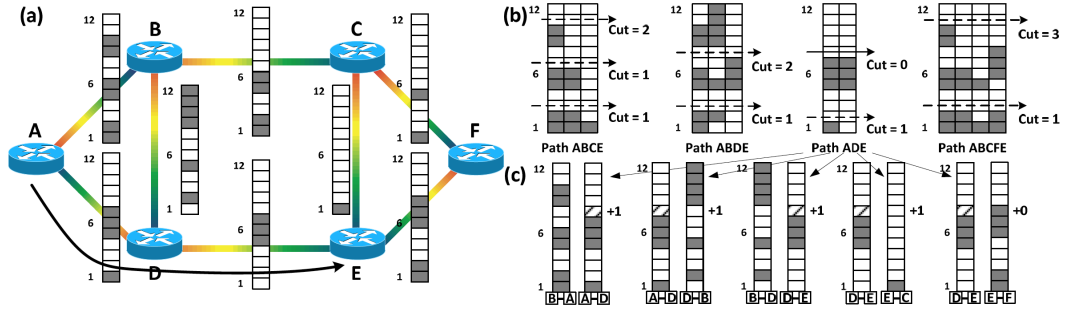


Figure 3.4: Example FISH network and the spectral assignment status on the links, (b) number of cuts to all the candidate solution to connection request A-E, and (c) alignment factor increase if choosing path ADE with slot 8 [4]

3.3 Defragmentation techniques

Even with the implementation of a fragmentation-aware RSA algorithm, the spectrum fragmentation is likely to occur. Defragmentation techniques focus on eliminating or decreasing the number of gaps already present in the network link spectrum. Defragmentation techniques are also known as reactive fragmentation-aware RSA algorithms, since they try to improve the network condition after spectrum fragmentation has already taken place. Various defragmentation techniques proposals are found in the literature. Most defragmentation solutions proposed are based on connection disruption and reallocation of resources into a new position on the spectrum grid. Figure 3.5 illustrates a defragmentation mechanism operation principle in a spectrum fragmented link.

The defragmentation mechanism may be periodic or path-triggered [74]. A periodic defragmentation is initiated either at pre-determined time intervals, or when the network wide spectrum fragmentation level have reached a pre-established threshold. The periodic defragmentation strategy intends to decrease the spectral fragmentation across all links in the network. It may disrupt many connections and is computationally expensive.

A path-triggered defragmentation is invoked when a connection request is blocked. When triggered, this defragmentation technique will only disrupt connections that share a link with the incoming demand's selected route. Therefore, path-triggered defragmentation will disrupt a fewer connections and may be implemented requiring less computational tasks.

The periodic defragmentation technique proposed in [75] intends to rearrange active connections in order to minimize the spectrum required to accommodate these connections and, hence, sparing spectrum for future connections. While

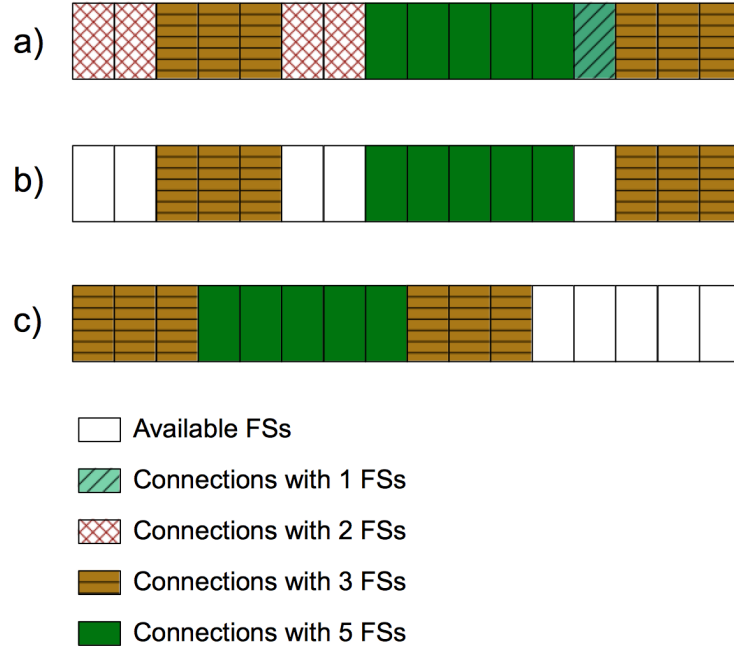


Figure 3.5: The diagram shows a) original link state before connections termination, b) spectrum fragmented link after connections termination and c) link state after defragmentation

achieving its objective, the problem, formulated as an integer linear program (ILP), tries to minimize the number of interrupted connections.

In the path-triggered defragmentation proposed in [74] when a demand is blocked the algorithm searches for a shortest route with sufficient available FSs whether contiguous or not. If such a route is found, the algorithm tries to create a group of contiguous available FSs to accommodate the demand. To this end, connections accommodated in links in common to the selected path will be reallocated to a different spectrum band in order to decrease fragmentation in such a way that the incoming request may be accommodated.

In [76] authors propose a defragmentation strategy where, whenever a connection is blocked, the algorithm tries to identify a group of FSs that could accommodate the demand by decreasing the number of active connections that would be disrupted. Then, the algorithm tries to find a new spectrum band that would accommodate all disrupted connections. If not found the demand is blocked and a new group of FSs is inspected.

Some authors propose non-disruptive defragmentation techniques relying on lightpath re-tuning and reconfiguration of allocated spectrum. In the defragmentation technique proposed in [21] as a connection is terminated, active connections that share a link with the terminated connection are shifted, whenever possible, to the lower end of the spectrum leaving a higher number

of contiguous available FSs at the higher end of the spectrum. This strategy promotes decreasing fragmentation level before demand blocking occurs. Because active connections are shifted via re-tuning, no connections are actually disrupted.

3.4 Fairness issue in EONs

As discussed in Chapter 2, service fairness issue regarding higher bandwidth requirement demands is a serious problem in EONs. As confirmed in [7] and [71] higher rate demands tend to be blocked much more often than lower rate demands. The level of unfairness across the various demand sizes may not always be acceptable by network operators demanding certain QoS requirements. Still, works studying and/or proposing solutions for service unfairness are very uncommon in the literature. In fact, after a literature review we have only found two articles that regard the service fairness problem. Indeed authors in [7] comment on the fact that the RSA algorithm articles they reviewed do not address this issue.

Some fragmentation-aware algorithms available in the literature may indirectly reduce unfairness. These algorithms, however, are not as effective in increasing service fairness as algorithms that focus on this purpose as analyzed in [7].

Authors in [7] and [71] propose spectrum partitioning and reservation as a means to increase service fairness in EONs. The algorithm proposed in [71] is described in Section 3.2. Simulations performance results in [71] indicate that DP have promoted the better level of fairness and decreased bandwidth blocking probability when compared to CS. SP presented lower level of fairness than DP but lower BBP than DP.

In [7] the authors propose a mechanism to promote fairness in EONs. Their proposal is developed to work in two rate EONs. Similar to SP algorithm in [71], the algorithm called Two Rate Reservation (TRR) partitions the spectrum for both dedicated and shared use. One spectrum range is reserved for the lowest bandwidth requirement connections, a second partition is reserved to serve only the highest BW requirement connections and a third spectrum may accommodate any of the two possible BW requirement demands. Each partition must have a previously calculated number of dedicated FSs.

When the shared partition has 0 FSs the TRR algorithm is referred to as Fixed RSA algorithm, where each group of demands is reserved a dedicated spectrum

band as in DP proposed by [71]. Demands with distinct rates may not share the same partition. In both algorithms proposed, first fit is implemented as spectrum allocation policy, and connections with a given BW requirement are accommodated from the left of the left border of their respective partitions.

Simulation performance results indicated that Fixed RSA algorithm provided a highest fairness level in detriment of highest blocking probability results when compared to TRR. TRR, on the other hand, presented higher fairness level when compared to the benchmark algorithms selected by the authors. However, TRR presented higher BP results than the benchmark algorithms.

The advantage of the work in [71] over [7], is that in [71] authors explain the optimum partitions size calculation, which is based on statistical data about each demand BW requirement arrival frequency and probability. In [71], the authors propose a solution for a three rate network. Authors present performance results based on the bandwidth blocking probability and do not do so on demands blocking probability results.

In general, dedicated spectrum partition and reservation solutions tend to increase the blocking probability of demands in the network. Thereupon, both [7] and [71] propose a spectrum band to be shared by all types of connections. This intermediate strategy provides better blocking probability results when compared to dedicated partitioning strategies.

4 Precedent contributions

Before developing the Priority Realloc mechanism for EONs, we have developed other studies and proposals for differentiated services on optical networks. We have previously focused on WDM networks and to this end we have studied current available priority of service strategy alternatives and developed a mechanism that promotes differentiation of resources distribution according to different classes of service. This differentiated resources allocation follows a constraint model that determines the maximum bandwidth a given CT value connection may be assigned and/or the amount of resources that would be reallocated to a higher priority demand. Part of this work has been published in a conference paper, while other remains unpublished.

Besides the contribution of this previous work to the research area of optical networks, this work have also inspired the creation and development of Priority Realloc. For these reasons, in this chapter, we present the study we have developed on priority of service on WDM networks and explain the differentiated service mechanism we have proposed for WDM networks.

The study and analysis on differentiated priority of service for WDM networks is presented in Section 4.1. We developed a differentiated resources distribution mechanism for WDM networks to be implemented in an offline scenario (explained in Section 4.2) and another version of the mechanism that operates in a dynamic scenario (explained in Section 4.3.1). Both versions of the mechanism rely on the RDM, previously cited in Chapter 2, as bandwidth constraint model. The adaptation of the original RDM into the proposed mechanism is explained in Section 4.2.

4.1 Priority of connection request processing

We have studied the available differentiated service in MPLS networks, with routing performed by the PCE [66], so we could propose a similar strategy for WDM networks. Since WDM networks may be controlled by Generalized

Table 4.1: BW requested and BW assigned following BC model

Priority field equals to	Description
Setup	The same value as the demand's set-up priority
Hold	The same value as the demand's holding priority
Average	The same value as the average of the demand's holding and setup priority values
Difference	The same value as the difference between the demand's holding and setup priority values

Multi-Protocol Label Switching (GMPLS) protocol suite [77] in tandem with the PCE, an adaptation of strategy is possible.

We have analyzed the priority field described in [65] for the PCE with different values. The PCE centralizes the route and resource assignment tasks in a network. In order for the PCE architecture to properly accommodate the differentiated service characteristics of MPLS [78] it must follow some requirements when computing a path.

In the PCE architecture, a path computation request (PCReq) message contains the requisites for the constrained based path computation [79]. The Request Parameters Object (RP) contains a Priority field (Pri field) with possible values which may be used by the PCE scheduler to determine in what order among many requests that specific request would be processed. Therefore the higher the Priority value of a demand more likely it will be processed before other requests.

The Label Switched Path Attributes (LSPA) Object contains required attributes for the establishment of a lightpath [79]. It contains, among other requirements, the setup and holding priority attributes of the requested path. This requirement is not necessarily considered by a PCE but, when it is considered, a connection request with higher setup priority may preempt a current connection with lower holding priority value to use its resources.

We extended the aforementioned concepts to a WDM network and tested the impact on network performance when Priority fields have different values relating to the setup and holding priority values.

4.1.1 Results and analysis

We implemented WDM network simulations as described in [64], where we tested different values for the Priority field as described in Table 4.1.

Network simulation results indicate that when the Priority field value equals the difference between the demand's setup and holding priority values the network blocking probability results are lower than the results achieved when the Priority field has the other tested values. However this Priority field value also presented the highest number of repeated connection request messages. A repeated connection request message refers to a request from a connection that was previously preempted.

Results also indicate that respecting the Priority field values, when ordering connection requests, increases the volume of resources assigned to demands with higher setup priority values. In this case the actual value of the priority field has little impact on the amount of resources assigned, even though when the value is equal to the demand's holding priority value more bandwidth were allocated to lower setup priority value connections in detriment of the highest setup priority value connections.

In general, it is possible to conclude that the combined use of preemption policies and the Priority field value equivalent to the difference between the demand's setup and the holding priority values is the most beneficial set of values in terms of performance. Once a preemption policy is implemented the demands priority field has direct impact on the WDM network performance.

4.2 Proposed RDM mechanism

In order to promote differentiated services in WDM networks, we proposed a resources differentiated distribution of resources and to this aim we developed a mechanism that adopts a bandwidth distribution constraint model. The bandwidth distribution constraint model we propose is adapted from the RDM, previously mentioned in Chapter 2, which was proven, among the available constraint models, to best adapt to the differentiated service bandwidth allocation policy by achieving high link utilization and guaranteeing quality of service to the various priority classes [80]. In the RDM, described in [59], a channels maximum capacity is shared by diverse CT values connections following a resources distribution constrained delineated by the model.

The WDM network considered implements a grooming technique as explained in Chapter 2, and therefore more than one connection may share a wavelength's full capacity. Thus, in a WDM link with many channels, the maximum capacity regarded by the RDM is a wavelength's maximum capacity. The constraint model

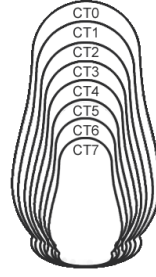


Figure 4.1: The Russian Dolls Model

is also used as a grooming policy to help determining which connections would share a channel's resource.

In the RDM a channel's maximum capacity is shared between connections with different CT values. Each connection's assigned resources follow an allowed bandwidth constraint (BC) usage determined by the accumulation of successive CTs and respective BCs. For example, CT7 may use resources up to the BC7 limit, while CT6 shares its BC6 constraint with CT7, CT5 shares its BC5 constraint with CT6 and CT7 and so on, as illustrated by Figure 4.1. In summary, a lower priority traffic may use the bandwidth reserved to a higher priority class, in case it is not in use, up to its own BC value, while a higher priority connection can preempt part of a lower priority connection's allocated bandwidth up to its own BC value [59].

Each CT's BC value is determined by network management taking into account SLA details. The BC values must be carefully selected as they determine the level of privilege over resources that higher priority connections will have. For instance, a situation in which connections with different CT values share the same channel's resource, and the difference between the BC values is a constant, connections with different CT values may be assigned the same amount of resources. This situation is illustrated in Figure 4.2. Consider, for example, a WDM network in which channels' capacity is 10 Gbps and BC values equals 10 subtracted the CT value in Gbps, so the difference between constantly BC values is always 1 Gbps. In a situation where a channel contains all CT values as 7 connections, each of which had resources requirements higher than 1 Gbps, each connection but CT7 connection will be assigned 1 Gbps. In such a scenario the only connection that would have differentiated service is connection with CT7 whilst all other connections would have no priority of resource use compared to one another as depicted in Table 4.2. However, if the difference between BC values increases as the CT value increases higher priority connections would be guaranteed more resources than lower priority ones as can be observed in Figure

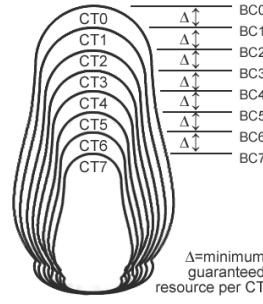


Figure 4.2: RDM with constant difference between BC values

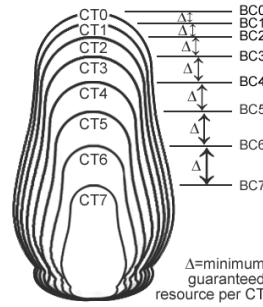


Figure 4.3: RDM with increasing difference between BC values

Table 4.2: BW requested and BW assigned following BC model

CT	BC	BW Required	BW Assigned
CT0	10 Gbps	3 Gbps	1 Gbps
CT1	9 Gbps	3 Gbps	1 Gbps
CT2	8 Gbps	3 Gbps	1 Gbps
CT3	7 Gbps	3 Gbps	1 Gbps
CT4	6 Gbps	3 Gbps	1 Gbps
CT5	5 Gbps	3 Gbps	1 Gbps
CT6	4 Gbps	3 Gbps	1 Gbps
CT7	3 Gbps	3 Gbps	3 Gbps

4.3.

The RDM is a resources distribution model. Throughout this chapter, however, we will refer to the RDM mechanism as our proposed mechanism that implements a similar version of this resources distribution model when performing the RWA algorithm.

We have implemented and tested the RDM mechanism in offline and dynamic WDM network scenarios and assessed the performance of the mechanism when compared to benchmark algorithms. In the following section we describe the RDM mechanism when implemented in an offline WDM network scenario.

4.3 Offline differentiated service for WDM networks

In order to implement an initial analysis on the RDM mechanism performance the proposed RDM mechanism is implemented in an offline scenario where the demand matrix is known in advance and resources are allocated in a planning phase [67]. The problem is formulated as a mixed integer linear programming (MILP) problem.

In the MILP problem an integer variable determines the amount of bandwidth assigned to a demand. D is the total number of demands at a given interval of time, index d . C is the total number of Class-Types (8 real Class-Types and one dummy), index c . p is the benefit of serving a demand of class c . b_c is the maximum reserved bandwidth of class c , b_d equals the bandwidth requirement by demand d . $b_c, c=1$ is the maximum capacity of the path. a_{dc} is 1 if demand d belongs to Class-Type c , and 0 otherwise. y_d is an integer variable that defines the amount of bandwidth to be assigned to a given demand. The MILP objective function is given by Equation 4.1, which is subject to Equations 4.2, 4.3, 4.4 and 4.5.

$$\text{Maximize } Z = \sum_d^D \sum_c^C a_{dc} \times p_d \times y_d \quad (4.1)$$

$$\sum_d^D y_d \times a_{dc} \leq b_c - \sum_c^C \sum_d^D y_d \times a_{dc+1}; \forall c \in C \quad (4.2)$$

$$\sum_d^D y_d \leq b_c; c = 1 \quad (4.3)$$

$$y_d \leq b_d; \forall d \in D \quad (4.4)$$

$$a_{dc} = [0, 1]; d, c, w, y_d \geq 0, \in \mathbb{Z}; b_d, b_c \in \mathbb{R} \quad (4.5)$$

The aim of the model is to maximize the bandwidth assigned to higher values CT demands, which objective function is described by Equation 4.1. The RDM for bandwidth constrain for each CT is defined by Equation 4.2, it guarantees that the allocated bandwidth for demand d belonging to class c is smaller than the maximum reserved bandwidth for that class minus the total used bandwidth

Table 4.3: BC values per CT values for the two tested scenarios

Scenario	CT0	CT1	CT2	CT3	CT4	CT5	CT6	CT7
RDM 1	200	190	178	164	146	126	106	82
RDM 2	200	188	176	164	152	140	128	116

of demands belonging to higher classes. In case of CT is 7 ($c=8$), its bandwidth use will be its bandwidth reservation limit because we stipulate a dummy class $c=9$ which requires no bandwidth. The total capacity of the path constrain is stipulated by Equation 4.3. Equations 4.4 guarantees that the amount of resources assigned to a demand d is not greater than the demand's requirement.

4.3.1 Results and analysis

As benchmark we consider a condition in which the MPLS preemption strategy explained in Chapter 3 is implemented in WDM networks. This condition is also formulated as a MILP problem and is denominated control model. In the control model setup and holding priority objects are the same and equivalent to the CT values. We assume that, in both control model and RDM mechanism, a connection may be established with less assigned bandwidth than originally requested.

We solved both control model and the proposed RDM mechanism on IBM CPLEX version 12.2. The offline network scenario we consider comprises 40 connection requests with uniformly distributed CT vales and bandwidth requirements between 5 Gbps and 49 Gbps. In this initial analysis we consider a fictitious condition with only one optical channel with a maximum capacity of 200 Gbps.

Simulations were held for two different scenarios each of which containing a different set of BC values as described in Table 4.3. In scenario RDM 1, the BC value for CT7 was smaller than in scenario RDM 2, so the highest priority class was less protected than in scenario RDM 2. However in RDM 1 the difference between the BC value from one CT value to the immediate subsequent CT value increases as the CT value increases, while in RDM 2 this difference remains constant. For instance, in RDM 1 the difference between BC for CT0 and BC for CT1 is 10 Gbps while the difference between BC for CT6 and BC for CT7 is 24 Gbps, in RDM 2 the difference is always 12.

Simulations results regarding number of connections established is depicted

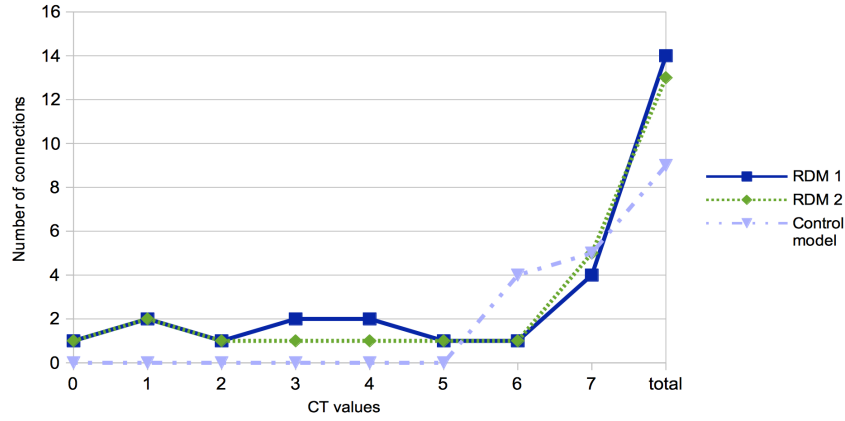


Figure 4.4: Number of connections established per CT values and total

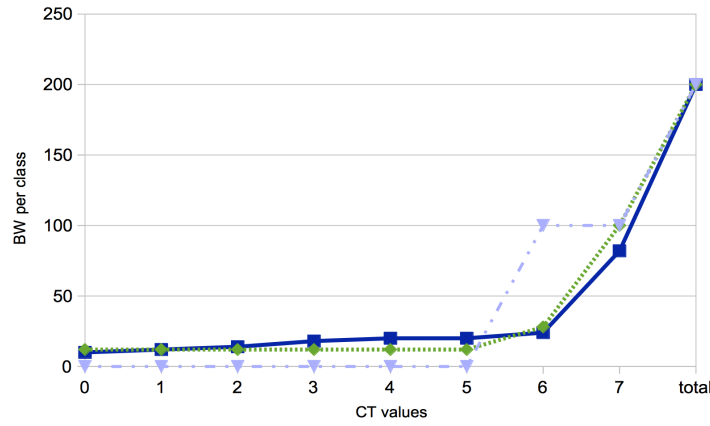


Figure 4.5: Amount of bandwidth assigned per CT values and total

in Figure 4.4. It is possible to observe that, in the scenarios where the RDM mechanism were implemented, at least one demand is served for each CT value, even though the resources assigned were less than the originally required value, while in the control model lowest priority demands are not served at all. It is also possible to note that the different CT values connections are more or less prioritized according to the sets of BC values adopted, for instance CT7 connections were assigned a larger amount of resources in scenario RDM 2 than in scenario RDM 1 where a higher amount of resources was distributed to lower priority connections.

In general the total number of demands assigned a connection is higher for when the RDM mechanism is implemented than in the control model, proving a fairer distribution of network resources. Furthermore, we believe that, by implementing the RDM mechanism, service providers have higher flexibility when planning service offer according to traffic priority levels.

The RDM mechanism performance analysis on the static network scenario have prompted us to enhance the mechanism to be implemented in a dynamic

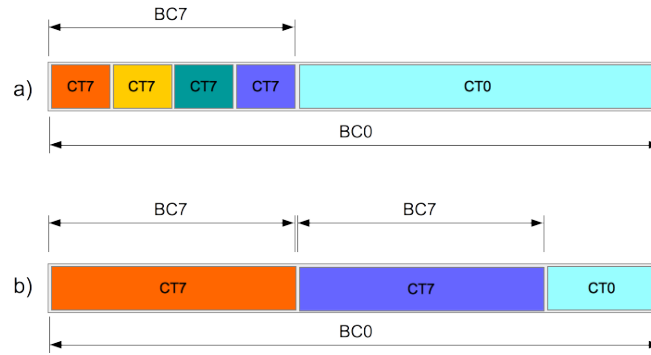


Figure 4.6: Variations on RDM bandwidth constraint use. a) depicts original RDM where a BC value is shared among all connections with same CT. b) depicts adapted RDM where each connection is assigned resources up to its own BC value.

scenario. The next section presents the RDM mechanism we propose for the dynamic scenario of a WDM network.

4.4 Dynamic differentiated service for WDM networks

When adapting the RDM mechanism for a WDM network dynamic scenario, the RDM model is not only used to determine how the various connections are going to share a wavelength's bandwidth in WDM network with grooming technology, but also the BC model is used to determine the amount of resources that are supposed to be preempted in order to accommodate a higher priority demand. The preemption occurs only when there is contention for resources. In the dynamic scenario, the mechanism is developed to perform a RWA algorithm determining resources allocation for incoming connection requests following the RDM model adopted.

In the original RDM a BC value is shared among all connections with same CT. Therefore, all connections in the same channel with same CT value share the same BC value of resources. If a channel has a large number of higher CT value connections and few lower CT value connections, the higher CT connections could be assigned less resources than the lower priority connections as can be observed in Figure 4.6a. In our proposed mechanism, each connection is assigned resources up to its own BC value, that may be shared only with higher CT connections as can be observed in Figure 4.6b.

Two versions of the mechanism can be implemented. One of the versions aims at fairness of resources distribution at the cost of higher computational complexity. In this option when a higher priority demand is assigned to a channel

and needs to use resources from lower priority connections, connections with same lower CT value would have equal amount of resources preempted. Similarly, when a higher priority connection is torn down, the resources released should be equally distributed to lower priority connections with same CT value. The other version is less computationally complex but does not treat same CT connections equally. In this version resources preemption is performed in a first fit basis and, to prevent excessive connection disruption and resource re-assignment, when a higher priority connection is torn down its resources are not re-assigned to lower priority connections. At this stage of the study we decided to implement the first fit version so that comparative results would be rapidly obtained.

4.4.1 Proposed algorithm

We propose two algorithm variations for the RDM, called RDM-full and RDM-less. In RDM-full, the bandwidth constraint limits the amount of resources assigned to a given class at all times. In this case, even if there is no contention for resources, whenever a demand arrives, the algorithm limits its resources assignment to the maximum amount allowed by its BC constraint. For instance, if a demand that has a BC value of 8 Gbps requires 10 Gbps, the algorithm will limit the bandwidth assignment to 8 Gbps, if, on the other hand, a demand with same BC value requires 6 Gbps, this bandwidth requirement is below its BC value, and the algorithm will assign the full 6 Gbps requirement.

In RDM-less the constraint is only enforced when the traffic load is greater than the system's capacity. In this scenario there is contention for resources and preemption of resources is necessary to accommodate incoming connection requests. In order to calculate the necessary amount of resources to be preempted the RDM mechanism is initiated and only at this moment the demands' bandwidth assignment is limited to its BC value. For instance, in a scenario in which RDM-less is implemented, if the network is working with light load and there is enough available resources to serve any demand requirements, there is no limitation on assignment or preemption of resources, and a demand with bandwidth requirement of 10 Gbps is assigned 10 Gbps. However if there are not enough resources available in the network, the demand's bandwidth requirement is limited to its BC value, for instance 8 Gbps, the RDM-less algorithm is activated in order to select connections and resources to be preempted and allocated to higher priority incoming demands.

Figure 4.7 illustrates two RWA dynamic scenarios implementing: grooming without policy mechanism, RDM-full and RDM-less algorithms. The CTs

bandwidth constraints and the channel's total capacity are depicted on the left side of the figure. Figure 4.7a) illustrates the resulting resources allocation to demands with different CT values according to the different mechanisms in a network scenario in which the third demand to arrive has a lower CT value than the CT values of the active connections. Preemption may not be performed, and therefore demand with CT3 is blocked by all mechanisms. However in both scenarios in which RDM-less and grooming are implemented, demands 1 and 2 are assigned their original resources requirements, whilst in RDM-full the bandwidth constraint is imposed at all times and demand 1 is assigned only its BC limit. The RDM-full algorithm limits the amount of resources assigned to the highest connection and the amount of resources left unused in the channel is larger than in grooming and in RDM-less scenarios. In the long run, the RDM-full tends to increase the number of connections with higher CT values and depending on the charging policy of a service provider it may be economically interesting to implement this algorithm version as can be observed in an economical analysis presented in Appendix A.

In both algorithms connections with different CT only share BC values when preemption is being performed. Consequently, when there is contention for resources, the RDM mechanism calculates whether there is enough resources from lower priority connections in order to, according the BC values, preempt part of the resources to accommodate a higher priority connection request. Figure 4.7b) presents a scenario in which there is contention for resources and the last demand to arrive has the highest CT value. In this case since the active connections have lower CT values preemption can be performed and the RDM mechanism is triggered in order to calculate the amount of resources to be reallocated to the incoming demand. In both RDM-full and RDM-less algorithms the bandwidth to be assigned to demand 1 is limited to its BC value, connection 3 has resources preempted to its minimum amount guaranteed by the model and the rest of resources required are preempted from connection with CT value 2, while by the grooming without policy mechanism the demand is blocked. It is possible to observe that in a dynamic RWA scenario the order in which demands arrive impacts the resources allocation.

In case the BC constraint is taken into account the demand's bandwidth requirement becomes the smallest value between its original value and the BC constraint.

Having established the resources amount to be assigned the algorithm selects the first route from the 3 alternative fixed possible routes. Then it searches, in first

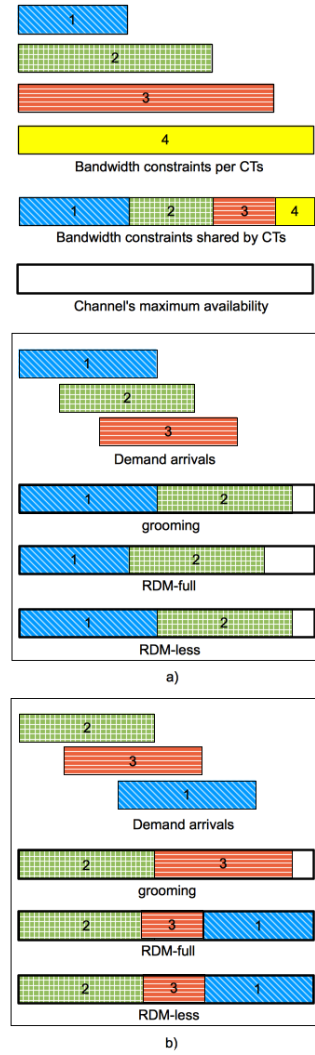


Figure 4.7: Connections and/or demands are represented by rectangles. The bandwidth required or assigned is represented by the rectangles lengths, the number in the rectangles represent both the demand's id and its CT value, being 1 the highest priority and 4 the lowest priority. Demands arrive in the order illustrated being the first the one from the far left and the last the one from the far right in the demand arrivals figures a) and b). In a) the last demand to arrive has a low CT value. In b) the last demand to arrive has the highest CT value.

fit order, a wavelength used by a connection established along the same route, so grooming may be performed on this lightpath. In case such a wavelength is found, the algorithm checks whether the lightpath's available resources are enough to accommodate the current demand. In case they are, the demand is assigned as a new connection to the lightpath. In case there is not enough resources available, the wavelength's *id* is recorded in case the RDM mechanism needs to be triggered later. If, however, a wavelength containing a connection using the selected route is not found, the algorithm searches, in first fit order, a not used wavelength in the selected route. If the process is not successful the tasks described above are consecutively performed for 2nd best and then 3rd best routes.

If a connection cannot be established after the previous steps, but a lightpath

containing a connection using the same route was found, then the RDM mechanism is triggered. When the option adopted is RDM-less the bandwidth constraint is enforced on the demand's BW requirement, whilst in RDM-full the algorithm will try to assign the amount of resources required. By accessing the information outputted from the grooming process the RDM algorithm already knows what lightpath contains a connection with same source destination node pair as the demand. It searches, in the selected lightpath, connections with the lowest possible priority value and calculates the amount of resources that can be preempted from the analysed connections. In case the resulting re-usable resource is not enough the procedure is repeated for all connections with the same lower CT value. This process is repeated for the consecutive CT values as long as their CT value is neither equal nor higher than the demand's and until the demand's BW requirement is met by the sum of all preemptable resources. The calculation of preemptable resources can be observed in the algorithm presented by Algorithm 1.

If after checking all the lightpath's connections the resulting total amount of resources that can be preempted is not enough to satisfy the demand request then the demand is blocked. Conversely, if enough resources are found, the lightpath is selected and, when assigned with the suggested reduced bandwidth, all channels active connections are updated.

4.4.2 Algorithm's complexity

We denote by p the demand's CT value, c is the total number of connections in the selected lightpath, and x is the CT value of the connection being analysed.

To calculate the amount of resources that can be reallocated the algorithm needs to find connections belonging to lower CT values. The algorithm starts searching connections with the lowest CT value. The search is iterated for all the consecutive increasing CT values as long as the necessary amount of resources to be reallocated is not met and the CT value being searched for is smaller than the demand's CT value. This step is described in Line 2 of algorithm 1 shown in Fig 1. In the worst case scenario, the algorithm needs to search all CT values that are lower than the demand's CT value, therefore the analysis of connections in the lightpath is repeated $p-1$ times.

Each time the algorithm searches for a connection with a specific CT value, it assesses the connections in the lightpath. This step is described in Line 3 of algorithm 1 depicted in Fig 1. In the worst case scenario the necessary amount of

Algorithm 1 RDM-less mechanism**Input:** *lightpath*, *demand*

```

1: thereIsRoute = false
2: resourceRequested = minimum between (demand's request ,
   demand's BC value)
3: total resource acquired = wavelength's resource available
4: i ← 0
5: j ← 1
6: while i < demand's CT do
7:   for each connection ∈ lightpath do
8:     if connection's CT == i then
9:       selectedConnection = connection
10:    while j ≤ demand's CT -
       selectedConnection's CT do
11:      for each connection ∈ lightpath do
12:        if connection's CT ==
           selectedConnection's CT + j then
13:          nextHigherBC = connection's BC
           selectedConnection's minimum BW
           guaranteed = (selectedConnection's BC -
              nextHigherBC)
14:          if selectedConnection's minimum BW
             guaranteed > 0 then
15:            selectedConnection's recyclable =
              (selectedConnection's BW assigned
              - selectedConnection's minimum BW guaranteed)
              total resources acquired = total resources acquired +
              (selectedConnection's recyclable)
16:            if total resources acquired ≥ Resources
              to be assigned then
17:              thereIsRoute's = true
              update wavelength and connections ∈
              wavelength.demandsAssigned;
18:            end if
19:          end if
20:        end if
21:      end for
22:      j ++
23:    end while
24:  end if
25: end for
26: i ++
27: end while

```

Output: *lightpath*, Resource to be assigned, *demand*

resources is not found until all connections in the lightpath have been analysed. In this case the number of iterations is equal to c .

When a connection belonging to the selected CT value is found on the lightpath the next CT value connection must be found. The first CT value to be searched is the selected connection's CT value + 1. If the necessary resources are not found this step is repeated until the analyzed CT value is equal to the demand's CT value as can be observed in Line 6 of algorithm 1 depicted in Fig 1. In the worst case scenario this step is iterated for the number of the demand's CT value minus the selected connection's CT value which is equal to $p-x$.

Each time the algorithm searches for a connection with the next CT value, it assesses the connections in the lightpath. This step is described in Line 7 of algorithm 1 in Fig 1. In the worst case scenario the next CT value is not found until all connections in the lightpath have been analysed. In this case the number of iterations is equal to c .

From the analysis above we conclude that the number of iterations is given by Eq. (4.6),

$$(p-1)[c(p-x)c], \quad (4.6)$$

which results in Eq. (4.7),

$$p^2c^2 - xpc^2 - pc^2 + xc^2. \quad (4.7)$$

The worst case corresponds to $x = 1$ resulting Eq. (4.8),

$$p^2c^2 - 2pc^2 + c^2. \quad (4.8)$$

From Eq. (4.8) we observe that the number of iterations is dominated by p^2c^2 and therefore the asymptotic algorithm's complexity is given by Eq. (4.9):

$$O((pc)^2) \quad (4.9)$$

In order to assess the RDM algorithm's added complexity we calculated the complexity of the grooming algorithm. Its complexity is dependent on the number of wavelengths in a link and the number of alternate available routes. The grooming algorithm first checks for a wavelength to groom the demand into it, and

not finding it will search for a non-used wavelength. In the worst case scenario the grooming algorithm has to assess all wavelengths in the first link of the selected route twice and then repeat the process for all available alternate routes. Given r as the number of alternate routes and w as the number of wavelengths in a link, the grooming algorithm complexity is equal to $O(r * 2w)$.

Consider a worst case RDM scenario with the following characteristics: selected lighpath's capacity is completely used by connections with smallest BW requirement and demand's CT value is the highest. The selected lightpath contains 10 connections of 10 Gbps each ($p = 10$) and demand's CT value is be 4 ($c = 4$). In the grooming scenario r is equal to 3 and w is equal to 40.

When comparing the RDM mechanism algorithm worst case scenario complexity value and the grooming algorithm complexity value it is possible to conclude that the RDM mechanism is 6.67 times more complex than the grooming algorithm. However it is important to emphasize that the RDM algorithm is only triggered when a demand is blocked via grooming. In the performed simulation, for instance, the RDM mechanism was triggered for only 2% of all demand arrivals, and its success rate was 60% as can be observed in Figure 4.9 presented in the next section.

For the simulation scenario described in the previous section we have measured the total running time of the simulations. The simulations were processed in an Intel Pentium (R) CPU G860, 3.4 Gb memory 3.00 GHZ x2 running a Ubuntu 12.10 64-bit operational system. Backbone networks rely on more robust route processors as, for example, a route processor for Cisco Carrier Routing System (CRS). The route processor for a CRS is an Intel Xeon quad-core at 2.13 GHz and 64-bit, with 6 or 12 GB Double data Rate-3 (DDR3) error correcting code (ECC) memory running Cisco IOS XR as operational system [81]. Regarding memory configuration this backbone router would run at least twice as fast as the computer we ran the simulations on. Furthermore, the use of an operational system dedicated to routing operations would, most likely, increase a backbone router's performance. For these reasons we can state that the extra time added in network performance due to the implementation of the RDM mechanism would be negligible.

The measured running times were, for grooming 53 minutes and 43 seconds, for RDM-less 1 hour 1 minute and 54 seconds and for RDM-full 1 hour 1 minutes and 37 seconds. The RDM-less mechanism simulation time was 15% higher than of the grooming scenario, while the RDM-full running time was 20% higher. From

Table 4.4: BW requested values distribution

BW requested value	10	40	100
Probability	0.80	0.15	0.05

the total running time for the grooming scenario it is also possible to estimate how long it would take to process one demand. If 5×10^5 demand arrivals take $53 \times 60 + 43$ seconds, than to process one demand would take $3223/5 \times 10^5$ which is equal to 6.44 milliseconds. If we consider that the RDM mechanism increases the demand processing complexity 6.67 times, then the amount of time it would take to process one demand would be increased proportionally and therefore it would take 42.95 milliseconds.

4.4.3 Performance study and analysis of results

In order to evaluate the performance of the proposed differentiated resources distribution algorithm, we have developed a Java based discrete event driven simulator. We ran a simulation using the German Nobel reference network topology with 17 nodes and 26 bidirectional links [82]. Each link in the network corresponds to one fibre comprising wavelengths with 100 Gbps bandwidth capacity each [83].

Connection requests are generated dynamically following a uniform distribution among node pairs for source and destination. All runs are averaged over 5×10^5 requests following a Poisson process with mean holding time (λ) set to 500 sec (exponential). Request inter-arrival times (μ) are also exponential and vary with loading. Offered traffic load is calculated in Erlang using the relation $E=\lambda\mu$ [84]. Bandwidth requests are non-uniformly distributed among 10, 40 and 100 Gbps, with distribution approximate to values from [83] that can be observed in Table 4.4.

Routing is performed as fixed alternative with 3 route options for each source destination node pair. Wavelength assignment is performed in a first fit basis. Wavelength-Continuity-Constraint (WCC) is enforced for path computation.

We have simulated the proposed mechanism with different network characteristics. We have observed that the number of source / destination node pairs and the number of wavelengths per link have a direct impact on how often the mechanism is triggered and its success on establishing a connection. We have simulated our proposed mechanism for networks with

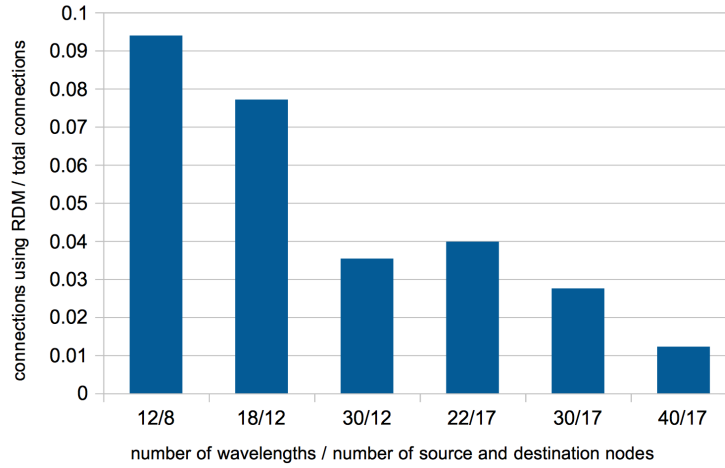


Figure 4.8: RDM connections per total number of connections for different scenarios with varied combinations of number of wavelengths and source and destination nodes for a network with offered traffic load of 1000 Erlang.

different characteristics and an offered traffic load of 1000 Erlang. We considered different numbers of wavelengths: 12, 18, 22, 30 and 40 wavelengths. The number of source/destination node pairs also varies according to the networks scenario, we tested scenarios with 8, 12 and 17 source and destination nodes. We analysed the proportion of connections established via the RDM mechanism and the total number of connections. As can be observed in Figure 4.8, the highest proportion between connections established via RDM occurred in the scenario with 12 wavelengths and 8 source and destination nodes in which more than 9% of the total number of connections were established via the RDM mechanism. In contrast, in the scenario with 40 wavelengths and 17 source and destination nodes roughly only 1% of all connections were established by the RDM mechanism.

The number of times the mechanism was triggered varied greatly. The mechanism may be triggered, but the computation of all preemptable resources may be insufficient to serve the demand's requirement and, consequently, the demand is blocked. To get a better understanding of the mechanism's performance we analysed the proportion of connections established using the RDM mechanism compared to the number of times the mechanism was triggered. In the scenario with 12 wavelengths and 8 source and destination nodes, the mechanism's performance was the lowest, meaning the mechanism had to be triggered more often in order to establish connections. Indeed as can be observed in Figure 4.9 in the aforementioned scenario 30% of the times the RDM mechanism was triggered a connection was successfully established while in the scenario with 40, 30 or 22 wavelengths with 17 source and destination nodes 60% of the times the RDM mechanism was triggered a connection was successfully

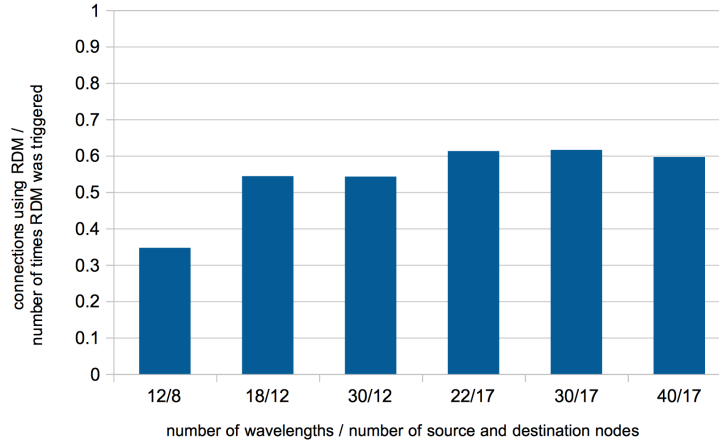


Figure 4.9: RDM connections per number of times RDM mechanism was triggered for different scenarios with varied combinations of number of wavelengths and source and destination nodes for a network with offered traffic load of 1000 Erlang.

established. This is easily explained as in the 12/8 scenario the level of resources usage is much higher than in the 40/17 for the same offered load and, therefore, it is not a figure of the mechanism's efficiency.

The performance of the RDM algorithm is also related to the offered traffic load. Since the RDM mechanism is triggered only when a demand is blocked it is plausible to assume that a network with low offered traffic load would have most demands served and therefore the RDM mechanism would seldom be triggered. We simulated the performance of the RDM mechanism for different offered traffic loads, and by analysing the results we could observe that the number of successful connections using the RDM mechanism increases significantly as the load increases. Results from these simulations may be observed in Figure 4.10, in which the proportion of RDM successful connections in a scenario with offered traffic load of 1000 Erlang is more than ten times higher than the proportion of RDM successful connections for an offered traffic load of 500 Erlang. Even though the proportion of RDM successful connections with offered traffic load of 1000 Erlang is approximately 1% of all connections established, this proportion of connections established via the RDM mechanism notably decreases blocking probability for higher CT connections and increases bandwidth assigned to these connections. This benefit also incurs in increased savings and profit as discussed in the Appendix A. For a network scenario in which the offered traffic load is 100 Erlang the RDM mechanism is never triggered.

In the MPLS diff serv model [78] 8 CT classes were described; however a network administrator may classify the traffic into as many CT values as necessary. We have tested the algorithm using different numbers of CT values.

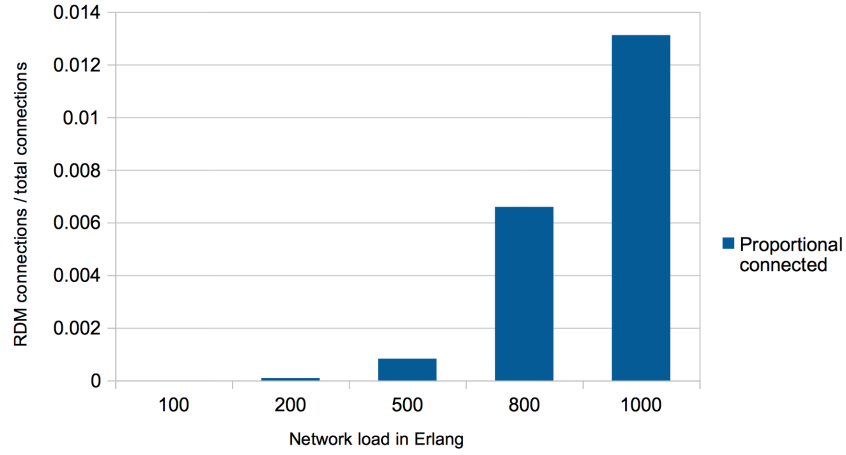


Figure 4.10: Proportion of RDM connections per total number of connections for scenarios with different offered traffic load.

Table 4.5: CT values distribution

CT value	0	1	2	3
Probability	0.60	0.25	0.10	0.05

Table 4.6: BC Model A

CT value	0	1	2	3
BC values (in Gbps)	100	97	79	47
Minimum BW guaranteed (in Gbps)	3	18	32	47
Max. preemptable (in Gbps)	0	3	21	53

Table 4.7: BC Model B

CT value	0	1	2	3
BC values (in Gbps)	100	97	88	20
Minimum BW guaranteed (in Gbps)	3	9	68	20
Max. preemptable (in Gbps)	0	3	12	80

Table 4.8: BC Model C

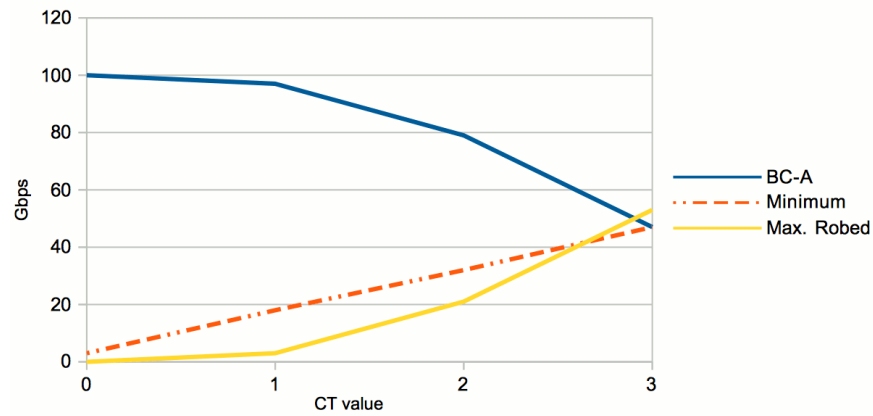
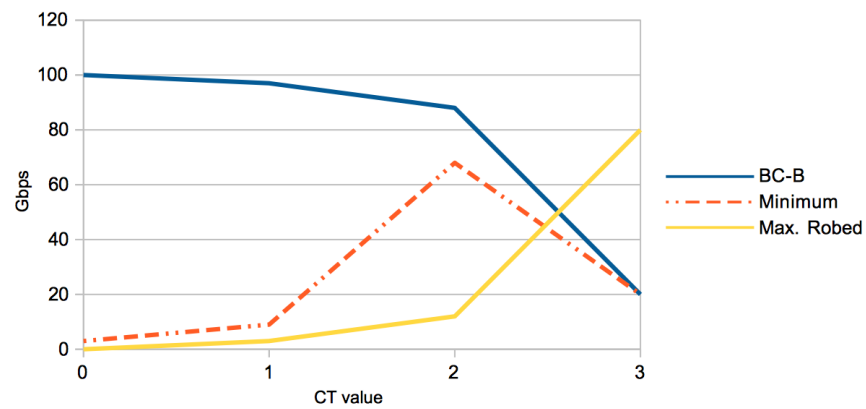
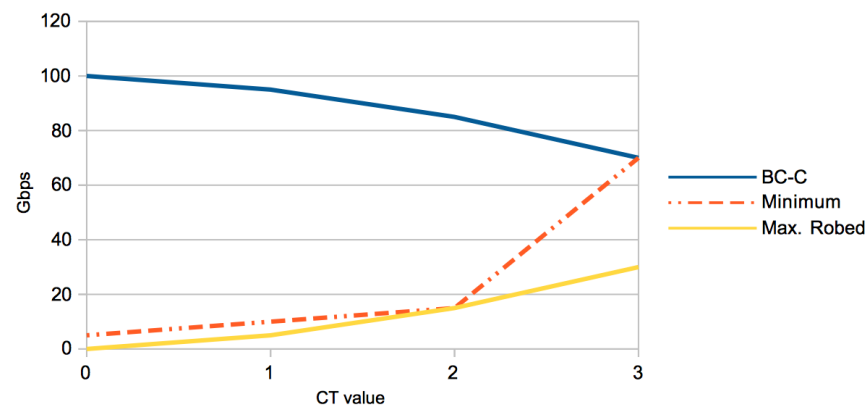
CT value	0	1	2	3
BC values (in Gbps)	100	95	85	70
Minimum BW guaranteed (in Gbps)	5	10	15	70
Max. preemptable (in Gbps)	0	5	15	30

We observed that 4 CT values represent a good trade-off between complexity and overall performance. The demands' 4 possible CT values follow a non-uniform distribution that can be observed in Table 4.5.

We have evaluated the algorithm for four different BC models. Such models, in this study, are arbitrary, but can be understood as different provider's policies to design a priority profile. Each BC model comprises i) BC values; ii) Minimum

Table 4.9: BC Model D

CT value	0	1	2	3
BC values (in Gbps)	100	90	70	40
Minimum BW guaranteed (in Gbps)	10	20	30	40
Max. preemptable (in Gbps)	0	10	30	60

**Figure 4.11:** Constraint values for BC model A**Figure 4.12:** Constraint values for BC model B**Figure 4.13:** Constraint values for BC model C

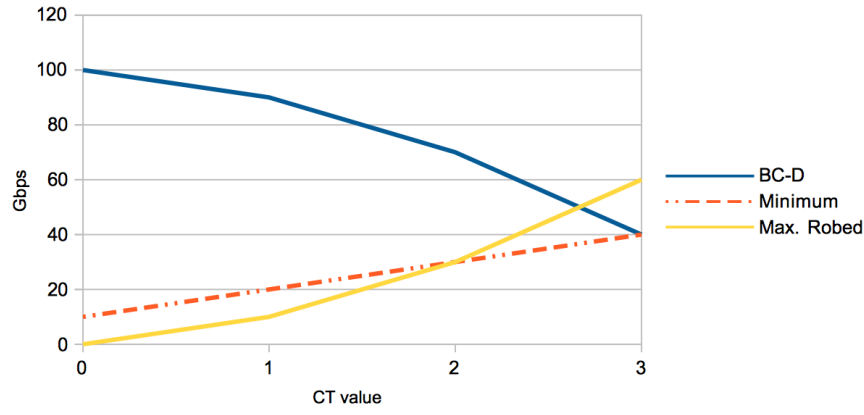


Figure 4.14: Constraint values for BC model D

guaranteed BW; iii) the maximum BW a CT can preempt from lower priority CTs, designated as Max. preemptable. Each of the four BC models tested are described in Tables 4.6, 4.7, 4.8, 4.9 and illustrated in Figs. 4.11, 4.12, 4.13, 4.14.

The performance of the proposed mechanism has been compared to a grooming scenario with no connection assignment policy. The performance metrics considered were blocking probability and the amount of resources allocated to connections. We ran simulations on a network with 40 wavelengths with 100 Gbps capacity, 17 source-destination nodes pairs and an offered traffic load of 1000 Erlang.

Simulation results indicate that both RDM-less and RDM-full mechanisms decrease the blocking probability rate when compared to the grooming scenario. Considering the total number of generated demands, the blocking probability is decreased roughly in 1% both in the scenario in which RDM-less is implemented - as illustrated in Figure 4.15 - and in which the RDM-full mechanism is implemented - as illustrated in Figure 4.16. In the figures it is also possible to observe that, when the total number of demands is being considered, the BC model adopted does not affect the blocking probability result once a RDM mechanism is being implemented.

When the total number of demands is being considered, the impact of the RDM mechanism in the blocking probability performance is partially justified by the fact that the blocking probability performs differently according to the connection's CT value. Indeed as can be observed both in Figure 4.17 and in Figure 4.18, for demands with the lowest CT value, the blocking probability is increased when the RDM mechanism is implemented. According to the distribution of CTs applied and described in Table 4.5, 60% of the demands tend to belong to CT value 0, therefore the overall blocking probability value is

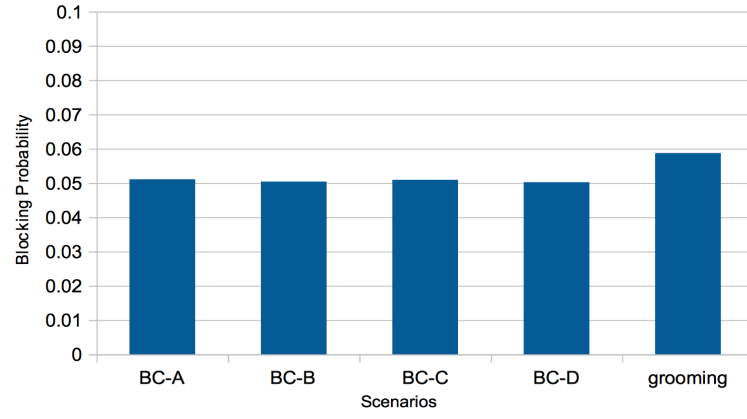


Figure 4.15: Blocking probability for RDM-less and grooming scenarios for total number of demands

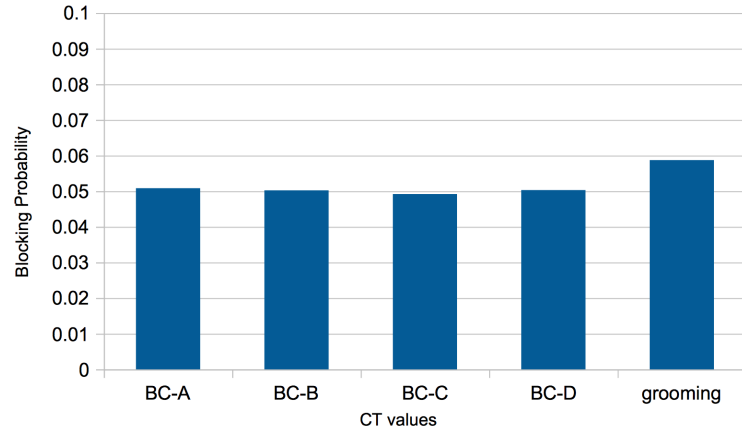


Figure 4.16: Blocking probability for RDM-full and grooming scenarios for total number of demands

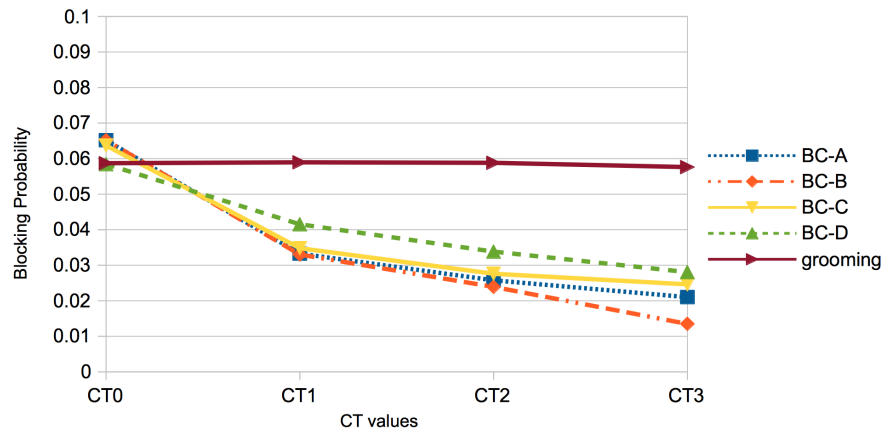


Figure 4.17: Blocking probability for RDM-less and grooming scenarios according to different CT values

increased due to results from demands belonging to this CT value.

As connections CT values increase their blocking probabilities decrease. As shown in Figure 4.17 and Figure 4.18 the blocking probability of connections with CT value 3 decreased most both in RMD-full and in RDM-less scenarios

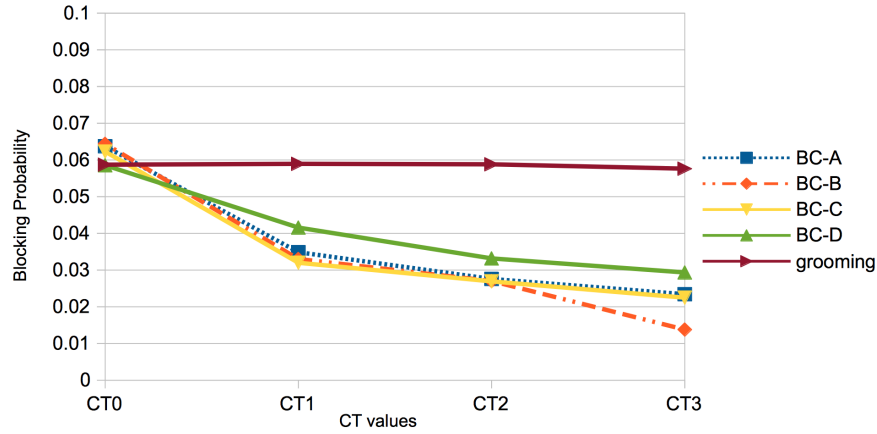


Figure 4.18: Blocking probability for RDM-full and grooming scenarios according to different CT values

the decrease percentage was approximately 5% when compared to the grooming scenario.

From the results it is also possible to observe that the BC model adopted has different impact on the blocking probability performance according to connections CT values. For example, both in RDM-less and in RDM-full scenarios the adoption of the BC model B resulted in a pronounced decrease in blocking probability for demands with CT value 3. The variation was approximately -3% when compared to the BC model D. This phenomenon occurs because, even though in the BC model B the bandwidth constraint for CT3 is more limiting than in the other models, in the BC model B demands with CT value 3 have a larger amount of resources that can be reallocated from connections belonging to CT2. The adoption of different BC models can be used by service providers to implement different SLA policies according to economic goals.

We have also analysed the proportion of resources allocated to connections in relation to the amount of resources requested by demands. RDM-less and RDM-full mechanisms have similar resources allocation results when the total number of demands is considered. In both cases the difference obtained by implementing the mechanism is quite small, as can be observed in the results illustrated in Figure 4.19 and in Figure 4.20. However, the RDM-less mechanism promotes an increase of 1% on the total amount of resources allocated, while RDM-full tends to decrease the total allocation of resources in, approximately, the same rate. When compared to the grooming mechanism, this difference in performance can be explained by the fact that the RDM-full mechanism always restricts the amount of resources allocated to connections, while the RDM-less mechanism only restricts resources allocation when there is contention

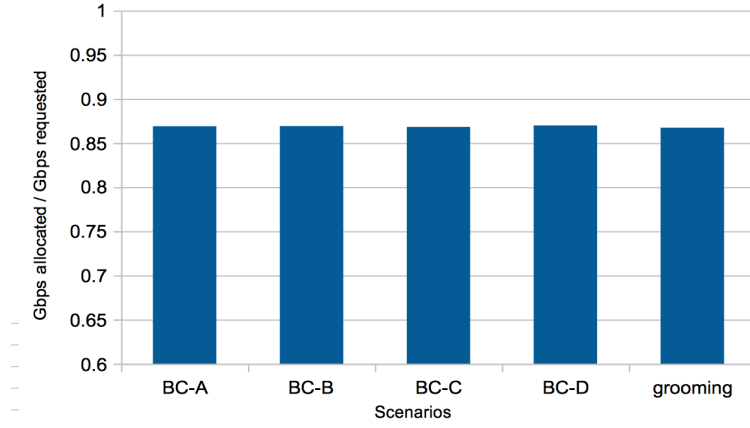


Figure 4.19: Proportion of total requested resources by total allocated resources for RDM-less and grooming scenarios.

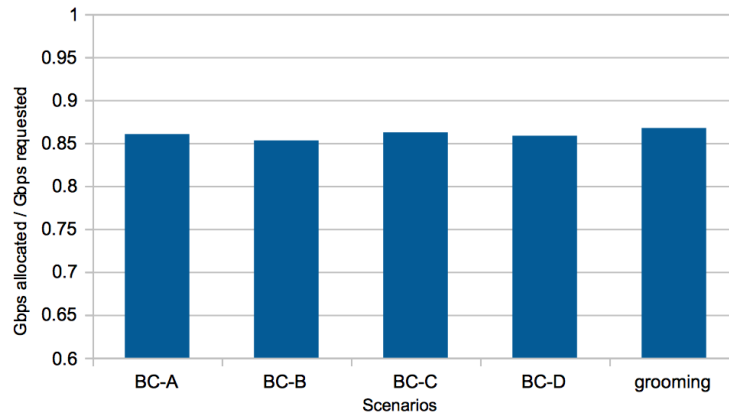


Figure 4.20: Proportion of total requested resources by total allocated resources for RDM-full and grooming scenarios.

for resources.

When the allocation of resources is analyzed according to connections' CT values, the RDM-less mechanism is more beneficial than the RDM-full mechanism, because it does not restrict the amount of resources allocated to connections before contention for resources occur. The RDM-less mechanism tends to benefit higher CT value demands in terms of resources allocation. Figs. 4.21 and 4.22 present results for RDM-less and RDM-full regarding the proportion of resources allocated per amount of resources requested for each of the connections 4 CT values. The results indicate that by implementing the RDM-full mechanism less resources are allocated to higher CT value connections. When BC model B is adopted the resources allocated to connections with CT value 3, are almost 30% less than the resources allocated to the same CT value connections in the grooming scenario. For the lower CT values connections implementing the RDM-full mechanism results in similar amount of resources allocation as in the grooming scenario.

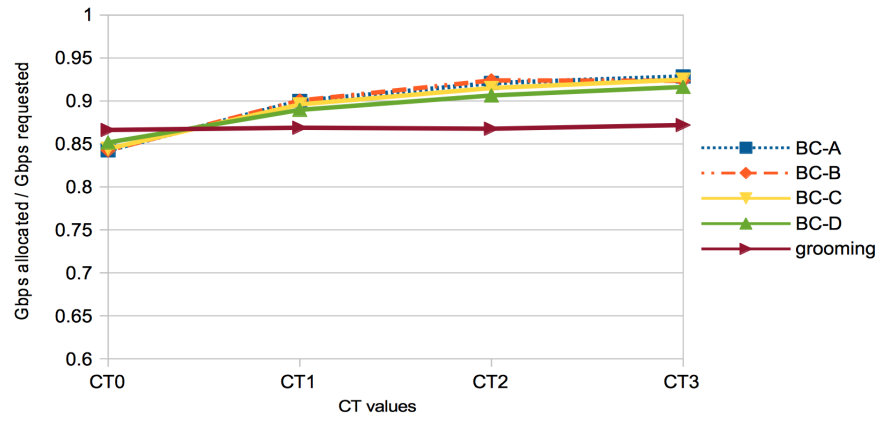


Figure 4.21: Resources allocation for RDM-less and grooming scenarios according to different CT values.

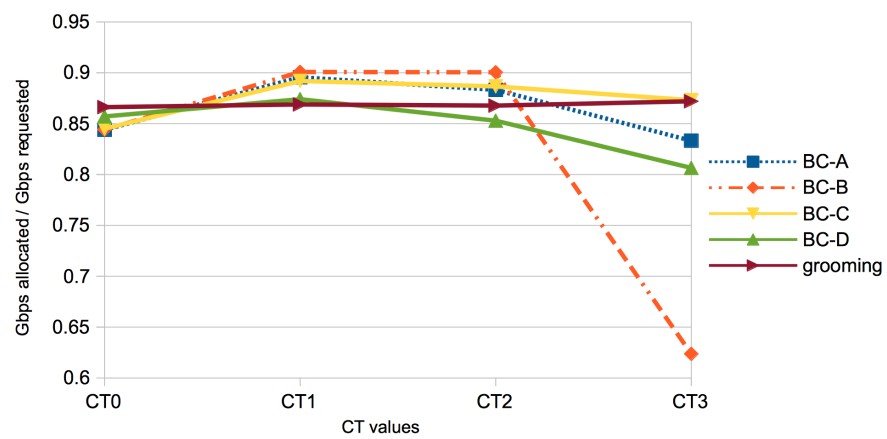


Figure 4.22: Resources allocation for RDM-full and grooming scenarios according to different CT values.

When RDM-less is implemented results for allocated resources are very different from results from the RDM-full scenario. In the RDM-less scenario, resources allocation are lessen only for connections with CT value 0, connections with higher CT values are assigned more resources than in the grooming scenario. As can be observed in Figure 4.21 the highest amount of resources allocation is for connections belonging to CT value 3 with the adoption of the BC model A: the amount of resources allocated to connections with CT value 3 is approximately 5% higher than in the grooming scenario.

From network simulation results, we observed that, besides increasing higher priority connections resource usage, the proposed mechanism also tends to optimize the network utilization and decrease blocking probability for heavy load traffic scenarios. By promoting better service to higher priority connections, implementing the mechanism might increase the net revenue of a network. Therefore we believe the RDM mechanism can be used as effective instrument to implement different SLA policies. A brief economical analysis on the economical impact promoted by the RDM mechanism in a WDM network may be appreciated in Appendix A.

5 Priority Realloc: a threefold RSA mechanism for EONs

In this Chapter we present our proposed mechanism denominated Priority Realloc. Priority Realloc aims at increasing the service fairness level towards highest bandwidth requirement demands by means of promoting differentiated service. To this aim, Priority Realloc treats highest rate demands as having priority over resources allocation. While allocating resources Priority Realloc also tries to prevent and reduce spectrum fragmentation.

Priority Realloc relies on the classification of connections according to their priority over service denominated Class-Type (CT). The mechanism considers 3 CTs, ranging from 0 (lowest priority) to 2 (highest priority). Highest priority connection requests may be reallocated FSs that were originally assigned to CT0 connections.

Priority Realloc presents two variations. In Priority Realloc HB (HB stands for highest bandwidth) only the highest bandwidth requirement connection requests are considered highest priority demands, in this variation CT2 demands that do not have a highest bandwidth requirement are ignored. In Priority Realloc HBCT (HBCT stands for highest bandwidth and Class-Type) both the highest bandwidth requirement demands and CT2 demands, regardless of their bandwidth requirement value, are considered as highest priority demands.

The Priority Realloc mechanism, independently of its variations, comprises two distinctive parts. In the first part, the mechanism will try to accommodate any incoming connection request in the existing gaps of contiguous available FSs. In order to do so, the mechanism relies on our proposed algorithm named Exact Gap Size with Fragmentation Level (EGS-FL). The ESG-FL algorithm is a fragmentation-aware algorithm similar to EF proposed by [19] and explained in Chapter 3.

The second part of the mechanism, identified as FSs reallocation, is only initiated if a highest priority demand is blocked by EGS-FL. The highest priority

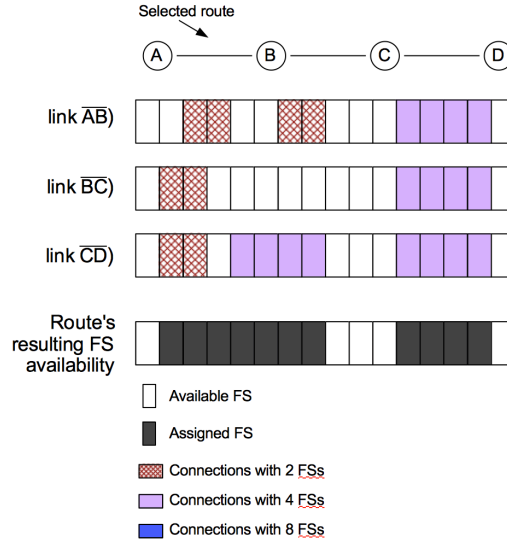


Figure 5.1: Links comprised by a selected route with busy FSs, the intersection of FSs in all the route's links results on the available FSs in the route

demand is a highest bandwidth requirement demand in HBCT version and either a highest bandwidth requirement and/or CT2 demand in HBCT version. In the second part, the mechanism will try to reallocate CT0 connections' FS to the incoming demand in order to guarantee its establishment. This part of the mechanism operates similarly to the path triggered defragmentation technique as explained in Chapter 2. It deallocates connections, or part of a connection's resources, that are preventing a gap from accommodating a demand and that is breaking a gap into smaller gaps.

The algorithm in the first part of the mechanism intends to decrease and prevent spectrum fragmentation level while accommodating incoming demands. It also tries to, whenever possible, establish the demand relying on the available resources so that the reallocation of resources promoted by the second part of the mechanism may be avoided. As observed in Chapter 2, reallocation of resources promotes network instability and increases the number of control messages exchange and should be averted.

In both algorithms, EGS-FL and FSs reallocation, a route's resources availability is scrutinized. A route's FS availability is calculated as the intersection of FSs availability in all links comprised by the route as illustrated in Figure 5.1. With the computed gaps of available contiguous FSs, a map of gaps and their size in number of FSs is generated. Figure 5.2 depicts an example of gap availability map. The gap availability map should be updated whenever a connection is established or terminated. The gap availability map aims at simplifying a route's resources availability inspection.

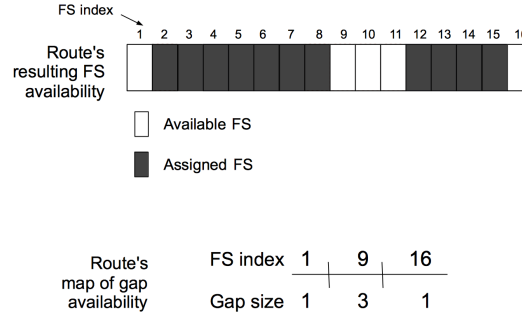


Figure 5.2: Gap availability map: gap index and respective gap size in number of FSs

Priority Realloc is designed to be implemented in an EON in which dynamic routing and resources assignment is centralized by one entity. GMPLS with PCE or a Software Defined Network (SDN) solution would be able to implement the centralized resources assignment task once control plane enhancement for EONs are concluded [49]. With few adaptations, the aforementioned control plane architectures could be able to perform Priority Realloc.

In the next sections we will explain the procedure of Priority Realloc and the two algorithms it comprises. In Section 5.1 we explain the EGS-FL, its objectives and procedures and in Section 5.2 we explain Priority Realloc's FSs reallocation mechanism.

5.1 Priority Realloc first part: Exact Gap Size with fragmentation level

We developed ESG-FL algorithm by adapting the EF algorithm proposed in [19] and explained in Chapter 3. Performance results from EON simulations proved that ESG-FL achieved better performance results than EF as can be observed in [85] and in Chapter 7.

Analogous to EF, in ESG-FL, when a demand arrives the algorithm tries to accommodate the demand in a gap which size, in number of contiguous available FSs, is exactly the same as the number of FSs the demand requires. Unlike EF, if such a gap is not available the gap with the smallest size in FSs and able to accommodate the demand is selected. We refer to a gap with smallest size in FSs and able to accommodate the demand as minimum size gap. Figure 5.3 illustrates the selection of exact size gap or a minimum size gap according to the link state.

In case there is more than a route with an exact size gap, the route with highest spectrum fragmentation level is selected. To calculate a route's spectrum

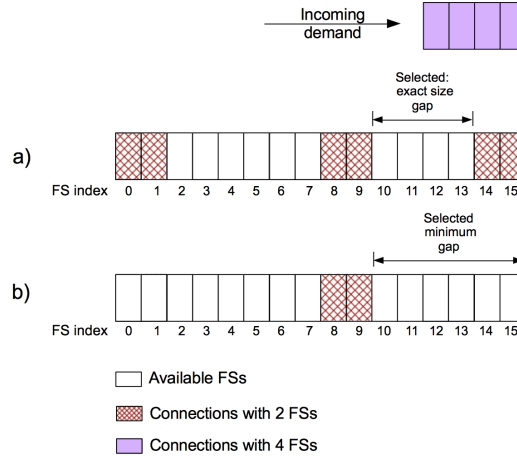


Figure 5.3: The diagram shows two different situations, in a) there are two gaps that can accommodate the demand, the algorithm selects the exact size one, and in b) there are two gaps that can accommodate the demand, the algorithm selects the smallest one

fragmentation level we relied on the external fragmentation measurement presented in [19] and explained in Chapter 3. If there is no route with exact size gap, the algorithm will select the shortest route containing a minimum size gap. If there is no gap able to accommodate the demand the second part of the mechanism is called. We offer a comprehensive step by step explanation of the algorithm in Section 5.3.

In ESG-FL, when there is no exact size gap to accommodate the demand the algorithm selects a minimum size gap instead of maximum gap as in [19]. We have selected this policy in order to spare largest size gaps to highest rate demands.

When there is more than a route with exact gap size the algorithm selects the route with highest fragmentation level instead of the route with fewest number of hops. We have adopted this policy because if a highly fragmented route is able to accommodate the demand it is more advantageous to assign this route and spare less fragmented routes to other demands.

All in all, the ESG-FL algorithm aims at sparing large gaps of available contiguous FSs to higher BW requirement demands. By focusing on accommodating a demand to a gap with the exact number of available FSs, the algorithm prevents established connections to fragment the available spectrum into smaller gaps of available FSs. It also aims at sparing least spectrum fragmented routes for demands that are less likely to be established due to their bandwidth requirements.

In the next section we explain the procedure of the second part of the

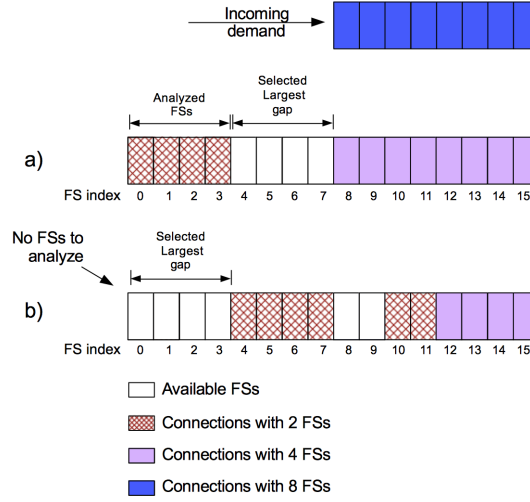


Figure 5.4: The diagram shows two situations, in a) the selected largest gap's index is 4 and therefore there are FSs on the left of the selected gap to be inspected and in b) the selected largest gap is 0 and therefore there is no FSs to the left of the selected largest gap to be inspected

mechanism. The FSs reallocation algorithm is called when a highest priority demand is blocked.

5.2 Priority Realloc second part: FSs reallocation

When the second part of the mechanism is called, its algorithm will attempt to reallocate FSs from CT0 connections to the prioritized demand. Prioritized demands may be highest bandwidth requirement demands in Priority Realloc HB and highest bandwidth requirement demands and/or CT2 demands in Priority Realloc HBCT. It is important to observe that CT0 connections may have any BW requirement, hence part of the resources from highest rate connections may be preempted.

All K alternative routes had their largest size gap previously calculated in the first part of the mechanism as will be explained in Section 5.3. When FSs reallocation algorithm is called, it will select the route with the largest size gap. The FSs located on the left of the largest size gap will be inspected for reallocation. For this reason, the index of the largest gap selected in the route cannot be 0 as illustrated by Figure 5.4. The decision to try to reallocate resources on the left of the selected gap is based on the principle used by KSP-FF to assign lowest indexed FSs first. This policy have resulted in efficient spectrum use as debated in Chapter 2.

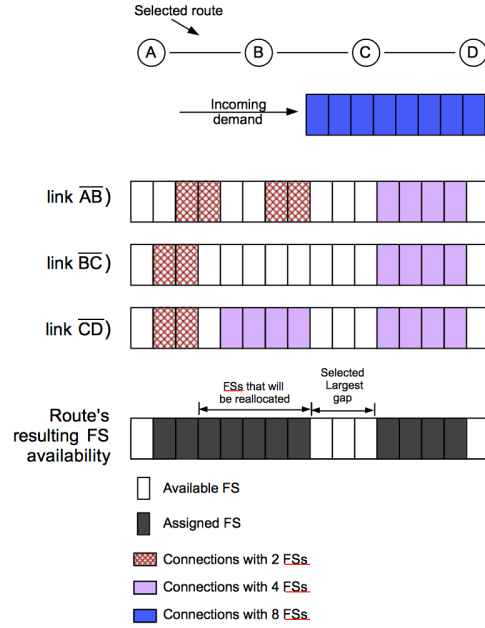


Figure 5.5: From the selected route's resulting gap availability map, the route's largest gap is selected. The FSs on the left of the selected gap are inspected for reallocation

In order to decrease the number of reallocated FSs, the algorithm selects the route with the largest size gap according to the route's map of gap availability. The difference between the demand's BW requirement and the size of the selected gap determines the number of additional FSs required to accommodate the demand. The algorithm will then check the required number of additional FS on the left of the selected gap on all links comprised by the selected route.

If any of the analyzed FSs are assigned to a connection with CT value higher than 0, the algorithm is either discontinued or this route is discarded and another route and its respective largest gap are considered. This step guarantees that the mechanism will not reallocate FSs from a higher priority connection. If all the FSs examined in all the links comprised by the route are either available or assigned to a CT0 connection the FSs reallocation may be established. Figure 5.5 illustrates the FSs reallocation according to the route's gap availability map. At this point the mechanism is considered successfully triggered. With the FSs reallocation, the incoming demand is accommodated by the selected gap and the inspected FSs. The process of FSs reallocation by link is illustrated in Figure 5.6. Section 5.3 presents a comprehensive step by step explanation of the algorithm.

The active CT0 connections originally accommodated by the reallocated FSs will be preempted from these FSs. The connections that were subject to FSs reallocation will be updated regarding the current amount of FSs assigned. Furthermore, if these connections were not accommodated in the same route as the selected route, the connection's route links will have the same indexed FSs

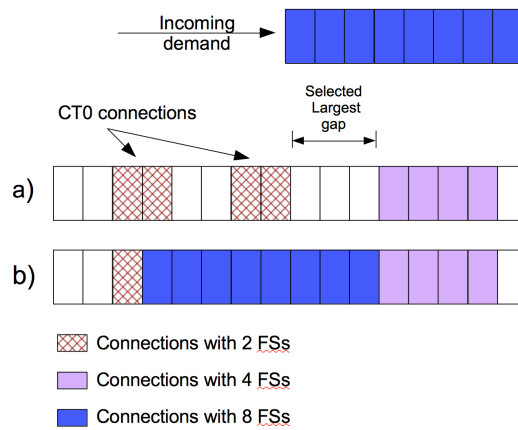


Figure 5.6: The diagram shows a) link state when connection request arrives, there is not enough number of available continuous FSs to accommodate the incoming demand, all connections on the left of the largest gap have CT value 0 and b) the necessary number of FSs are reallocated to the incoming demand

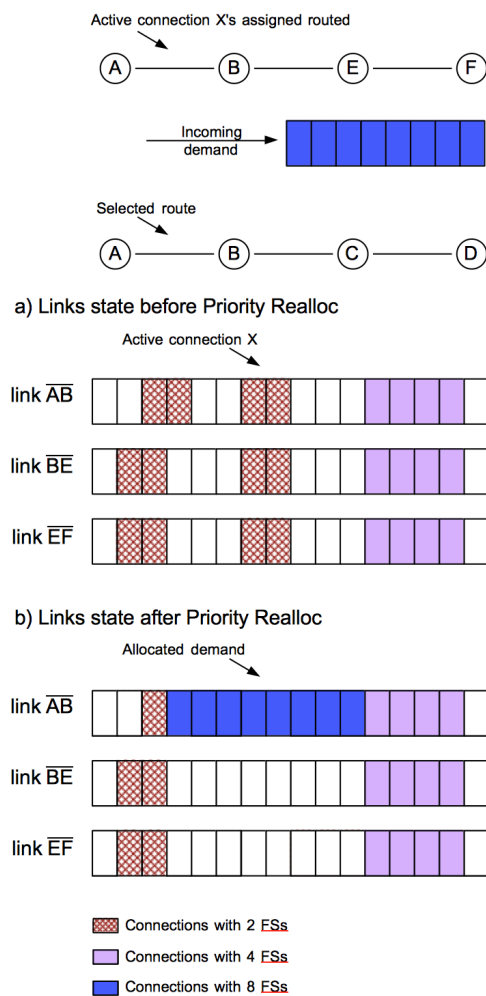


Figure 5.7: The diagram shows a) link state before Priority Realloc: connection X is accommodated in a different route from the selected route but both routes have one link in common and b) link state after Priority Realloc: connection X have all its FSs preempted. In the common link the preempted FSs are reallocated to the incoming demand, in the other links from connection X's route the FSs remain available

preempted. This condition is better visualized in Figure 5.7.

When the FSs reallocation algorithm results in available FSs in links not comprised by the selected route, these FSs may accommodate future incoming connection requests, decreasing the system's blocking probability. Furthermore, by allocating a highest rate connection, when this connection is terminated the resulting gap of available FSs comprises a larger number of FSs than each of the original smallest gaps. This largest size gap will be able to accommodate either a highest rate connection or a higher number of combinations of different rate connections. Therefore, the mechanism promotes an indirect benefit on the network performance beyond the accommodation of a highest rate demand.

When a connection's FSs are reallocated, it may happen that the reallocated FSs corresponds to all of the connection's assigned resources in which case the connection will be, in fact, disrupted. This occurrence is more likely to happen with lowest rate connections, since a smaller number of reallocated FSs could result in the connection's disruption. This is an indirect way to promote service fairness since lowest rate demands are more likely to be established than highest rates demands as discussed in Chapter 2.

It is important to observe that preemption of resources will not always occur as soon as the preempted connection is established. In the majority of times the reallocation of resources will occur after some time the connection has been active with all of its original resources assigned. In a superficial analysis, if we consider that FSs reallocation is equally probable to happen in any point in time, and thus are uniformly distributed in discreet values of percentage of active time, we have Equation 5.1 which equals to 50.5. Meaning that, in average, connections that suffer reallocation of resources would keep all of its original resources 50.5% of its active time.

$$\frac{\sum_{i=1}^{100}(i)}{100} \quad (5.1)$$

Another characteristic of the mechanism is that, in some cases, the FSs reallocation from a connection located on the left border of the selected gap may enable the assignment of available FSs located in a gap on the left of the preempted connection. Therefore, by reallocating a connection's FSs, two gaps of available FSs are filled by establishing the incoming demand as illustrated in Figure 5.6. In the example one connection is accommodated in two of the additional FSs required on the left of the selected gap, preventing the demand's accommodation. With the reallocation of two FSs from the active connection

it was possible to allocate a connection with 8 FSs, and eliminate gaps of available FSs that would not be able to accommodate highest BW requirement demands. The next Section details the algorithms comprised by the Priority Realloc mechanism.

5.3 Analysis and explanation of proposed algorithms

In the first step of ESG-FL the algorithm inspects the gaps in the route's map of gap availability in search for a gap with exact size in number of contiguous available FSs as the demand's FS requirement. During the inspection of gaps, if an exact size gap is found the iteration is interrupted. However, the exact size gap may either be found in the last gap of the map or not be found at all. In such cases the algorithm will iterate through all the gaps in the map. The number of elements in the map of gap size availability may be large, increasing the number of algorithm's iterations and, consequently, the algorithm's complexity.

In order to avoid iteration over all elements of map of gap availability more than once, while inspecting FSs to find the exact size gap, the algorithm also computes if the inspected gap is the minimum or the largest gap of available FSs. In case all gaps in the route's map are inspected the route's minimum and largest size gaps will be found and registered for posterior steps. If an exact size gap is found before the end of the map a route's minimum and largest gap will not be required and the iteration may be interrupted. If there are more than one minimum or largest gap in the route, the selected ones will be the ones first computed, thus, the ones with smallest index number.

If there is more than a route with exact gap size the mechanism will select the route with higher level of spectrum fragmentation. If there is no route with exact gap size the algorithm will select the first route in the list of KSP and its minimum size gap. The first route in the list of KSP is the route with smallest number of links. Since the gap selected will not be entirely filled the aim of this policy is to decrease the number of links assigned. The ESG-FL pseudo-code may be appreciated in Algorithm 2.

When filling gaps by selecting exact size gaps, or sparing larger gaps by selecting minimum size gap the algorithm cannot guarantee every link in the route will have an exact or a minimum size gap assigned. However the route itself is an entity that may or may not be able to accommodate incoming demands

and hence, optimizing the selection of its gaps of available FS may improve the probability this route will be able to accommodate a demand in the future.

Algorithm 2 ESG-FL algorithm

Input: demand, alternative routes

```

1: condition ESG found = no
2: for each K alternative routes do
3:   largest gap size = 0, smallest gap size = 999
4:   for each gap in G gaps of available slots in map of gap availability do
5:     if current gap size == demand's FS requirement then
6:       route's selected gap = current gap
7:       condition ESG found = yes, stop FOR
8:     else
9:       if (current gap size > largest gap size) and (current gap size' id > 0) then
10:        largest gap size = current gap size
11:      end if
12:      if (current gap size < smallest gap size) and (current gap size ==> demand's
13:        FS requirement) then
14:        smallest gap size = current gap size
15:      end if
16:    end if
17:    route's smallest gap = smallest gap index
18:    route's largest gap = largest gap index
19:  end for
20: if condition ESG found == yes then
21:   highest fragmentation level = 0
22:   for each K alternative routes do
23:     if (route's selected gap == demand's FS requirement) and (route's fragmentation
24:       level > highest fragmentation level) then
25:       selected route = this route
26:     end if
27:   end for
28: else
29:   for each K alternative routes do
30:     if route's smallest gap size != 999 then
31:       selected route = this route, route's selected gap = route's smallest gap, stop
32:       FOR
33:     end if
34:   end for
35:   if selected route == null then
36:     call mechanism's second part
37:   end if

```

Output: selected route, selected gap index

When the Priority Realloc's FSs reallocation is called, the route with largest size gap is selected and the algorithm calculates the number of additional FSs necessary to accommodate the demand. As commented in Section 5.2, the selected largest gap's index cannot be equal to zero because in such a case there would be no FSs on the left of the gap to be inspected.

It may occur that the selected largest gap's index is lower than the number of extra FSs required to accommodate the demand, meaning the number of FSs on the left of the selected largest gap is not enough to attend the demand's BW requirement. When that happens the number of additional FSs required is determined to be equal to the largest gap's index and the demand is under-provisioned. This situation, though, is not likely to happen, in fact, the probability of occurrence is given by Equation 5.2, where R is the number of FSs in the highest bandwidth requirement in the network, and the number of FSs in an EON link is 320 for a link with 4,000 GHz spectrum and a FS width of 12.5 GHz.

$$\frac{\sum_{i=1}^{R-1} (R - i)}{\text{number of FSs in the link}} \quad (5.2)$$

The algorithm inspects all additional FSs required in all route's links. If any inspected FSs is assigned to a connection with CT higher than 0 the algorithm will disregard this route and select another route with largest size gap within the remaining routes in K alternative routes. This process is repeated either until the demand is established or until there is no remaining route in the list of KSP. When there is no route remaining in the list of KSP, the algorithm is interrupted and the connection is blocked. If the inspected additional FSs allow reallocation, the connection is established. The algorithm's pseudo-code may be appreciated in Algorithm 3.

5.3.1 Algorithms procedure alternatives

Both ESG-FL and Priority Realloc's FSs reallocation algorithms would admit different steps and decision policies from the ones we adopted and described in the previous Sections. Some variations would increase the probability of the mechanism to be successfully triggered, others would decrease the number of reallocated FSs. In this Subsection we comment on the alternative possibilities of algorithm steps and policies, their benefits and our decisions to not implement these variations.

Different policies could be chosen to lead the route selection process. For instance, the route could be selected by smallest number of hops. The benefit of this policy would be link usage reduction and simplicity of route selection procedure since the first route in the list of KSP would be selected eliminating the need of iterating through all routes. The disadvantage of this policy would

Algorithm 3 Priority Realloc's FSs reallocation algorithm

Input: demand, alternative routes

```

1: for each K alternative routes do
2:   largest gap = 0, selected route= null
3:   if route's largest gap > largest gap then
4:     selected route= this route
5:   end if
6: end for
7: if selected gap index < additional FSs required (F) then
8:   additional FSs required (F) = selected gap index
9: else
10:  additional FSs required (F) = (selected route largest gap size) - (demand's FS
    requirement)
11: end if
12: condition for reallocation = positive
13: for each link in L links in route do
14:   for each FSs in F additional FSs required do
15:     if the FS is not available and FS accommodated connection CT value > 0 then
16:       condition for reallocation = negative, stop FOR
17:     end if
18:   end for
19:   if condition for reallocation = negative then
20:     stop FOR
21:   end if
22: end for
23: if condition for reallocation = positive then
24:   trigger reallocation, stop FOR
25: else
26:   K = K-1
27:   while K>0 do
28:     repeat lines 1 to 26
29:   end while
30:   if condition for reallocation = negative then
31:     block demand
32:   end if
33: end if

```

Output: selected route, selected gap index

be the increase in number of reallocated FSs.

Another possibility would be selecting the route with the highest number of links in which the route's selected exact size gap is also an exact size gap. The benefit of this policy is to promote spectrum fragmentation decrease in a higher number of links, which means decreasing horizontal fragmentation, however, this include another iteration on the algorithm increasing its complexity.

Other steps of the algorithm could also follow different decision processes. For instance, when the algorithm is inspecting a connection's CT value it could also investigate the amount of time the connection has been active in relation to its holding time. With this information the algorithm could try to only reallocate resources from connections that have already been active most of their holding time. This policy would decrease the amount of time a connection is disrupted or have its assigned resources decreased. The unfavorable characteristic of this policy is that it would decrease the number of times the mechanism is triggered.

Other decision process in the algorithms could be questioned. As an example, when the selected largest gap in the route becomes ineligible due to the higher priority connections accommodated by FSs on its left border, another largest gap could be selected in the same route. The benefit of this decision would be the increase in the number of times the mechanism is triggered. The drawback would be the increase in procedure complexity and iteration size. Procedure complexity would be increased due to the register of more than one largest size gap and iteration size would increase due to the increase in the number of elements the algorithm would inspect.

In the algorithm, only FSs on the left of the selected largest gap are inspected, when the FSs are ineligible the FSs on the right of the selected gap could also be inspected. This procedure would increase the probability of triggering the mechanism at the cost of increasing algorithm complexity. Furthermore this policy is a counteract in regard of the policy of firstly allocating FSs from the left hand side of the spectrum.

All in all, the main benefits promoted by the algorithm variations would be increasing the probability of the mechanism being triggered and the number of prioritized demands established, decreasing the number of reallocated FSs and further decreasing spectrum fragmentation level.

After testing most of the variations we have decided not to implement them for many reasons. Most algorithm variations promoted a negligible increase in

performance benefit, not justifying the increase in algorithm complexity. Some decision policies would required a significant increase in the amount of information stored in the nodes state database, usually known as Traffic Engineering Database (TED). Some variations would magnify the impact of the mechanism that, as indicated by results in Chapter 7, already provides a significant increase in service fairness. We believe that allowing the mechanism to not be triggered in some occasions would be an indirect manner of moderating the promoted benefit towards prioritized connections. Ultimately, the mechanism's aim is to promote fairness and not to unbalance the service provision towards highest rate connections.

5.3.2 Algorithm's computational complexity

In order to evaluate the Priority Realloc algorithms' complexity we have considered all iterations in the algorithms' steps. We observed that the algorithms complexity are mainly composed by the iterations over the number of gaps of availability, the number of links in the selected route, the number of alternative routes in KSP, and the number of additional FSs required.

The ESG-FL algorithm contains the following iterations: the iteration over K routes in KSP in each of which the algorithm iterates over G number of gaps in the map of gap availability. If an exact gap size is found, there is an iteration over K routes in KSP to select the route with largest fragmentation level, otherwise, there is an iteration over K routes in KSP to select a route with a minimum gap able to accommodate the demand. Either way there will be one more iteration over K routes in KSP. The ESG-FL algorithm complexity is, therefore, given by Equation 5.3.

$$\text{ESG's complexity} = O(K \times G + K) \quad (5.3)$$

The FSs reallocation algorithm contains the following iterations: the iteration over K routes in KSP to select the route with largest gap size. The iteration over L links in the selected route in each of which the algorithm iterates over the F number of additional required FSs. If after inspection the selected route is not eligible for mechanism trigger this route is extracted from KSP and the algorithm iterates over the K remaining routes in KSP to select another route with largest size gap and so on so forth until KSP contains only one element and either the FSs reallocation is triggered or the demand is blocked. So, in fact, the mechanism

iterates K times over $K - i$ routes where i varies from 1 to K , which means the algorithm performs $\sum_{i=1}^K i$ iterations. From the analysis above we conclude that the FSs reallocation algorithm computational complexity is given by Equation 5.4, simplified into Equation 5.5 and further simplified into Equation 5.6.

$$\text{FSs reallocation's complexity} = O\left(\sum_{i=1}^K i + L \times F\right) \quad (5.4)$$

$$\text{FSs reallocation's complexity} = O((0.5K^2 + 0.5K) + (L \times F)) \quad (5.5)$$

$$\text{FSs reallocation's complexity} = O((K^2 + K) + (L \times F)) \quad (5.6)$$

From the analysis above we can compute the mechanism's complexity by adding the two algorithms computational complexities resulting in Equation 5.7. By observing Equation 5.7, it is possible to infer that the mechanism complexity is dependent mainly on K , given by $O(K^2 + K)$.

$$\text{Priority Realloc's complexity} = O(K \times G + K + K^2 + L \times F) \quad (5.7)$$

In order to be able to estimate the added computational complexity promoted by the Priority Realloc when compared to the benchmark algorithms, we have calculated the computational complexity of KSP-FF and EF proposed in [19]. Both algorithms, in a worst case scenario would iterate through the K routes in KSP and through all the gaps of available FSs in each route. Therefore both algorithms' complexity are given by Equation 5.8.

$$\text{benchmark algorithms' complexity} = O(K \times G) \quad (5.8)$$

To calculate a numerical value for ESG-FL computational complexity, we consider the network condition in which we simulated an EON as described in Chapter 7. In those simulations $K = 3$ in KSP. The largest route from all pre-calculated routes contains 7 links ($L = 7$). The EON link contains 320 FSs. In a worst case scenario, every other slot is assigned to a connection so the number of gaps in array of slot availability (G) is given by the total number of slots in the link divided by 2 ($G = 160$). In the simulated network configuration the highest

rate demand required 8 FSs. A highest rate demand may require at the most 7 additional FSs ($F = 7$).

If we substitute the network configuration values into the computational complexity equations' variables we will get numerical values for each of the algorithms' computational complexity. For the benchmark algorithms we substitute the network condition values into Equation 5.8, which results in Equation 5.9. For ESG-FL complexity, we substitute the network condition values into Equation 5.3, which results in Equation 5.10. For Priority Realloc's FSs reallocation algorithm, we substitute the network condition values into Equation 5.5, which results in Equation 5.11.

$$\text{benchmark algorithms' complexity} = K \times G = 3 \times 160 = 480 \quad (5.9)$$

$$\text{ESG-FL's complexity} = K \times G + K = 3 \times 160 + 3 = 483 \quad (5.10)$$

$$\begin{aligned} \text{FSs reallocation's complexity} &= K \times K + K + L \times F = \\ &3 \times 3 + 3 + 7 \times 7 = 6 + 49 = 55 \end{aligned} \quad (5.11)$$

To calculate the added computational complexity promoted by implementing the Priority Realloc mechanism when compared to the benchmark algorithms we have to consider that the ESG-FL would be implemented for every incoming connection request, while the FSs reallocation will be only called by blocked highest priority. For example, EON simulation results proved that, for an offered traffic load of 1,110 Erlang, highest priority demands were blocked 3.7% of all the connection requests. The ESG-FL algorithm is 0.625 % more complex than the benchmark algorithms. When called, the FSs reallocation algorithm adds 11% of benchmarks algorithms' computational complexity.

In the next section we present DSEON-Jsim, an EON simulator we have developed in Java that implements the algorithms described in this chapter. DSEON-JSIM aims at testing Priority Realloc performance benefits.

6 DSEON-Jsim: an ad-hoc event driven Java based simulator for EONs

Network simulation is an important tool in optical network research, aiding researchers to promptly validate and evaluate the performance of new algorithms without the need of installing and managing network testbeds [86]. Besides, in a testbed not all algorithms and mechanisms may be tested because most of the optical network equipment is proprietary vendor with restricted programmable features. When enabled, implementing new algorithms in testbed equipment may be a complex and time consuming task as it requires accessing, controlling and programming devices low level capabilities [86].

Most of the optical network simulation tools available emulate WDM networks and not EONs. In many cases the tool is designed by researchers in order to study a specific problem or to test a new proposed algorithm. Due to their exclusive scope and the type of network they emulate, the available optical network simulation tools would have to be reprogrammed and adapted to be able to implement the proposed mechanism and assess the required variables under the necessary conditions. However as observed in [86]: “most of the available solutions are limited in scope, difficult to use or not totally open”. In most cases, the exclusive simulation platform, models and assumptions result in a programming ambient difficult to re-use and adapt. Furthermore, many of the available tools are partially deprived of documentation a.

The EON resources assignment paradigm is novel and EON simulation tools are not common in the literature. EonSim is the sole EON simulator for open use we have found available. EonSim is described in [87] and available in [88]. EonSim is able to simulate various RSA algorithms and output performance metric files containing blocking probability and the network bandwidth occupation. EonSim provides a user manual and a graphic user interface which promotes ease of use. However, EonSim does not provide differentiation of service and preemption of

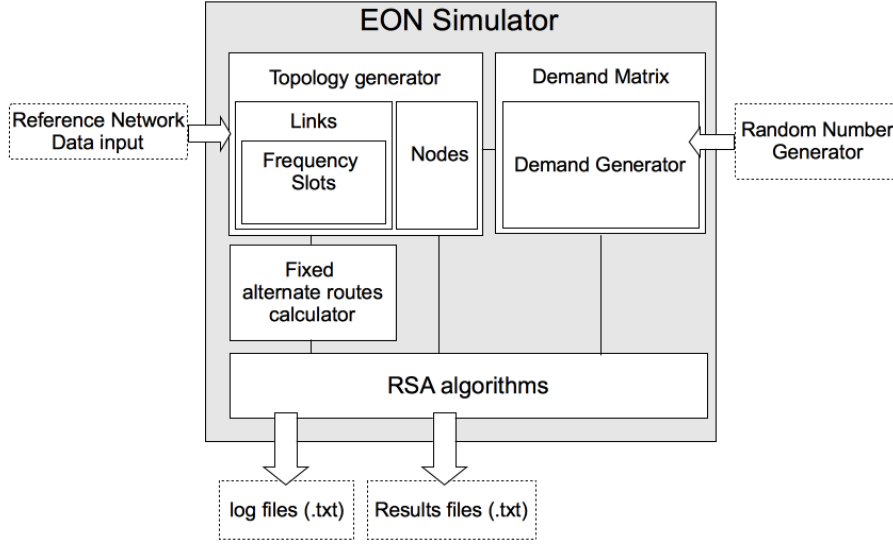


Figure 6.1: DSEON-Jsim software architecture diagram

resources which are the main focus of study in this thesis. Adapting a simulator to consider classes of service and perform preemption of resources would require a programming working time equivalent to writing a new simulator that would focus exclusively on the features we needed to test.

Due to the aforementioned reasons we have developed, in Java, an ad-hoc discreet event driven simulator that implements the algorithms proposed in this thesis. The Java based simulator EON is called DSEON-Jsim, the DS prefix refers to the ability of implementing differentiated services provisioning. DSEON-Jsim is available for open use [89].

6.1 Operation description

The DSEON-Jsim consists on computing available resources for incoming demands following a network topology state. The simulator architecture can be observed in Figure 6.1.

In DSEON-Jsim, a time interval represents the simulation running time, and is repeatedly generated as a discreet sequential number starting at zero. As a new simulation process starts, an inter-arrival value is generated following an exponential distribution with mean λ . Each time a new time interval is generated this value is compared to the inter-arrival value. When the current running time equals the inter-arrival time value plus the time interval of the last demand arrival a new demand is generated. When a demand is created its variables are determined. A demand's variables are:

- Bandwidth requirement: randomly selected from a group of possible pre-determined values represented in number of FSs. The bandwidth requirement values may follow either a uniform or a non-uniform distribution probability.
- CT value: randomly selected from a pre-determined group of possible values. The CT values may follow either an uniform or a non-uniform distribution.
- Holding time: determines the number in time intervals during which a connection is active before being released. It is determined by a random value generator that follows a Poisson distribution with mean value μ .
- Time of setup is equivalent to the time interval at which the demand is generated.

Part of the bandwidth variables rely on user defined values. The values defined by the user are:

- Mean μ used for the computation of holding time.
- Mean λ used for the computation of inter-arrival time.
- Number of CT values.
- CT values probability distribution.
- Connection requests' bandwidth requirements (in number of FSs).
- Bandwidth requirements probability distribution.

Once a demand is generated an RSA algorithm is triggered in order to try to accommodate the demand in the network's available resources. The RSA algorithm implemented is selected by the user. In any selected RSA algorithm the routing problem considers K shortest alternate fixed routes computed offline for each source/destination node pair. The K shortest paths are inputted in the system according to the network topology selected by the user. The K paths are ordered according to their number of hops so that the shortest route is the first inspected for available contiguous FSs. To compute resources availability the simulator considers user defined network information, which are:

- Reference network topology.

- Number of FSs per link.
- FS width in Ghz.

In parallel to the RSA algorithm initiation, whenever a new time interval is generated, active connections are inspected to check whether they should be terminated. This inspection calculates if the connection's holding time plus its setup time are equivalent to the current time interval. For the connections that are terminated their assigned resources are liberated in all links in the assigned route.

DSEON-Jsim has a specific manner of regarding the network state. In DSEON-Jsim each link has an array of slots availability which number of elements is equivalent to the link's number of FSs. The elements of this array are integers 1 and 0, 1 representing an available FS and 0 an assigned FS. The array position refers to the FS index. From the links array of slots availability the routes array of slots availability are calculated. Similar to the links' array of slots availability route's array of slots availability comprises 1 and 0s representing FSs availability, however, this array is achieved by the multiplication of all links FSs availability in the route. The aim is to generate the resulting slots availability for the route. For instance, if a given FS in a link is not available, this FS in the route array of availability will also be unavailable even if the FS is available in other links in the route.

A gap availability map simplifies the route array of slots availability, saving computational time in resources availability inspection. A gap availability map is a Java treemap that has a gap index and its respective size in number of contiguous available FSs. A gap index is defined as the index of the first FS in a group of contiguous and available FSs. The gap availability map is used by the RSA algorithm when checking if the analyzed route contains the minimum number of available contiguous FSs.

After the RSA algorithm is concluded, a new inter-arrival time value is generated and the time interval generation process continues. If the connection is successfully established, the links in the selected route are updated regarding FSs availability and accommodated connection. The flowchart in Figure 6.2 illustrates the simulator main steps. Whenever the computation of routes and resources availability is concluded, performance metrics are calculated and registered. Variable values are also registered in log files to assess the simulator correct operation. When the total number of generated connection requests reaches the total number of demands previously stipulated by the user, the simulation is terminated.

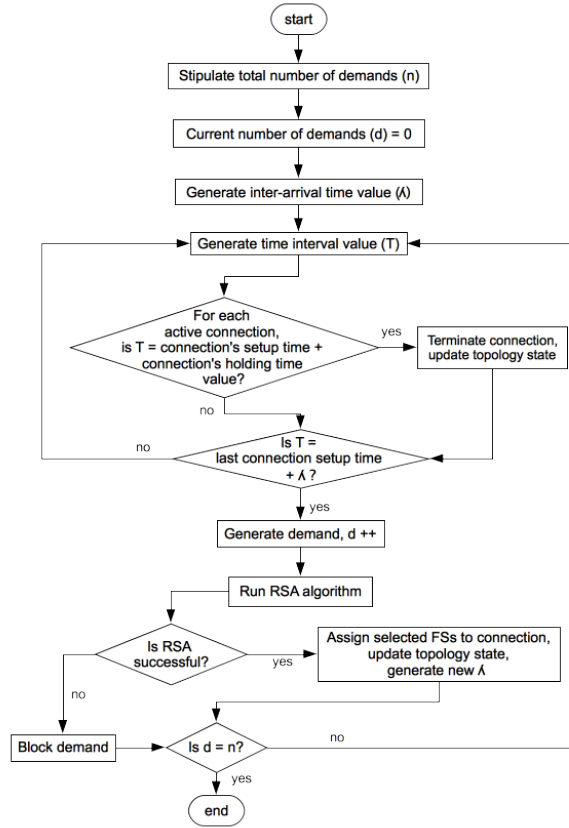


Figure 6.2: DSEON-Jsim operation flowchart

The simulator also outputs .txt files with network's performance results. A file containing number of connections established permits calculating total blocking probability and blocking probability per CT values. A file containing amount of bandwidth assigned permits evaluating the total amount of resources assigned and the amount of resources assigned per CT value and per bandwidth requirement. Other performance results files contains system's routes fragmentation levels.

6.2 Validation process

We implemented different validation procedures to guarantee the simulations were correctly performed and that the simulation results are reliable. The adopted validation procedures are:

- Comparison between simulator holding and inter arrival time values generated and the values generated by another mechanism available in the literature.
- Analysis of simulator log files.
- Assessment of performance results statistical properties.

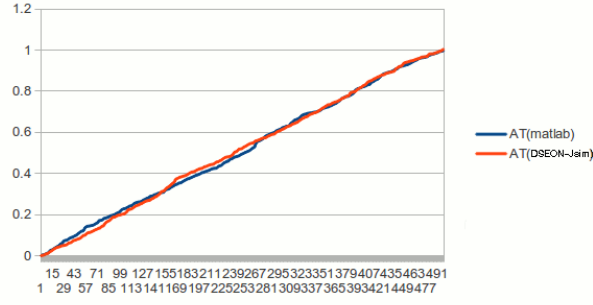


Figure 6.3: Plotted results generated by Matlab code and Java code used in the simulator

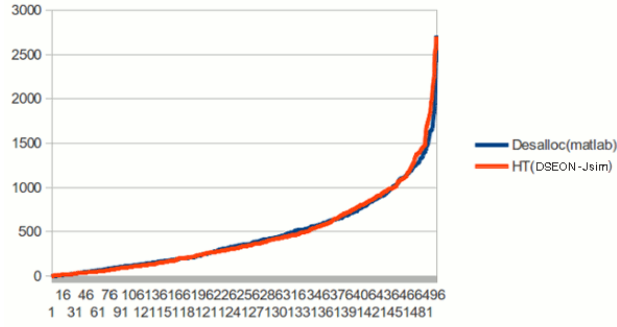


Figure 6.4: Plotted results generated by Matlab code and Java code used in the simulator

- Comparison between DSEON-Jsim results and results from simulations available in the literature with similar configuration.

6.2.0.1 Random values generator

In DSEON-Jsim connection requests follow a Poisson arrival process, in which the mean inter-arrival time λ varies with load. The demand lifetime is random following an exponential distribution with mean holding time equal to μ . The random values are generated by a Java method. In order to assess whether the random values generated follow a correct distribution we have compared results generated in DSEON-Jsim and the Matlab based connection requests generator adopted in [90]. Mean inter-arrival time λ is set to 0.2 and mean holding time $\mu = 500$. Figure 6.3 and 6.4 present the values generated after 500 occurrences. As can be observed, both inter-arrival time values (AT in both generators) and holding time values (HT in DSEON-Jsim and Desalloc in the Matlab generator) have similar results and curvature.

6.2.0.2 Log files

In order to guarantee the simulator is operating correctly, we analyze log files containing variable values registered at selected time intervals. In the main

log file, called “updating connections”, whenever a connection is established or terminated, network state, connection and assigned route information is registered. The connection’s information is:

- Bandwidth requirement.
- Source and destination nodes.

The selected route information is:

- Route id.
- Source and destination nodes.
- Array of slot availability before and after network state update.
- Map of gap size and position before and after network state update.

The information from “updating connections” log file assures that:

- The amount of FSs assigned to a connection is correct.
- FSs availability status is adequately updated.
- The selected route initiates and terminates at the demand’s source and destination nodes.
- All K alternative routes are being considered.

When a route is discarded for not being able to accommodate a demand, its map of gap size and position and the demand’s bandwidth requirement is outputted in a log file. This information is used to assure no gap of contiguous FSs in the inspected route has enough available FSs to accommodate the demand requirement.

The Priority Realloc mechanism has a complex structure and therefore it generates its own log files. Priority Realloc mechanism log files contain information that assesses:

- Whether the mechanism was successfully triggered.
- If the route largest gap index minus the amount of extra FSs required equals the FSs index selected by the FS reallocation mechanism.

Table 6.1: Statistical metrics for simulations results implementing KSP-FF bandwidth requirement scenario 4 with load equivalent to 1,000 Erlang

Statistical metric	BP	prop. BW	BP of Highest BW req
Average	0.069380	0.843422	0.677208
Variance	0.000014	0.000046	0.000319
Standard deviation	0.003771	0.006800	0.017866
Sample size	12	12	12
Upper bound	0.071513	0.847270	0.687317
Lower bound	0.067246	0.839574	0.667099
Confidence interval			
95% level	0.002133	0.003847	0.010108
Confidence interval			
99% level	0.002804	0.005056	0.013284

- In case the mechanism is blocked, what causes the blockage. The mechanism may not be triggered because the demand's CT value is not 2 or the route's largest gap index is 0 or one of the connections served by the extra FSs required has a CT value higher than 0.
- If the total number of FSs assigned to connections with CT value 0 are reduced when the mechanism is successfully triggered.

6.2.0.3 Results statistical properties analysis

We performed simulations in DSEON-Jsim in order to generate 12 samples of results for KSP-FF algorithm with bandwidth requirement scenario 4. Based on this sample we assessed the statistical properties of the results as can be observed in Table 6.1.

As can be observed, the sample's performance metrics have a small margin of error represented by the confidence interval. Blocking probability results for highest bandwidth requirement demands present highest margin of error of 0.013 for a confidence level of 99%. This means that there is a probability of 0.99 that for any simulation run BP results for highest bandwidth requirement demands will lie within the interval of the mean plus or minus the confidence interval. For general BP results the confidence interval for a confidence level of 99% is 0.002, which means that there is a probability of 0.99 that, for any simulation run, BP result will lie within the interval of the mean plus or minus 0.002. In both cases the reliability of performance results is high.

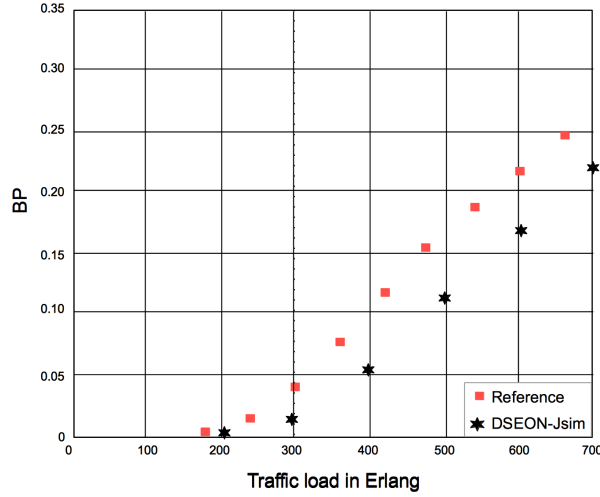


Figure 6.5: BP results achieved by simulation described in [4] and by DSEON-Jsim simulation

6.2.0.4 Literature simulations reproduction and results comparison

We adopted DSEON-Jsim to reproduce EON simulations that are available in the literature. We compared a benchmark algorithm (KSP-FF) results achieved by the selected literature simulations and DSEON-Jsim with the same or similar network configuration. Since there are not many EON dynamic scenario simulations fully described in the literature two simulations, among the four simulations performed, were reproduced using different network topologies.

We reproduced the simulation conditions described in [4]. BP results achieved by the DSEON-Jsim and in [4] can be observed in Figure 6.5. Blocking probability results achieved with DSEON-Jsim are similar but slightly better than the results achieved in [4], this can be partially justified by the fact that the K shortest paths may be different, most of the K alternate routes considered in DSEON-Jsim are disjoint for the same source/destination node pair.

Authors in [5] describe a simulation performed in the 14-node Japanese network, we have performed a simulation with similar configuration using the NSFNET topology. Even though the network topologies adopted are different, results achieved by DSEON-Jsim closely matches the ones achieved by the simulation described in the article as can be observed in Figure 6.6.

We reproduced the simulation configurations described in [6] in which the distribution of the bandwidth requirements is non-uniform and classified according to the distance between sources and destination nodes. We interpreted the equivalent number of FSs requirements in DSEON-Jsim. The simulation in [6] is performed in pan-European Nobel-EU network, we performed the DESON-Jsim

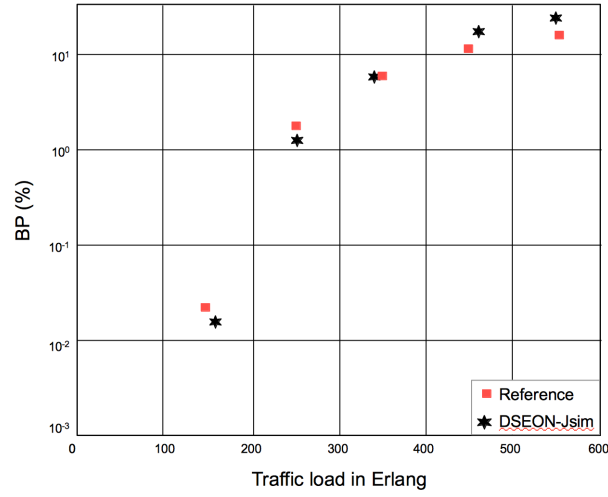


Figure 6.6: BP results achieved by simulation described in [5] and by DSEON-Jsim simulation

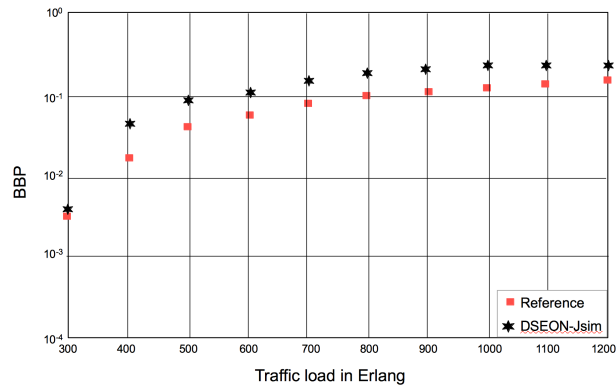


Figure 6.7: BBP results achieved by simulation described in [6] and by DSEON-Jsim simulation

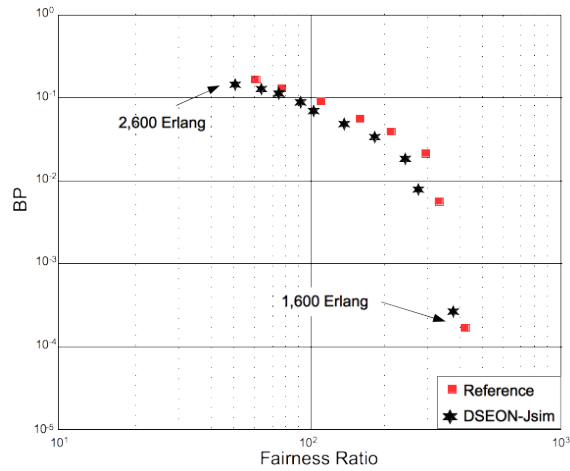


Figure 6.8: Comparison between BP and fairness ratio results obtained by DSEON-Jsim and those presented in [7]

simulations in NSFNET. DESON-Jsim KSP with $K=3$ is equivalent to the article's CP3 algorithm. The BP results from the simulation described in [6] and DESON-Jsim BP results can be observed in Figure 6.7.

In [7] performance metrics include, besides the blocking probability, the fairness level of service provision as described in Chapter 2. We reproduced the conditions of the simulations described in the article and achieved similar blocking probability and fairness level results with DSEON-Jsim as depicted in Figure 6.8. The fairness level is given by the ratio of highest bandwidth requirement demands blocking probability value connections to the lowest bandwidth requirement demands blocking probability.

In the four reproduced simulations, DSEON-Jsim achieves BP and BBP results similar to the BP results achieved by simulations described in the literature, thus indicating that DSEON-Jsim operates correctly.

7 Simulation Results

In this Chapter we present performance results achieved by simulations performed in DSEON-Jsim, an ad-hoc event driven Java based simulator described and validated in Chapter 5.3.2. The simulations results we present in this chapter refer to EON performance compared to WDM networks (Subsection 7.1.1), EONs performance according to bandwidth requirement characteristics (Subsection 7.1.2), and Priority Realloc performance compared to benchmark algorithms (Subsection 7.2).

The simulations main performance metrics adopted are blocking probability (BP) and bandwidth blocking probability (BBP). We remind that BP refers to the ratio of the number of blocked connections requests to the total number of connection requests received. BBP refers to the ratio of the blocked bandwidth to the total bandwidth requested. In general, in EONs, BBP results are higher than connection requests BP. That occurs because highest bandwidth requirement connections are blocked more often, as explained in Chapter 2 in which the fairness issue is debated.

In the EON simulations the bandwidth required by the connection requests is represented in number of FSs. All EON simulations consider only one modulation format, binary phase-shift keying (BPSK) with 1 bit per symbol [85]. The EON simulated does not consider guardbands as in simulations described in [6].

In all simulations, connection requests are generated dynamically following a uniform distribution among source and destination node pairs. All simulations run comprise 5×10^5 connections requests following a Poisson process with mean holding time (λ) set to 500 sec (exponential). Request inter-arrival times (μ) are also exponential and vary with loading. The benchmark algorithm adopted is KSP-FF for all EON simulations. The KSP-FF algorithm is explained in Chapter 2. Unless stated otherwise, all bandwidth requirements and CT values follow a non-uniform distribution properly described in each respective section. We decided to adopt a non-uniform distribution for these variables in order to represent a realistic traffic scenario as described in [83].

The network simulations runs were based either on National Science Foundation Network (NSFNET) or Nobel German network reference topologies. The NSFNET has 14 nodes and 21 links [91]. Its mean nodal degree is 3.00, mean number of hops for working paths is 2.14, mean link length is 1,086 km. NSFNET topology is depicted in Figure 7.1.

The Nobel German network has 17 nodes and 26 bidirectional links [82]. Its mean nodal degree is 3.06, mean number of hops for working paths is 2.7, mean link length is 143.1 km. Nobel German network topology is presented in Figure 7.2.

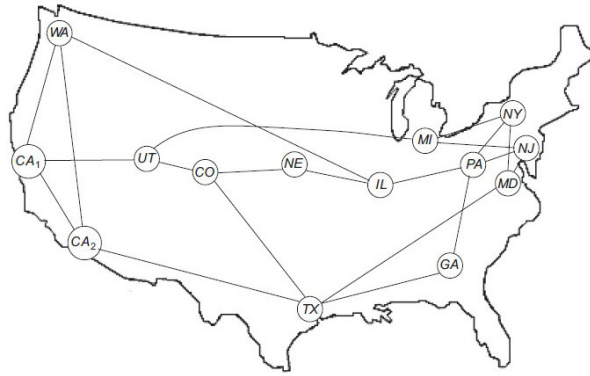


Figure 7.1: NSFNET reference network topology

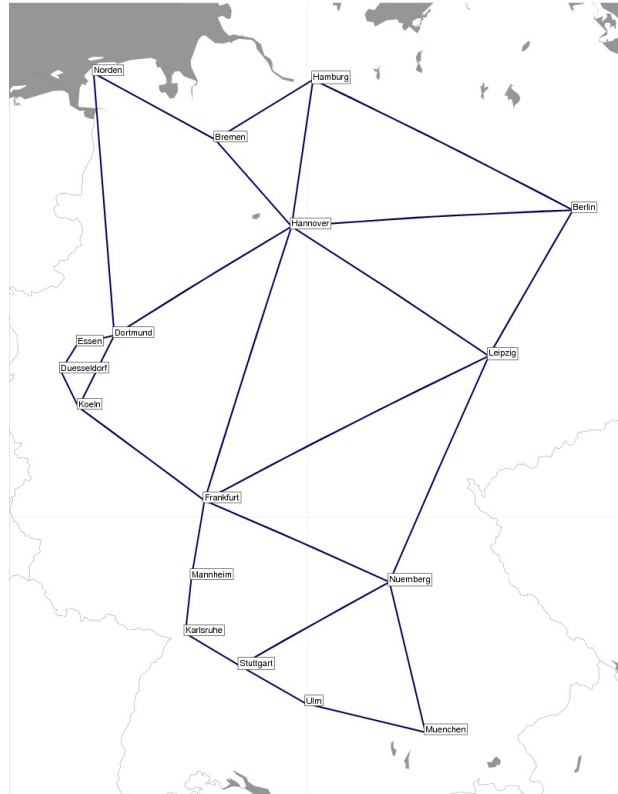


Figure 7.2: Nobel German reference network topology

7.1 EON simulations performance results and analysis

In this Section we present performance comparisons between EON and WDM networks and between different EON scenarios with diverse bandwidth requirement scenarios. In Subsection 7.1.1 we present simulation results for WDM networks and EONs with similar configurations so that the results between the two types of networks can be compared.

In Subsection 7.1.2 we present results and performance analysis for the KSP-FF algorithm for different bandwidth requirement scenarios. The aim of analyzing these scenarios is to be able to assess the impact of the BW requirement characteristics on EONs performance.

7.1.1 Comparison between EON and WDM network with grooming performances

In order to have a fair comparison, we performed simulations for a WDM network enhanced with grooming and simulations for EONs with similar configuration characteristics. In both network conditions we considered the Nobel German network topology (refer to Figure 7.2). Spectrum continuity and contiguity constraints are enforced for path and resource assignment computation in the EON, while only wavelength continuity constraint is enforced in the WDM network.

The WDM network we simulate implements a grooming mechanism, where, as briefly mentioned in Chapter 2, the total capacity of a wavelength may be shared by more than one connection. Therefore a lightpath will accommodate one or more connections as long as the sum of the connections bandwidth assigned are equal to or less than a wavelength's maximum bandwidth capacity. The aggregation of connections into a lightpath is performed electronically at the lightpath's end nodes.

The WDM network uses the KSP-FF algorithm for RWA, we implement the equivalent algorithm, also called KSP-FF, as the RSA algorithm in EON simulations. In both cases, we fix $K=3$.

In the WDM network, each fiber link contains 40 wavelengths of 100 Gbps each resulting in a link capacity of 4,000 Gbps. Each channel (wavelength) occupies 100 GHz [92] and each link comprises 4,000 GHz. The

bandwidth requirement considered in the simulations were 10, 40 and 100 Gbps non-uniformly distributed as depicted in Table 7.1.

To establish a network condition of EON simulations that would be similar to the WDM simulations, we had to establish bandwidth requirements in FSs that would relate to the bandwidth requirements of the WDM network simulations. A 4,000 GHz link in an EON comprises 320 FSs of 12.5 GHz each [92]. To determine the values of bandwidth requirement in the EON we considered how many connections of a given bandwidth value would fit in a WDM link and reproduced the same amount with respective BW requirements for an EON link.

A WDM link with grooming would accommodate 400 connection of 10 Gbps, in an EON the minimum resource requirement would be 1 FSs and an EON link would accommodate 320 connections of 1 FSs. A WDM link would accommodate 80 connections of 40 Gbps (2 per wavelength), an EON link would accommodate 80 connections of 4 FSs. If a WDM link was not divided into wavelengths but could have its resources continuously assigned, a WDM link with grooming would accommodate 100 connections of 40 Gbps, in an EON a link would accommodate a 100 connections of 3 FSs. A WDM link with grooming would accommodate 40 connections of 100 Gbps, one per wavelength, the equivalent to 40 connections of 8 FSs in an EON link. With this relation of bandwidth requirements in FSs we delineated scenarios EON 1 and EON 2 as described in Table 7.1.

Due to the fact that the minimum resource requirement in an EON is 1 FS, scenarios EON 1 and EON 2 may suffer discrepancy relating to the WDM scenario. The minimum resource requirement in the WDM network is 10 Gbps that would be equivalent to 10 GHz and not 12.5 GHz as afforded by 1 FS. This difference in bandwidth requirement may decrease the EON performance level when compared to the WDM network. For this reason we have also considered a scenario where each network link would contain 400 FSs and 5,000 GHz. Indeed there are studies in the literature that consider such capacity for an EON network link as described in [4] and [7]. In this scenario, denominated scenario EON 5 and detailed in Table 7.1, one EON link would accommodate 400 connections of 1 FSs, 80 connections of 5 FSs and 40 connections of 10 FSs. The bandwidth requirements for the delineated scenarios follow the same non-uniform distribution detailed in Table 7.1.

We compared the network performance of scenarios WDM, EON 1, 2 and 5, regarding BP and BBP. The graphics presented here depict the results in logarithm scale and, for these reason, values equivalent to zero are not illustrated.

Table 7.1: Distribution of bandwidth requirements

Scenario	BW Requirement		
	10 Gbps	40 Gbps	100 Gbps
WDM	10 Gbps	40 Gbps	100 Gbps
EON 1	1 FS	3 FSs	8 FSs
EON 2	1 FS	4 FSs	8 FSs
EON 5	1 FS	5 FSs	10 FSs
probability	0.80	0.15	0.5

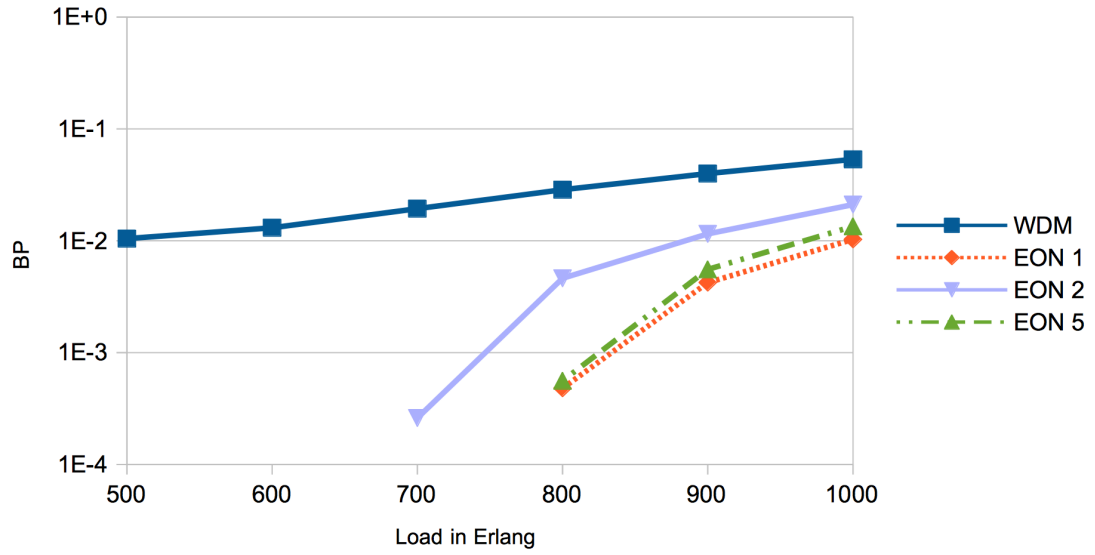
**Figure 7.3:** BP results for WDM and EON scenarios 1, 2 and 5 using KSP-FF algorithm

Figure 7.3 presents performance results regarding BP in WDM network and EON. As can be observed, as offered traffic load increases, the EON network scenarios perform better than WDM with grooming. For an offered traffic load of 1,000 Erlang, scenario EON 2 achieves BP result 60% lower than the BP for the WDM network, while scenarios EON 1 and 5 achieve blocking probability at least 75% lower than the BP for the WDM network with grooming.

Figure 7.4 presents BBP results for EON and WDM network scenarios. It is possible to observe that, as offered traffic load increases, EON scenarios perform better in terms of BBP than the WDM network. Specifically, for an offered traffic load of 1,000 Erlang, scenario EON 2 BBP result is 39% lower than the value achieved in the WDM network while scenarios EON 1 and 5 decreased BBP results in 64% the value achieved with WDM with grooming.

In general, from the simulations performed, it was possible to conclude that an EON with equivalent connection bandwidth requirements as the WDM network

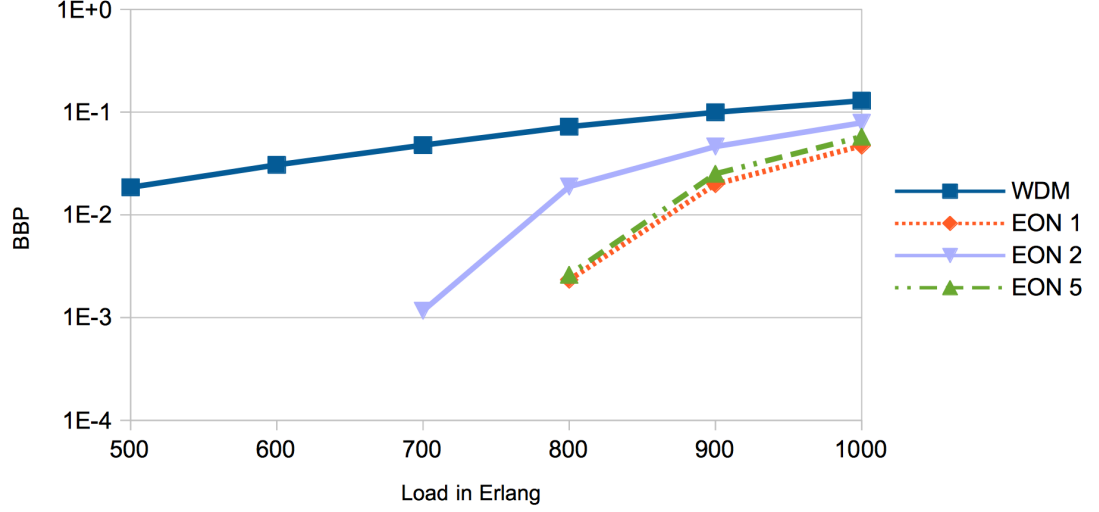


Figure 7.4: BBP results for WDM and EON bandwidth requirement scenarios 1, 2 and 5 using KSP-FF algorithm

tends to outperform the WDM network in number of connections established and efficiency of resources distribution.

7.1.2 EON performance with diverse BW requirement scenario

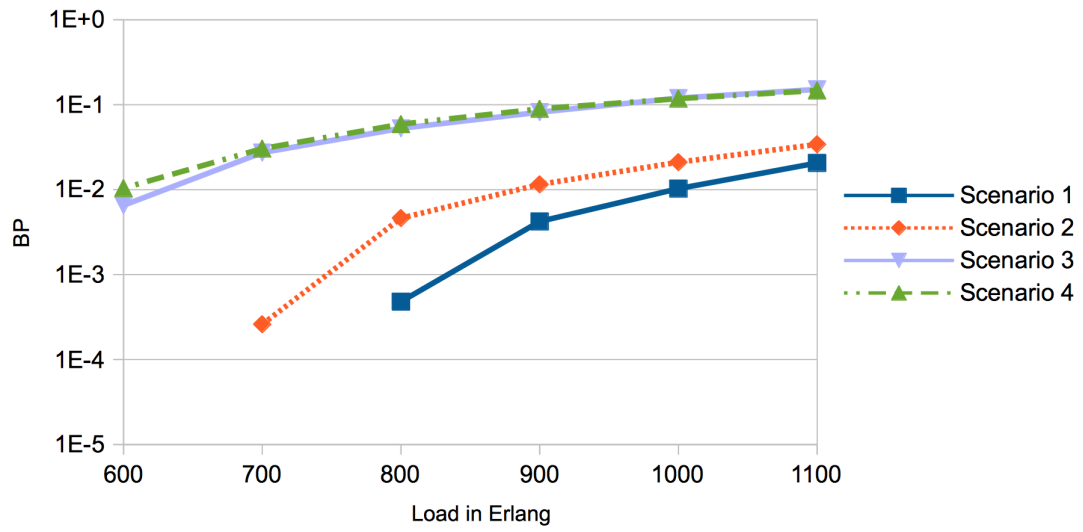
As explained in Chapter 2, in an EON, the demand matrix characteristic interfere on the resource usage efficiency. We compared the performance of EONs with diverse bandwidth requirement scenarios. All simulations were performed either on the Nobel German network topology or on the NSFNET topology (refer to Figure 7.1) and implement the KSP-FF algorithm with $K=3$. Each fiber link has 320 FSs of 12.5 GHz, resulting in 4,000 GHz spectrum capacity.

We simulated the aforementioned conditions for BW requirement scenarios 1 and 2 described in Subsection 7.1.1 and two other bandwidth requirement scenarios in which the smallest bandwidth requirement value is equal to 2 FSs instead of 1 FS. The four BW requirement scenarios simulated can be observed in Table 7.2. Bandwidth requirement values are selected randomly following a non-uniform probability distribution previously adopted for scenarios 1 and 2 and detailed in Table 7.1.

The BP of the different bandwidth requirement scenarios in Nobel German network topology may be observed, in logarithmic scale, in Figure 7.5 and in NSFNET network topology in Figure 7.6. Comparing BP results for the two topologies it becomes clear that simulations in NFSNET network topology have,

Table 7.2: Bandwidth requirement scenarios (in number of FSs)

scenarios	Total number					sum	average
	of FSs per link	FSs	FSs	FSs	FSs		
1	320	1	3	8	-	12	4
2	320	1	4	8	-	13	4.34
3	320	2	3	8	-	14	4.67
4	320	2	4	8	-	13	4.34

**Figure 7.5:** BP for various BW requirement scenarios in Nobel German network topology

in general, better performance than in Nobel German network topology. However, in both network topologies it is possible to observe that BW requirement scenarios 1 and 2 present lower BP results. BW requirement scenarios 3 and 4 have higher BP results, and, as the offered traffic load increases, the difference between blocking probability for scenarios 3 and 4 and for scenarios 1 and 2 increases. For an offered traffic load of 1,100 Erlang, for instance, the BP results for scenario 1 is 86% lower than BP result for scenario 4 in Nobel German network topology, and 93% in NSFNET network topology.

It is interesting to observe that, for higher traffic loads, over 700 Erlang in Nobel German network topology and over 800 Erlang in NSFNET network topology, BP results for BW requirement scenarios 3 and 4 are virtually the same. Since BW scenario 4 requires a higher sum of FSs it would be expected that the BP for this BW scenario would be higher. However, all values of FSs requirements of BW requirement scenario 4 have one common denominator,

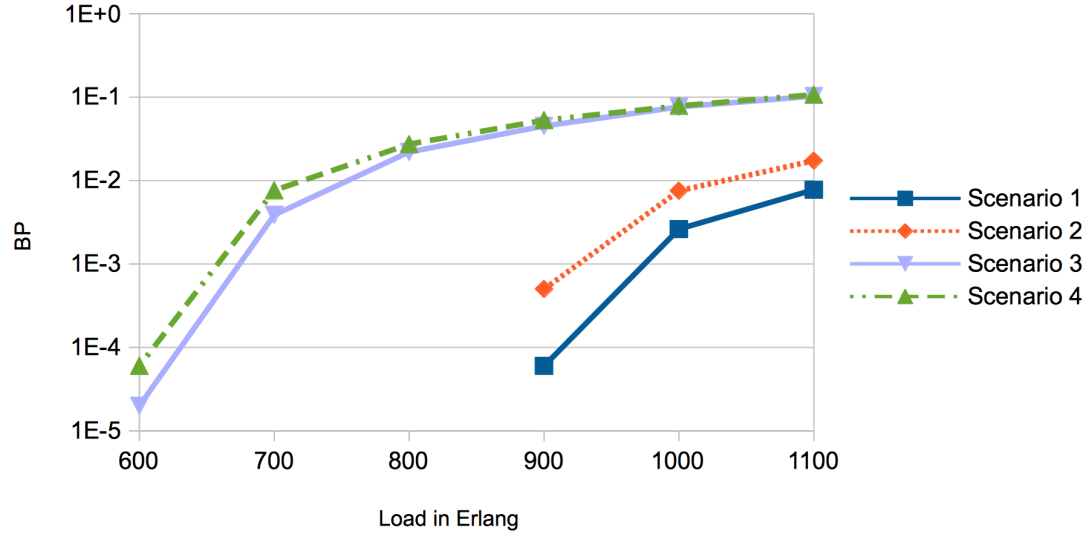


Figure 7.6: BP for various BW requirement scenarios in NSFNET network topology

therefore the resulting spectrum fragmentation with BW requirement scenario 4 permits a better fitting of incoming connections requests than BW requirement scenario 3. The relation of a common denominator for FSs requirements and spectrum efficiency allocation is explained in Chapter 2 .

Fairness of service regarding highest BW requirement demands blockage when compared to lower BW requirement connection requests is a serious issue in EONs as explained in Chapter 2. In both topologies, for all tested offered traffic load, the BP of lowest BW requirement demands is null in BW requirement scenarios 1 and 2, this result is partially justified by the fact that connections requests that require only 1 FS may be accommodated in any gap of available FSs. For this reason, BP fairness level in BW scenarios 1 and 2 is solely dependent on the BP of the highest BW requirement demands.

We analyze network service fairness level as the ratio of the BP of highest BW requirement demands to the BP of lowest BW requirement demands as proposed in [7]. The highest the ratio result the lower the service fairness level. The closer the ratio result is to 1 the better is the service fairness level.

The ratio of BP results is presented, in logarithmic scale, for Nobel German network topology in Figure 7.7 and for NSFNET network topology in Figure 7.8. Since lowest BW requirement connections BP results for scenarios 1 and 2 are null only BP ratios for scenarios 3 and 4 are presented. Please note that for some traffic loads the BP result is zero for the lowest bandwidth requirement demands, and, for these reason there is no ratio result for these traffic loads. In both topologies, for bandwidth requirement scenarios 3 and 4 the fairness level

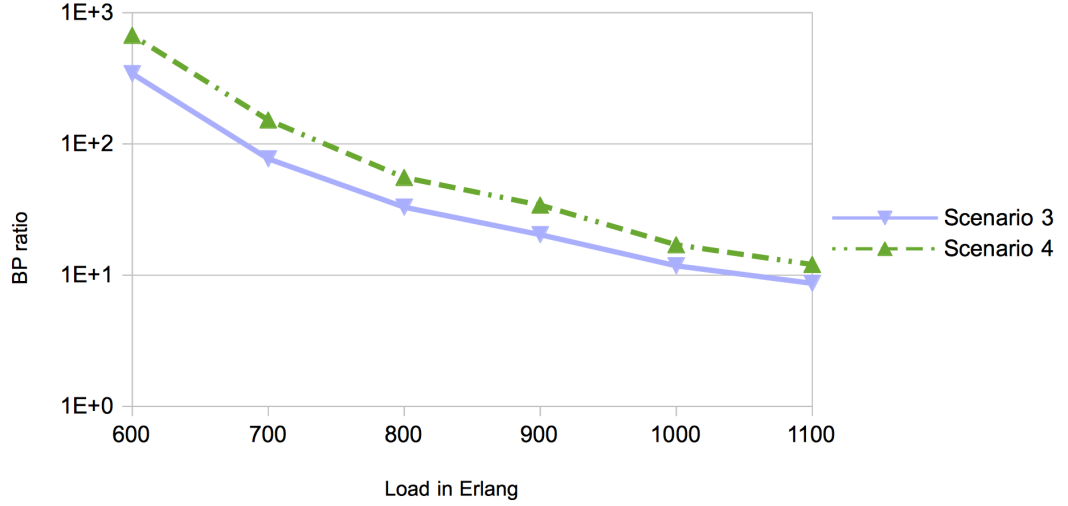


Figure 7.7: Ratio between highest and lowest BW requirement demands BP in Nobel German network topology

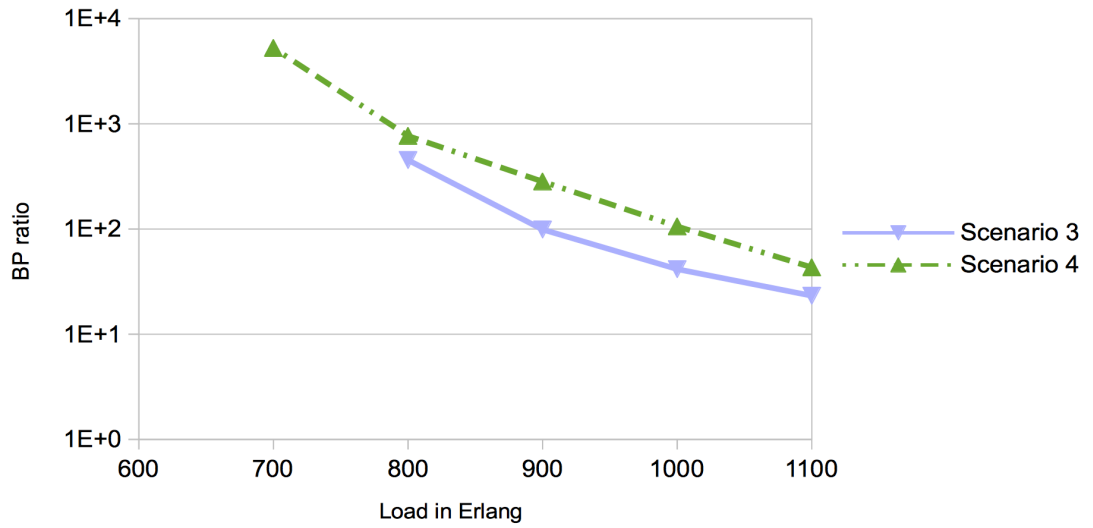


Figure 7.8: Ratio between highest and lowest BW requirement demands BP in NSFNET network topology

tend to decrease as the offered traffic load increases, that happens due to the increase in BP of lowest BW requirement connection requests (refer to Figures 7.11 and 7.12).

Due to the fact that lowest BW requirement demands BP results are null in scenario 1 and 2, we also assess fairness level as the difference between highest and lowest BW requirement demands BP. The difference between blocking probability results of highest and lowest bandwidth requirement connections for Nobel German network topology is presented in Figure 7.9 and for NSFNET network topology in Figure 7.10. It is possible to observe that in scenarios 1 and 2 the difference in blocking probability is lower than in BW requirement scenarios

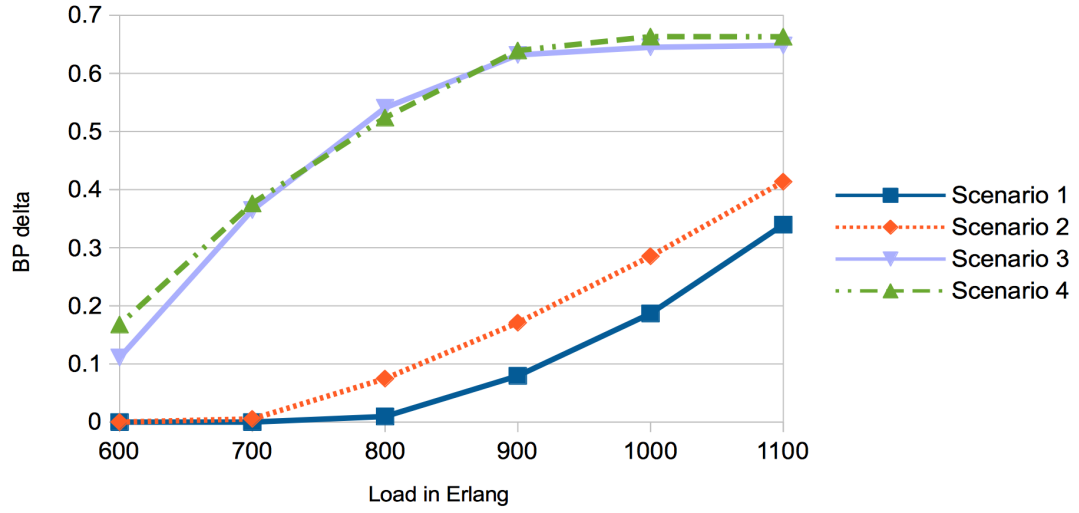


Figure 7.9: Difference between highest and lowest BW requirement demands BP results in Nobel German network topology

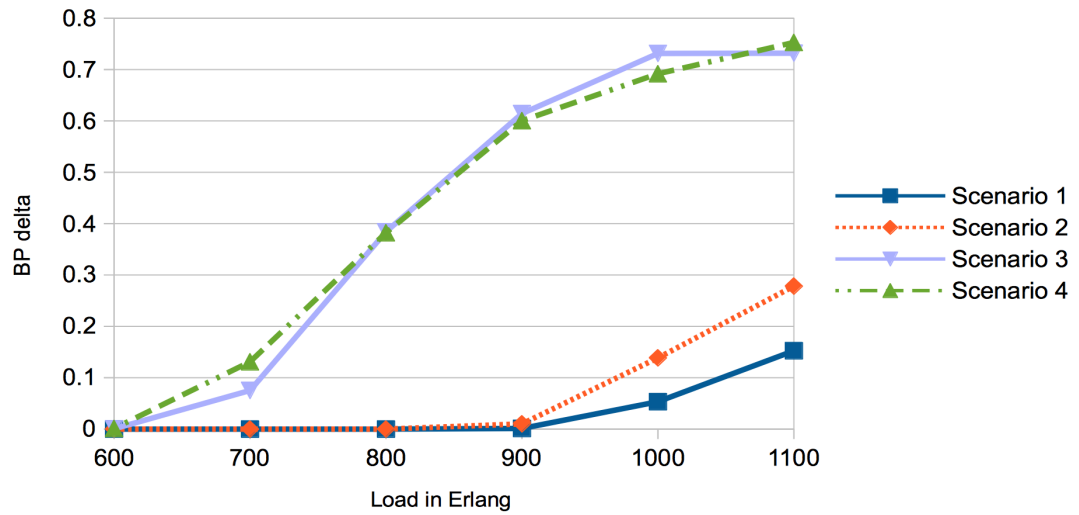


Figure 7.10: Difference between highest and lowest BW requirement demands BP results in NSFNET network topology

3 and 4. In Nobel German network topology, for an offered traffic load of 1,100 Erlang the absolute difference in BP between highest BW requirement demands and lowest BW requirement demand is 0.33 for BW requirement scenario 1 and 0.66 for BW requirement scenario 4. For the same load, in NSFNET network topology the difference in BP between highest BW requirement demands and lowest BW requirement demand is 0.15 for BW requirement scenario 1 and 0.75 for BW requirement scenario 4.

While the BP of 1 FS is either very low or null, the BP for the demands that require 2 FSs is much higher, as can be observed in Figure 7.11 for Nobel German network topology and in Figure 7.12 for NSFNET network topology. For

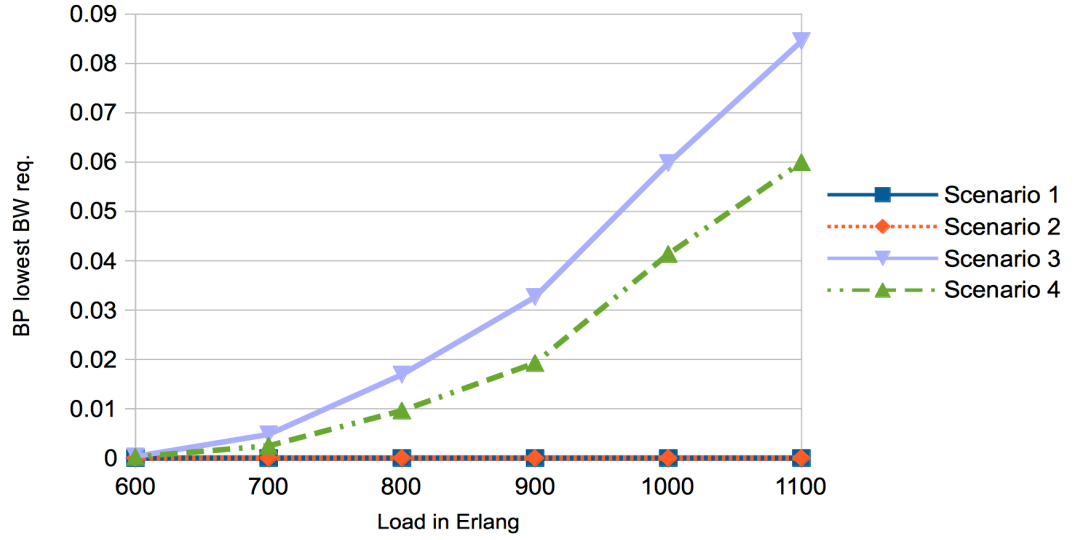


Figure 7.11: BP for lowest bandwidth requirement connections in Nobel German network topology

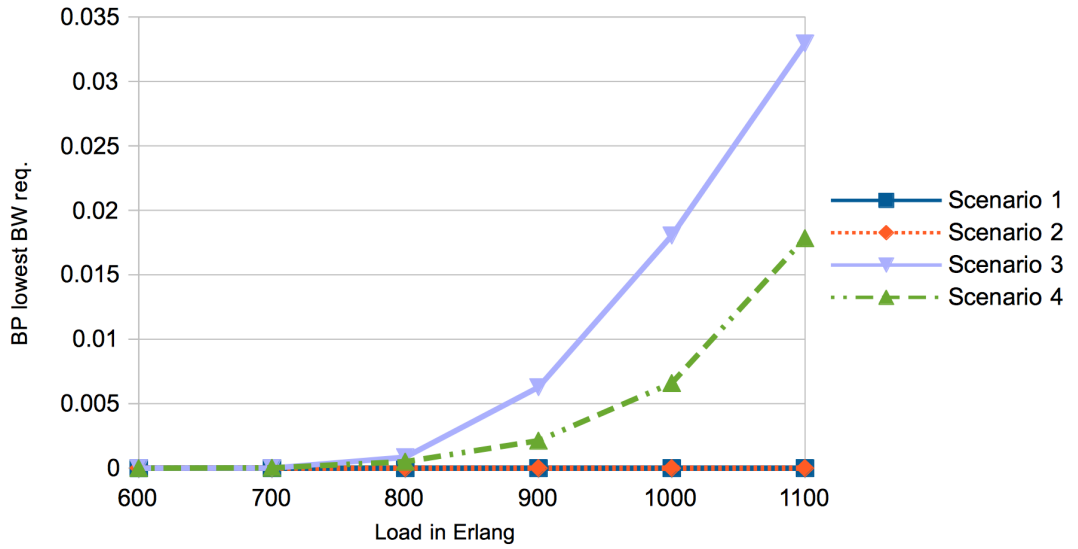


Figure 7.12: BP for lowest bandwidth requirement connections in NSFNET network topology

a traffic load of 1,100 Erlang the blocking probability for lowest BW requirement demands in Nobel German network topology is 8.5% for scenario 4 and 6 % for scenario 3, while in NSFNET network topology it is 3% and 1.7% respectively.

The higher value of FS requirement in lowest BW requirement demands has its toll on highest BW requirement demands, because the amount of available resources is lessen after accommodating these lowest rates connections. This explains why the blocking probability difference in scenarios 3 and 4 is higher than in scenarios 1 and 2 as can be observed in Figures 7.9 and 7.10.

Connections with lowest bandwidth requirement value represent 80% of all

connection requests, therefore their low blocking probability results tend to decrease the overall blocking probability results of all connection requests as can be observed in Figures 7.5 and 7.6.

Even though simulation conditions were different, the BP ratio values observed in our simulations were very similar to the values observed in [7]. Thus, we can conclude that the fairness issue regarding the establishment of highest BW BW requirement connections is indeed grave and habitual in EONs. We have also observed, from the aforementioned simulation results, that the higher the sum of bandwidth required, the less is the amount of resources available to accommodate highest BW requirement connections. However, we could observe that by guaranteeing a common denominator for all BW requirement values this prejudicial effect on highest BW requirement connection request tends to be diminished.

We analyze the spectrum fragmentation level of the network routes with each of the studied scenarios. Fragmentation level results for Nobel German network topology can be observed in Figure 7.13 and for NFSNET network topology in Figure 7.14. From the results in NSFNET network topology, it is possible to observe that, for scenarios 1, 2 and 3, the spectrum fragmentation level increases as offered traffic load increases until an inflection point of offered load in which the tendency is interrupted. In Nobel German network topology, in scenario 1 and 2 the spectrum fragmentation increases until 900 Erlang or 1,000 Erlang, and for higher loads the spectrum fragmentation levels maintains the same value.

We note that for all scenarios, and in both networks, after a given value of offered traffic load, as the load increases the spectrum fragmentation level starts to decrease. This occurrence can be explained by the fact that as traffic offered load increases, the number of available FSs decreases reaching a point in which there are almost as much FSs available as the number of contiguous FSs available in a gap, decreasing the result for external fragmentation level equation.

In both networks the spectrum fragmentation level decrease with BW requirement scenario 4 is outstanding. For offered traffic loads higher than 800 Erlang, spectrum fragmentation with scenario 4 is always lower than the spectrum fragmentation with other BW requirement scenarios.

The studied scenarios presented very different spectrum fragmentation results. Scenario 4 is the scenario in which the sum of FSs required is the highest when compared to the other tested scenarios. For this reason, with lower offered traffic load values, the spectrum fragmentation was higher for this scenario

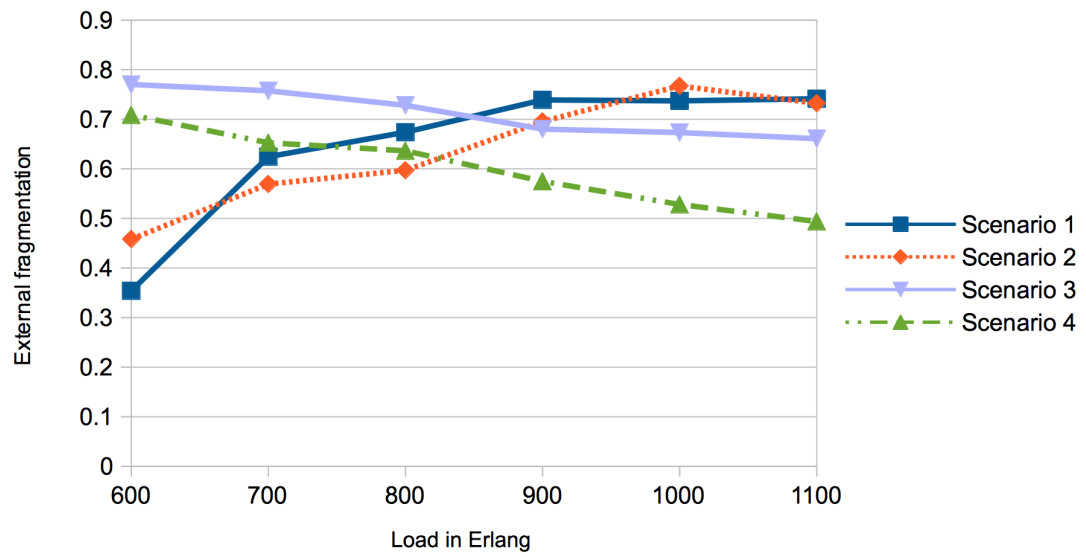


Figure 7.13: Spectrum fragmentation level in NSFNET network topology

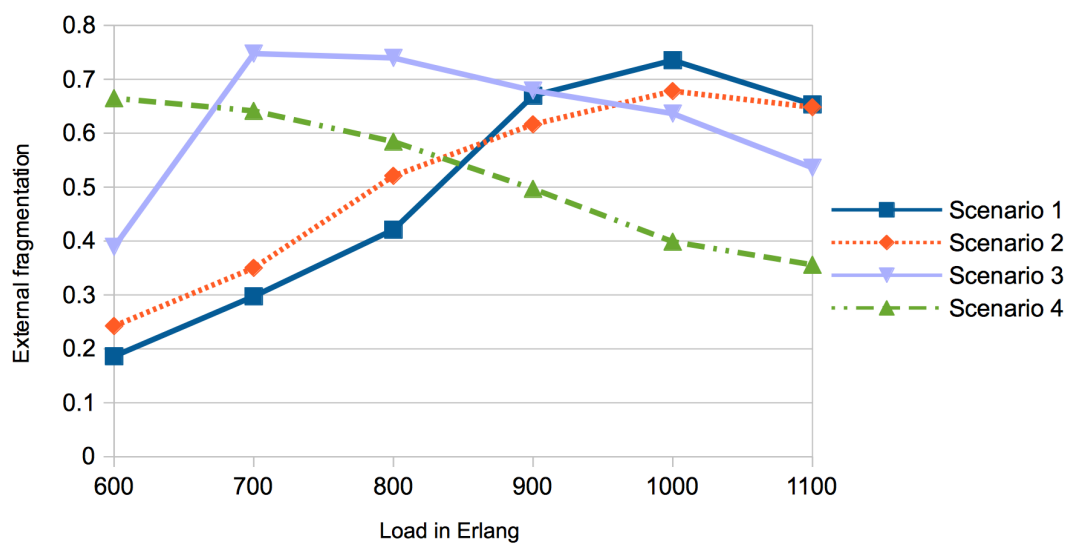


Figure 7.14: Spectrum fragmentation level in NSFNET network topology

Table 7.3: BW requirement and CT value probabilities for BW requirement scenario 4

probability	0.85	0.15	0.05
number of FSs	2	4	8
CT value	0	1	2

because it requires more bandwidth, there were less available FSs, increasing the fragmentation level equation. However after a given value of offered traffic load, the spectrum is being fully assigned and gaps of recently terminated connections are allocated to incoming demands. Scenario 4 has a higher optimization of gaps assignment and therefore presents lower spectrum fragmentation levels.

7.2 Simulation results for Priority Realloc mechanism performance in EONs

In this Section we present simulations performance results for our proposed mechanism denominated Priority Realloc. Simulations were performed in the NSFNET network topology. This network topology was selected due to its broad adoption in simulations available in the literature and also due to its results regarding fairness levels of highest BW requirement connection establishment with the KSP-FF algorithm as described in Subsection 7.1.2.

CT values are randomly selected in the range (0-2), following a non-uniform distribution probability described in Table 7.3. Bandwidth requirement values, in number of FSs, are randomly selected following a non-uniform distribution probability (refer to Table 7.3), between the possible FSs requirement values defined in bandwidth requirement scenario 4 (refer to Table 7.3). In simulations described in Subsection 7.1.2, this bandwidth requirement scenario presented high values of blocking probability and low fairness level regarding highest BW requirement connection establishment. Under the described conditions the Priority Realloc mechanism would be triggered more often than in other network scenarios. A network condition where the analyzed proposed mechanism would be triggered this often would enable adequate results for mechanism performance assessment.

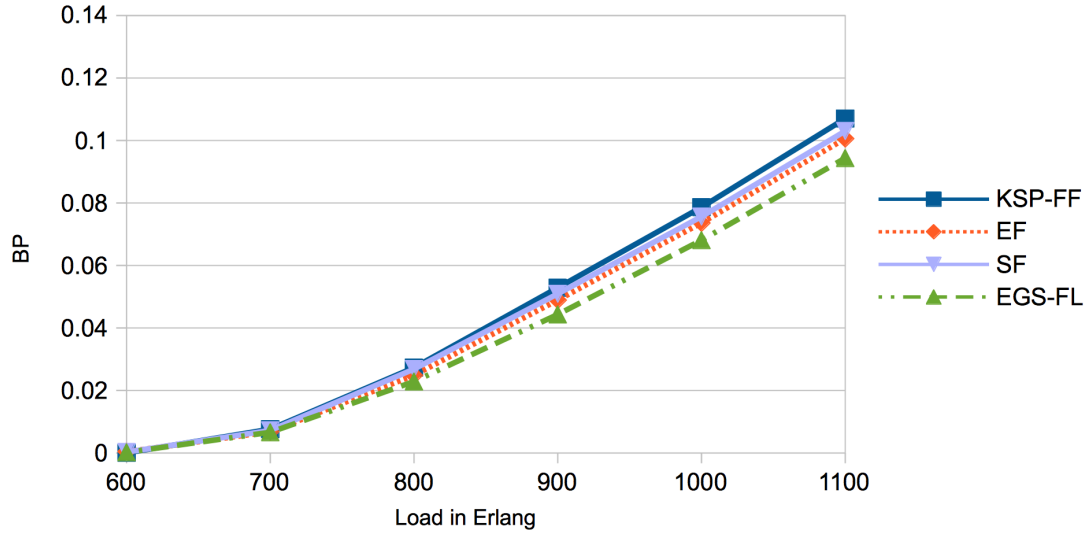


Figure 7.15: BP results of tested RSA algorithms

7.2.1 ESG-FL algorithm results

In this Subsection we exclusively analyze the performance of the mechanism's first algorithm, ESG-FL. We want to assess the level of benefit provided by ESG-FL in relation to other fragmentation-aware RSA algorithms available in the literature. To this aim we consider KSP-FF algorithm as benchmark and compare performance results between ESG-FL, EF and SF algorithm (these algorithms are explained in Chapter 3).

The performance metrics we adopt are blocking probability, bandwidth blocking probability and external fragmentation (proposed in [19] and explained in Chapter 2).

Figure 7.15 presents blocking probability results for the tested algorithms. It is possible to observe that any fragmentation-aware algorithm achieves better BP results than KSP-FF. However it is also possible to observe that the decrease in blocking probability provided by each of the tested algorithms when compared to KSP-FF is modest.

Figure 7.16 presents the proportional decrease in BP results promoted by each of the tested algorithms over KSP-FF. EGP-FL provides the highest decrease in blocking probability when compared to KSP-FF. For an offered traffic load of 1,100 Erlang the BP result with EGS-FL is 12% lower than the BP result with KSP-FF. For the same offered load the BP result decrease promoted by EF over KSP-FF is 6% and for SF it is 4%.

We have also analyzed the algorithms proportional amount of blocked

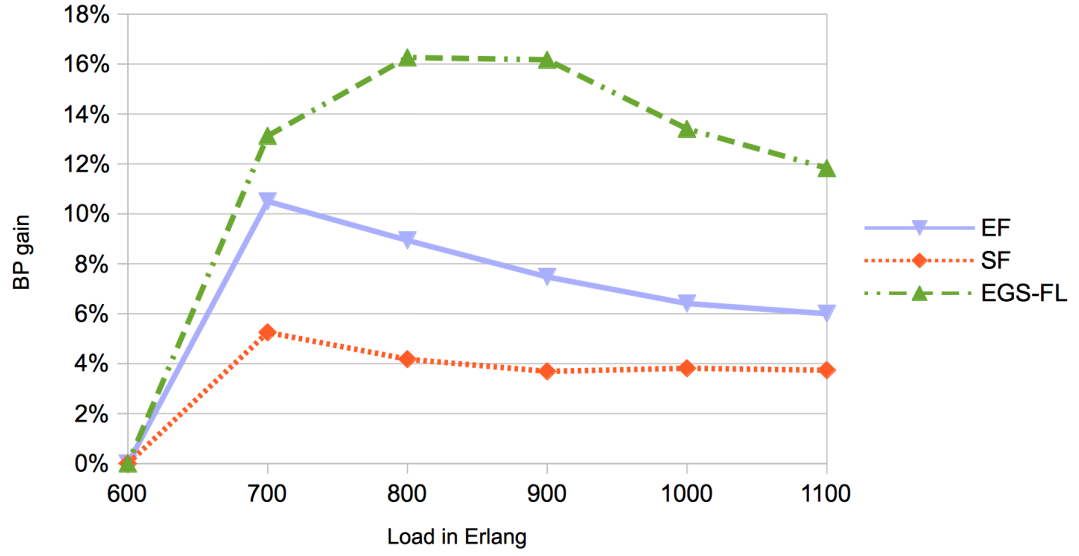


Figure 7.16: BP reduction gain of tested algorithms over KSP-FF

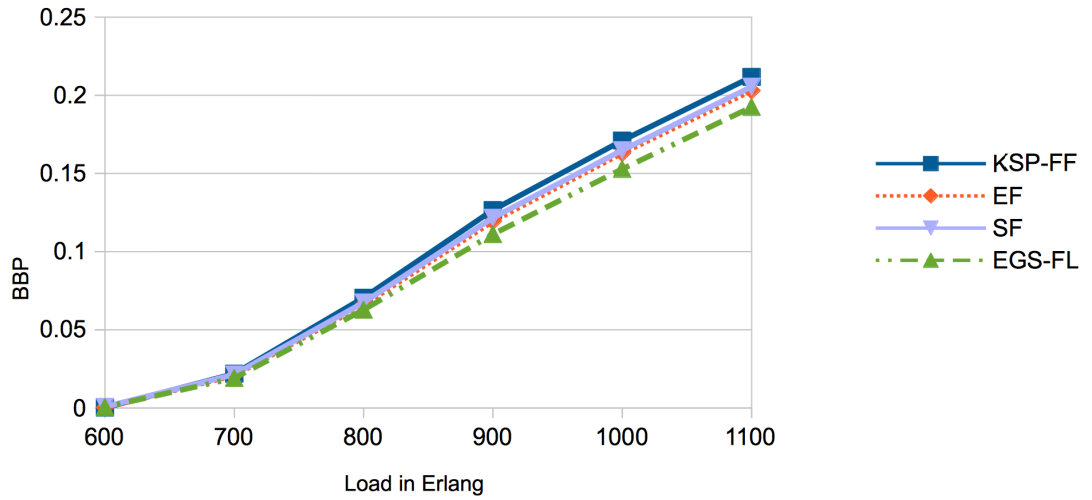


Figure 7.17: BBP results for tested algorithms

resources represented by the bandwidth blocking probability and depicted in Figure 7.17. The BBP results are higher than BP results which is characteristic to EONs, and previously explained in Chapter 2. As occurred to BP results and as expected, BBP results increase with load. When compared to KSP-FF all tested RSA algorithms presented lower BBP results. However the decrease provided was modest.

The BBP decrease promoted by the tested algorithms BBP results and KSP-FF BBP results represents the benefit of the tested algorithms over the benchmark and can be observed in Figure 7.18. The BBP benefit promoted by ESG-FL when compared to KSP-FF is more noticeable than the benefit promoted by the other fragmentation-aware RSA algorithms. As traffic load increases the

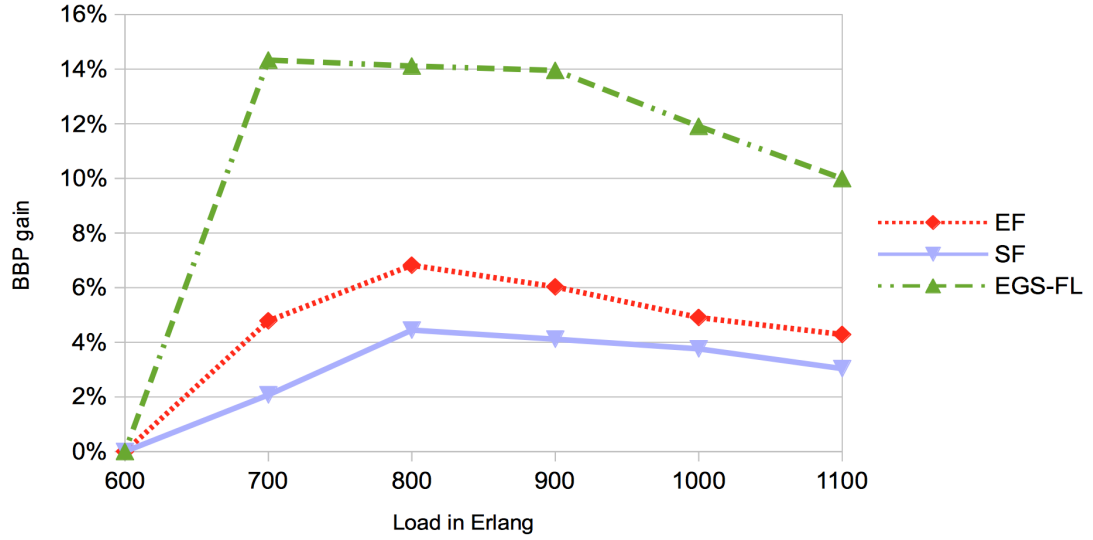


Figure 7.18: BBP reduction gain of tested algorithms over KSP-FF

ESG-FL benefit becomes even higher when compared to the other algorithms. For an offered traffic load of 1,100 Erlang, ESG-FL promoted BBP decrease of 10 % when compared to KSP-FF while EF achieved a 4 % decrease and SF a 3 % decrease. To this extent, the BBP benefit provided by ESG-FL is representative while the benefit promoted by EF and SF is almost negligible.

Since RSA algorithms focus on decreasing network spectrum fragmentation level we analyzed the spectrum fragmentation level achieved by the RSA algorithms and KSP-FF, the results are presented by Figure 7.19. The spectrum fragmentation results presented are the average external fragmentation value of all routes and are achieved by the sum of the external fragmentation of all routes divided by the number of pre-calculated routes. As expected, KSP-FF have a higher level of spectrum fragmentation for any offered traffic load. The fragmentation-aware RSA algorithms do decrease spectrum fragmentation when compared to spectrum fragmentation resulted from implementing KSP-FF.

All in all, we note that the studied fragmentation-aware RSA algorithm, in general, promote a very moderate benefit in EONs regarding connections establishment. This circumstance is explained by the fact that, even though the analyzed algorithms focus on decreasing the route spectrum fragmentation, there is no manner to control the effects on connections establishment and termination on the links that are used by other routes in what is known as the horizontal fragmentation (refer to Chapter 2). However decreasing the number of route spectrum gaps whenever possible does improve the spectrum fragmentation level in the network as we observed by the results presented in this section.

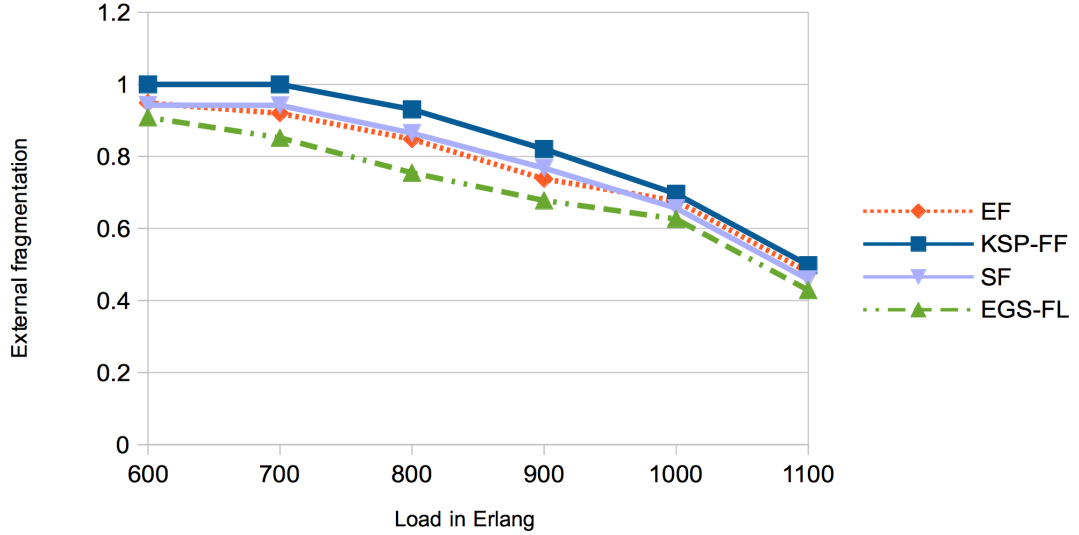


Figure 7.19: Spectrum fragmentation level for tested algorithms and KSP-FF

7.2.2 Priority Realloc mechanism results

We adopt KSP-FF and EGS-FL as benchmark algorithms, which have been previously explained in Chapter 2. The performance improvement of EGS-FL over KSP-FF is analyzed in the previous Subsection. The decision of adopting EGS-FL as benchmark algorithm relies on the need to assess whether the Priority Realloc promoted benefit is higher than the benefit promoted by EGS-FL.

In order to measure the mechanism performance we rely on the same performance metrics considered in Subsection 7.1.2: blocking probability, bandwidth blocking probability and the fairness level. We also analyze proportion of times the Priority Realloc mechanism was triggered and, since the proposed mechanism tends to improve resources use efficiency, we also analyzed the average routes spectrum fragmentation level.

The preemption of resources from lower priority connections, promoted by Priority Realloc mechanisms, has a direct impact on bandwidth blocking probability results and impel interpretation of blocking probability results. Consequently, in Priority Realloc, BP and BBP per demand type present different results, whilst in KSP-FF and EGS-FL the results are equal. A numerical analysis on the Priority Realloc procedure influence over the BP and BBP performance metrics is outlined in Subsection 7.2.2.1.

The Priority Realloc HBCT mechanism presents a negligible interference on Priority Realloc HB overall network performance, partially explained by the negligible increase in trigger occasions when compared to Priority Realloc HB, as

analyzed in Subsection 7.2.2.2. For this reason we do not present BP, BBP, and fairness level results for Priority Realloc HBC T as those are virtually the same values as the ones achieved with Priority Realloc HB. However Priority Realloc HBC T presents improvement in service for CT2 connections and therefore we present performance analysis according to connections CT values for Priority Realloc HBC T in Subsection 7.2.2.7

7.2.2.1 Interpretation of BP and BBP performance metrics for Priority Realloc mechanism

Regarding the Priority Realloc mechanism, the performance metrics represent a given point in time of the resources allocation condition, they do not consider the proportional amount of time the resources have been allocated before preemption.

When the Priority Realloc mechanism is implemented, in some cases, the whole amount of resources assigned to a given connection may be preempted. When this happens it would be correct to consider the connection is, in fact, terminated. These active connections disruptions are not considered as blocked connections and therefore are not accounted for in the blocking probability results. However it is important to analyze the probability at which this situation would happen, so we can interpret the blocking probability results.

In Priority Realloc HB, only demands with the highest BW requirement may trigger preemption of resources, that only occurs when this demand is blocked with the EGS-FL mechanism. The proportion of times the mechanism was successfully triggered by the total number of connection requests is depicted in Figure 7.20. For an offered traffic load of 1,100 Erlang the mechanism preempts resources in 2% of all connection requests.

The probability of preemption is uniformly distributed in a given moment of a connection's active time, it is possible to infer that, in average, connections maintain their original resources assigned for 50.5% of its active time, as justified by Equation 5.1 in Chapter 5.

A request for 8 FSs, after finding a gap of available FSs, may require from 1 to 7 extra FSs with the same probability. Connections with 8 FS will never be disrupted. Connections with 4 and 2 FSs may be disrupted, but they will not be disrupted every time preemption of resources takes place.

If an active connection has 2 FSs it has 0.5 probability that all of its FSs are within the range of reallocated FSs and if it has 4 FSs it has 0.25 probability that

all of its FSs are within the range of reallocated FSs. In case a connection has all its assigned FSs in the range of reallocated FSs the connection may be disrupted. If a connection has 4 FSs, the reallocation of 7, 6, 5 or 4 FSs would disrupt the connection, so there is $4/7$ (0.57) chances the connection would be disrupted. If a connection has 2 FSs, the reallocation of 7, 6, 5, 4, 3 and 2 FSs would disrupt the connection, so there is $6/7$ (0.86) chances the connection would be disrupted.

So, in case preemption of resources occur, which may happen in 2% of all connection requests for a traffic load of 1,100 Erlang, there is a chance a connection with 2 FSs will be disrupted with probability 0.43 (0.86×0.5) in 50% of its holding time. And there is a chance a connection with 4 FSs will be disrupted with probability 0.14 (0.57×0.25) in 50.5% of its holding time.

The resources extracted from an active connection are not deducted from the total amount of resources assigned since these resources are being reallocated to another connection. On the other hand, the reallocated resources are deducted from the amount of resources assigned to the type of connection it was extracted from. For instance, if FSs are deallocated from CT0 connections these resources will be subtracted from the registered amount of FSs assigned to CT0 connections, if the FSs are extracted from highest BW requirement connection the amount of resources will be deducted from the registered amount of resources assigned to this type of connection. These resources deduction alters BBP results for the specific types of connections, but do not interfere in the BBP result for all connection requests.

7.2.2.2 Priority Realloc mechanism trigger analysis

The Priority Realloc mechanism is called when a prioritized demand is blocked by EGS-FL algorithm, and is only successfully triggered, preempting FSs, when all connections accommodated by the reallocated FSs have CT0. Therefore, the mechanism trigger depends on the proportion of prioritized demands in all connection requests and the proportion of CT0 connections in all active connections.

In Priority Realloc HB, only demands with highest BW requirement may trigger the mechanism. In the simulated scenario only 5% of connection requests require 8 FSs (refer to Table 7.3), therefore, the proportional number of times the mechanism was triggered in relation to all connection requests is low. In Figure 7.20 it is possible to observe the proportion of times the Priority Realloc HB and Priority Realloc HBCT mechanisms were successfully triggered in comparison to

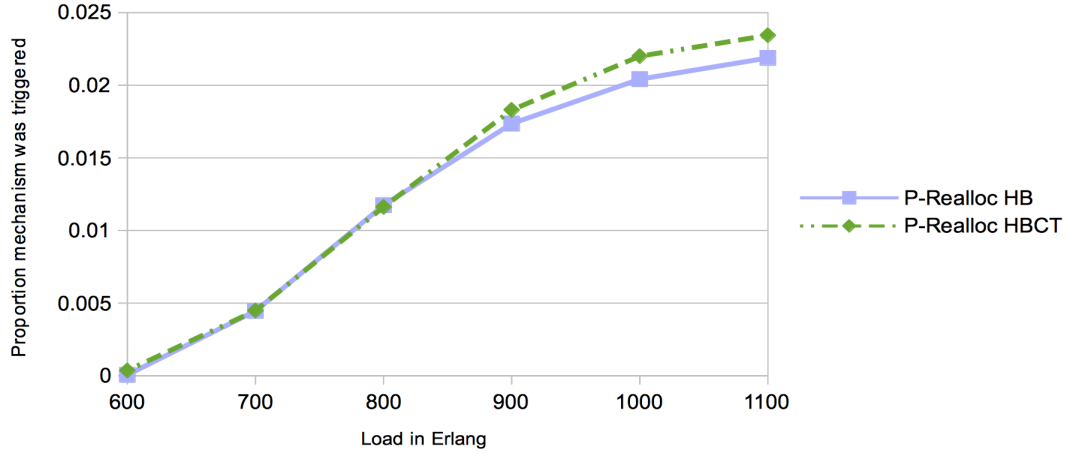


Figure 7.20: Proportion of times mechanism was triggered compared to the total number of demands

the total number of demands in the network. As offered traffic load increases contention for resources increases and augment the proportion of times the mechanism is triggered. For an offered traffic load of 1,100 Erlang only 2.2% of connection requests would successfully trigger Priority Realloc HB.

Over 900 Erlang, Priority Realloc HBCT is triggered a little bit more often than Priority Realloc HB. For an offered traffic load of 1,100 Erlang only 2.3% of connection requests would successfully trigger Priority Realloc HBCT. This negligible increase in occurrence is justified by the fact that CT2 demands represent 5% of all connection requests, 0.25% of which has highest BW requirement. Furthermore, CT2 connections are not blocked as often as highest BW requirement demands. The blocking probability of CT2 demands is the same as the general BP. When EGS-FL mechanism is implemented, the general BP is 0.02% for 600 Erlang and 9% for 1,100 Erlang, whilst BP for highest BW requirement demands is 0.3% for 600 Erlang and 73% for 1,100 Erlang.

In Figure 7.21, the proportion of times the mechanism was triggered is considered in relation to the number of highest BW requirement demands for Priority Realloc HB and in relation to the number of CT2 demands and/or highest BW requirement demands for Priority Realloc HBCT. For an offered traffic load of 1,100 Erlang, Priority Realloc HB is triggered 44% of all highest BW requirement connection requests, whilst Priority Realloc HBCT is triggered 24% of the sum of highest BW requirement and CT2 connection requests. Due to the higher value of its blocking probability, the percentage of time Priority Realloc HBCT is triggered is mainly dependent on the highest BW requirement connection requests.

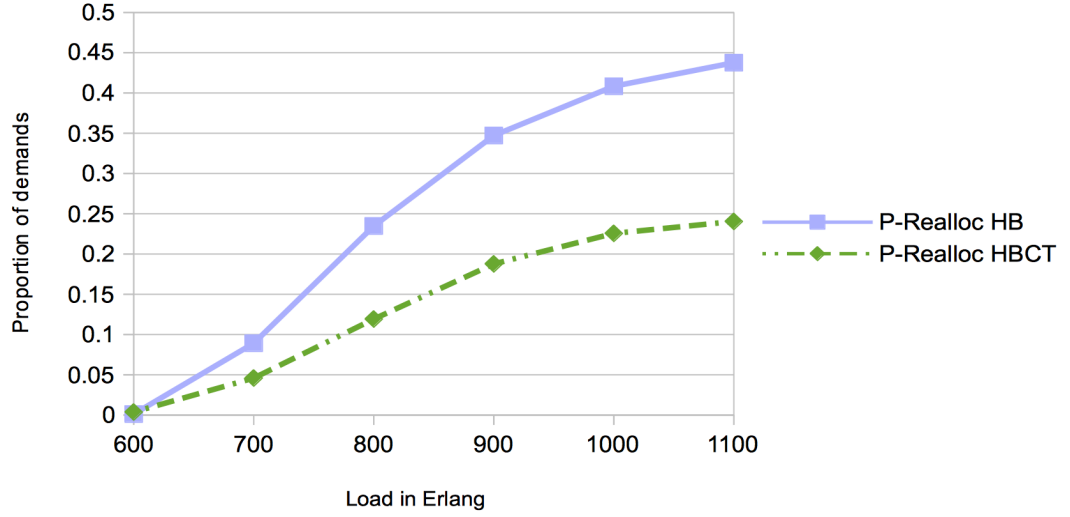


Figure 7.21: Proportion of times mechanism was triggered compared to the number of highest BW requirement demands for Priority Realloc HB and compared to the number of CT2 and highest BW requirement demands for Priority Realloc HBCT

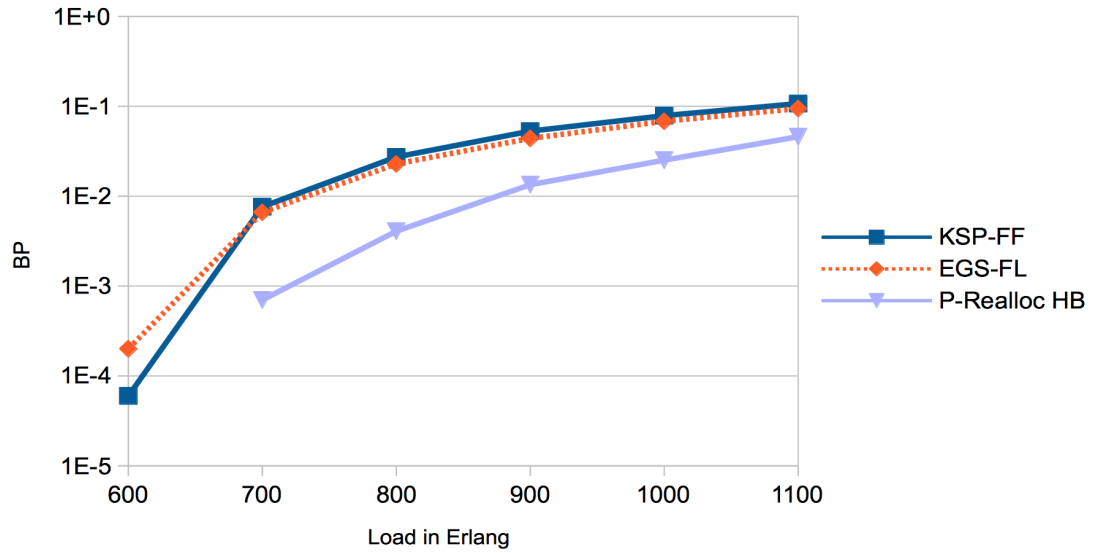


Figure 7.22: BP results for KSP-FF, EGS-FL and Priority Realloc HB mechanisms

7.2.2.3 Priority Realloc blocking probability and bandwidth blocking probability results

By analyzing simulations results we observed that, when Priority Realloc HB is implemented, a higher number of connections is successfully established when compared to KSP-FF and EGS-FL algorithms. Figure 7.22 presents blocking probability results for the three algorithms. It is possible to observe that as offered traffic load increases blocking probability increases for all algorithms, however Priority Realloc HB blocking probability is maintained lower than the other mechanisms for all offered traffic loads considered.

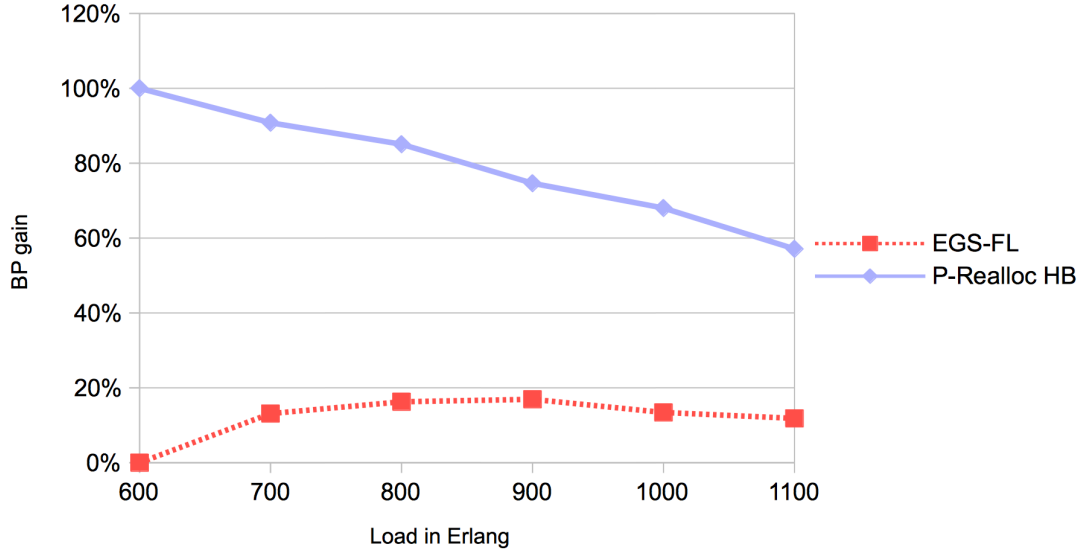


Figure 7.23: BP decrease gain of Priority Realloc HB and EGS-FL mechanisms when compared to KSP-FF mechanism

We quantified the benefit of implementing Priority Realloc HB and EGS-FL when compared to KSP-FF mechanism. Figure 7.23 presents the proportional decrease in BP results promoted by these algorithms. For an offered traffic load of 1,100 Erlang, for instance, EGS-FL decreases blocking probability in 11%, while Priority Realloc HB decreases blocking probability in 57% when compared to KSP-FF. It is also possible to observe in Figure 7.23 that for all offered loads the decrease in blocking probability for Priority Realloc HB mechanism is always higher than the decrease promoted by EGS-FL.

As observed in Subsection 7.2.2.2, for an offered traffic load of 1,100 Erlang, only 2.2% of connections requests successfully triggers Priority Realloc HB, therefore it is not expected that the BP decrease promoted by Priority Realloc HB would be so high when compared to EGS-FL algorithm. However a connection that has part of its resources preempted may be assigned different links from the ones comprised by the incoming demand's selected route. As an example consider that a CT0 active connection in route UT-CO-NE-IL-PA has 4 FSs preempted. Consider the demand to which this 4 FSs will be reallocated uses route TX-CO-NE. In this case the FSs in link CO-NE will be reallocated to a new connection, while the preempted FSs in links UT-CO, NE-IL and IL-PA will remain available. The resources preempted in other links will not be allocated to the incoming connection and will be available for other demands, increasing the number of connections established.

Priority Realloc HB also improved network performance regarding BBP. In Figure 7.24 it is possible to observe that the BBP when Priority Realloc

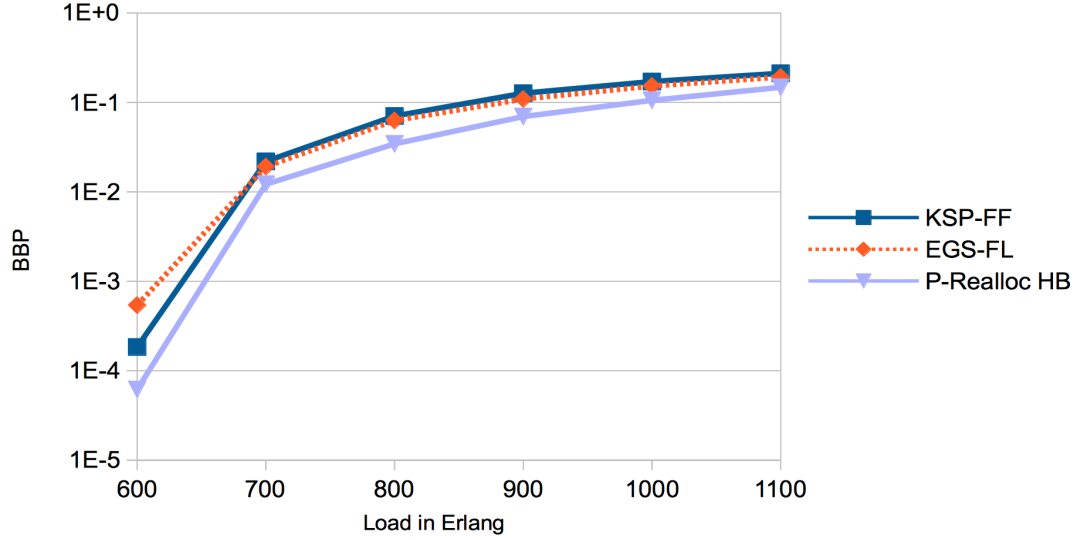


Figure 7.24: BBP results for KSP-FF, EGS-FL and Priority Realloc HB mechanisms

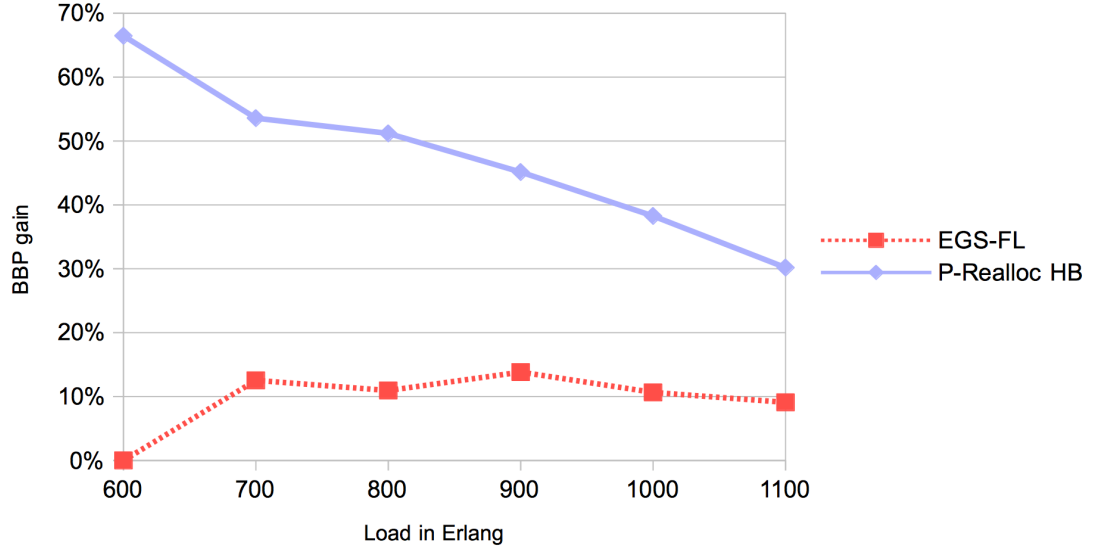


Figure 7.25: BBP decrease gain of EGS-FL and Priority Realloc HB mechanisms when compared to KSP-FF mechanism

HB mechanism is implemented is always lower than KSP-FF and EGS-FL mechanisms.

As can be observed in Figure 7.25, the benefit promoted by Priority Realloc HB mechanism regarding BBP is greater than the benefit promoted by EGS-FL for any offered traffic load. As an example, for an offered traffic load of 1,100 Erlang the BBP with Priority Realloc HB is 30% lower than KSP-FF, while EGS-FL mechanism decreases BBP in 9%. This decrease in BBP results promoted by Priority Realloc HB is due to the increase in resources assigned to highest BW requirement demands as analyzed in Subsection 7.2.2.4.

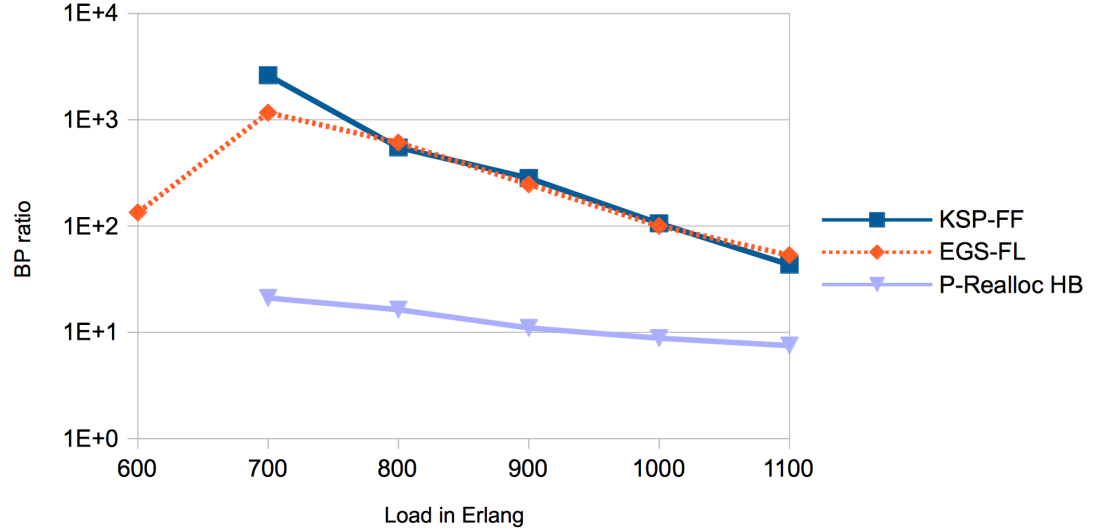


Figure 7.26: Ratio between highest and lowest BW requirement demands BP results

7.2.2.4 Priority Realloc mechanism fairness level

As debated in Chapter 2, in EONs, there is a low level of service fairness experienced by different BW requirement connections. We assess the fairness level as the ratio between highest and lowest BW requirement connection requests blocking probability and bandwidth blocking probability, as proposed in [7]. When the ratio value equals 1 there is absolute fairness of service between highest and lowest BW requirement connection requests. The higher the ratio value the lower the service fairness level.

Figure 7.26 presents results for BP ratio. When the Priority Realloc HB is implemented the fairness level is higher, represented by lower ratio values, compared to KSP-FF and EGS-FL for any offered traffic load. It is also possible to observe that, for all tested algorithms, the BP ratio tends to decrease as the offered traffic load increases, which means BP fairness level is increased. That phenomenon is explained by the fact that as contention for resources is higher, lowest rates demands are blocked more often than in a condition with lower contention for resources, as confirmed by results in Figure 7.28. For an offered traffic load of 1,100 Erlang the BP ratio is 53 for EGS-FL and 7.5 for Priority Realloc HB, while for an offered traffic load of 700 Erlang the BP ratio is 1163 for EGS-FL and 21 for Priority Realloc HB.

When Priority Realloc HB mechanism is implemented the BP fairness level increase is promoted by the blocking probability decrease of highest BW requirement connection requests as can be observed in Figure 7.27. On the other hand, implementing Priority Realloc HB mechanism does not interfere on

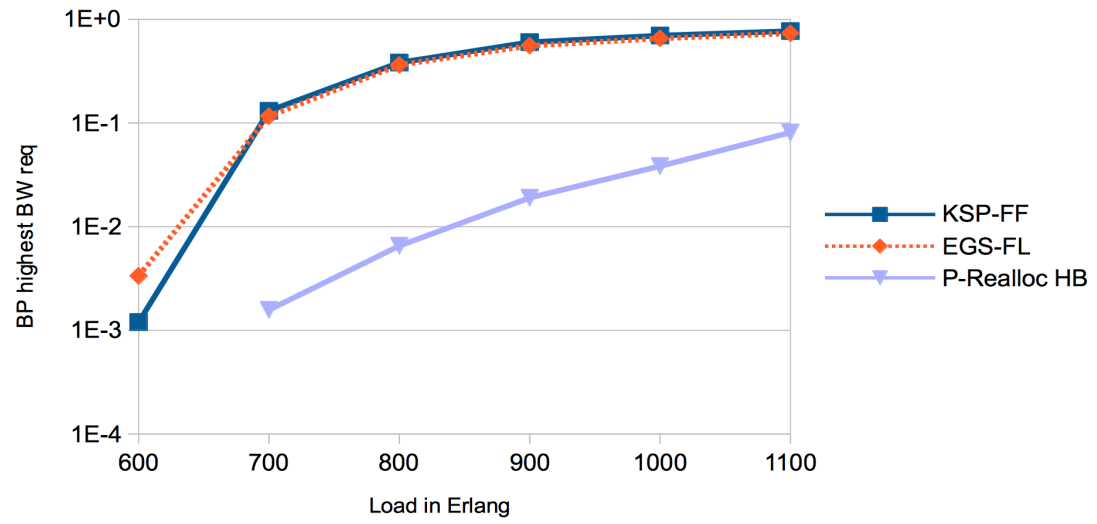


Figure 7.27: BP results for highest BW requirement demands

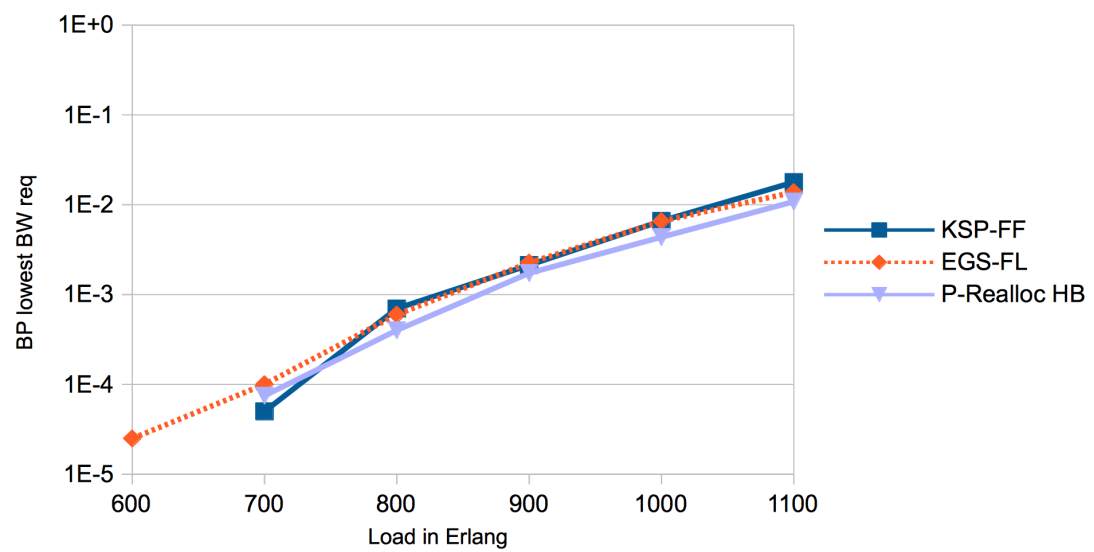


Figure 7.28: BP results for lowest BW requirement demands

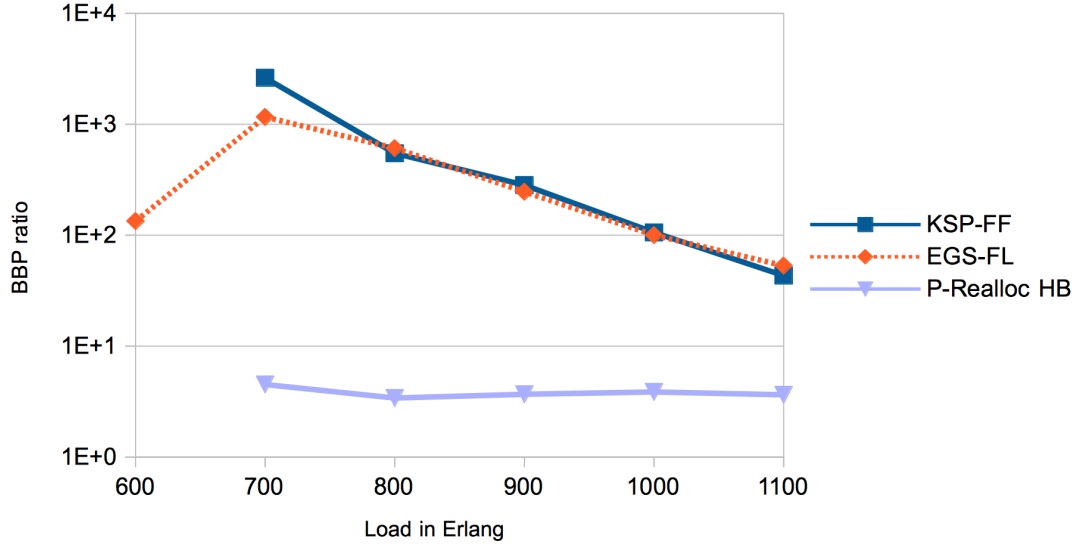


Figure 7.29: Ratio between highest and lowest BW requirement demands BBP results

blocking probability results of lowest bandwidth requirement connection requests, as can be observed in Figure 7.28.

The fairness level regarding bandwidth blocking probability can be observed in Figure 7.29. It is possible to observe that the BBP ratio value is lower when Priority Realloc HB is implemented indicating a higher level of fairness of service. For an offered traffic load of 1,100 Erlang, for instance, the ratio between highest BW requirement demands BBP and lowest BW requirement demands BBP is 3.6 when Priority Realloc HB mechanism is implemented and approximately 50 for both KSP-FF and ESG-FL. Similar to what happens to BP fairness level, for BBP fairness level, as the offered traffic load increases the BBP ratio decreases indicating an improvement on BBP fairness level.

When the BBP is considered, implementing Priority Realloc HB increases the fairness level not only by decreasing BBP of highest BW requirement connection requests, as can be observed in Figure 7.30, but also by increasing BBP for lowest BW requirement demands as illustrated by Figure 7.31. That increase on lowest rates demands BBP is instituted by the reallocation of resources from CT0 connections to highest BW requirement demands.

From the simulations performed we observed that Priority Realloc HB improved overall network performance and the fairness level of service shared among different BW requirement connections.

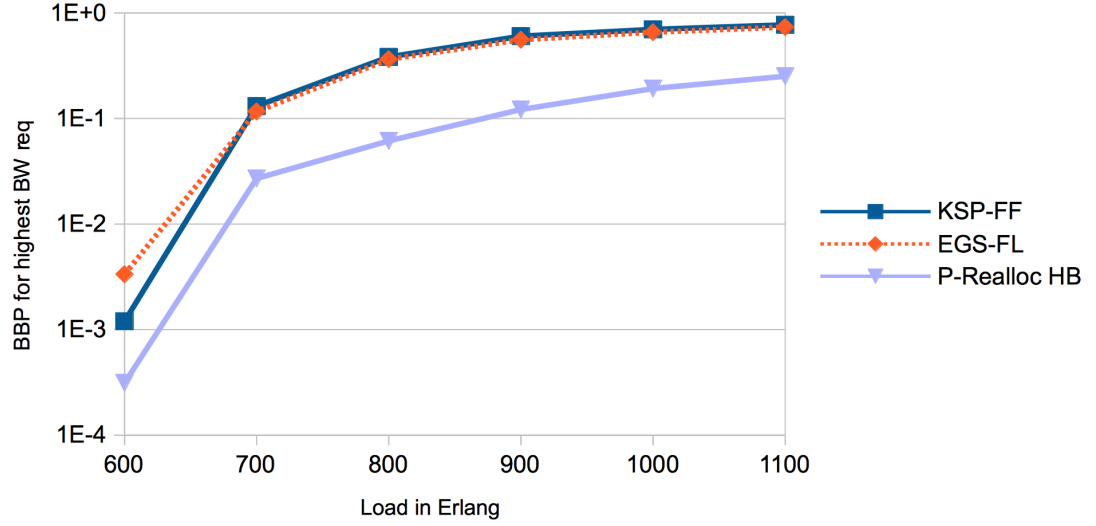


Figure 7.30: BBP results for highest BW requirement demands

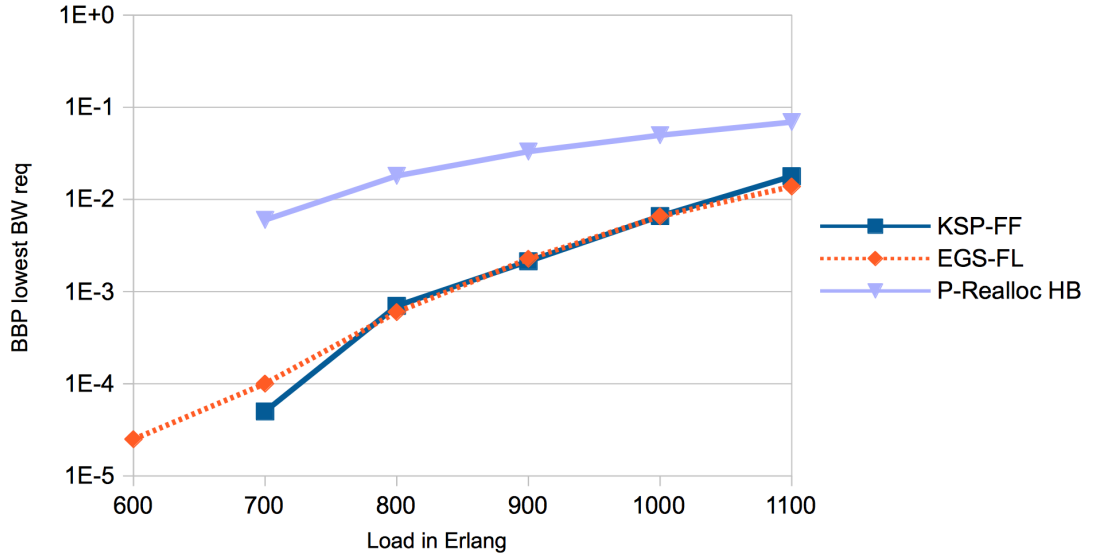


Figure 7.31: BBP results for lowest BW requirement demands

7.2.2.5 Comparison between Priority Realloc HB and TRR [7] mechanism results

We reproduced the network simulation conditions adopted in [7] to simulate Priority Realloc HB in order to compare the performance results achieved by TRR algorithm, the mechanism proposed in [7] as described in Chapter 3, and Priority Realloc HB.

We have plotted the BP and fairness level results achieved with TRR [7] and Priority Realloc HB. The fairness level results were calculated as the BP ratio proposed in [7] and explained in Subsection 7.2.2.4. As can be observed in Figure 7.32, Priority Realloc achieved better BP results for any of the tested offered

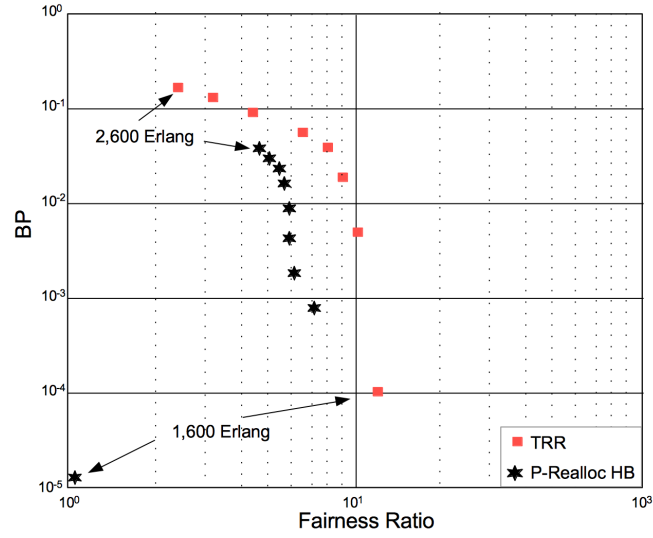


Figure 7.32: For each simulated offered traffic load in Erlang, dots represent the resulting fairness ratio and respective BP for Priority Realloc HB and TRR [7] algorithms

traffic loads and better fairness level for the 5 lowest traffic offered load values. For the three highest offered traffic load values, TRR achieved better fairness level results at the cost of higher BP results.

This result is expected because Priority Realloc HB decreases blocking probability and increases fairness ratio when compared to KSP-FF, while TRR improves fairness but increases BP when compared to KSP-FF as demonstrated in [7].

7.2.2.6 Priority Realloc mechanism and spectrum fragmentation

We assessed the spectrum fragmentation level achieved by the tested algorithms, via the external fragmentation measurement proposed in [19] and explained in Chapter 2. In external fragmentation measurement the closer the value is to 1 the higher is the spectrum fragmentation level, and the lower the value the lower the spectrum fragmentation level. The average routes external fragmentation value is achieved by the sum of all routes external fragmentation divided by the number of pre-calculated routes.

The highest improvement in route spectrum fragmentation is achieved with EGS-FL mechanism. Priority Realloc HB mechanism also implements EGS-FL mechanism promoting at least the same amount of decrease in spectrum fragmentation. However, in Figure 7.33, it is possible to observe that Priority Realloc HB promotes a further improvement of spectrum fragmentation. That is explained by the fact that with Priority Realloc HB when a connection is blocked with EGS-FL the demand is accommodated in a gap of available FSs even if

this gap does not have the minimum amount of FSs required by the demand. Therefore, with Priority Realloc HB, a higher number of gaps may be filled in the selected route's links decreasing the route's spectrum fragmentation.

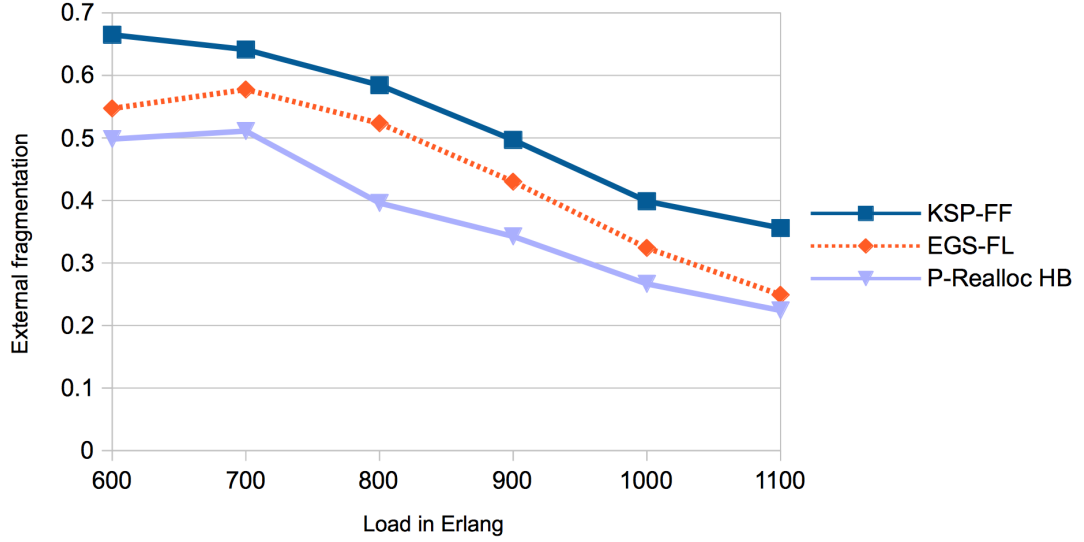


Figure 7.33: Average external fragmentation of routes

7.2.2.7 Priority Realloc effect on connections CT values performance metrics

Since Priority Realloc HBCT presents improvement in service for CT2 connections, in this Subsection we present BP and BBP results according to connections CT values for EGS-FL, Priority Realloc HB and Priority Realloc HBCT.

For an offered load of 1,100 Erlang, the BP results according to connections CT values may be observed in Figure 7.34. For EGS-FL and Priority Realloc HB algorithms, BP results do not vary according to CT values. Priority Realloc mechanisms do not promote differentiated service by blocking CT0 demands, and Priority Realloc HB does not prioritize establishing CT2 connections. However, when Priority Realloc HBCT is implemented it is possible to observe that BP result for CT2 connections is 75% lower than BP for the CT0 demands and 73% lower than BP for the CT1 demands.

When BBP is analyzed it is possible to observe that, when Priority Realloc HBCT is implemented, CT2 connections present lower BBP results when compared to the other CT value demands. Furthermore, for both Priority Realloc HB and Priority Realloc HBCT, CT0 demands present higher bandwidth blocking probability when compared to CT1 and CT2 connection requests. That occurs

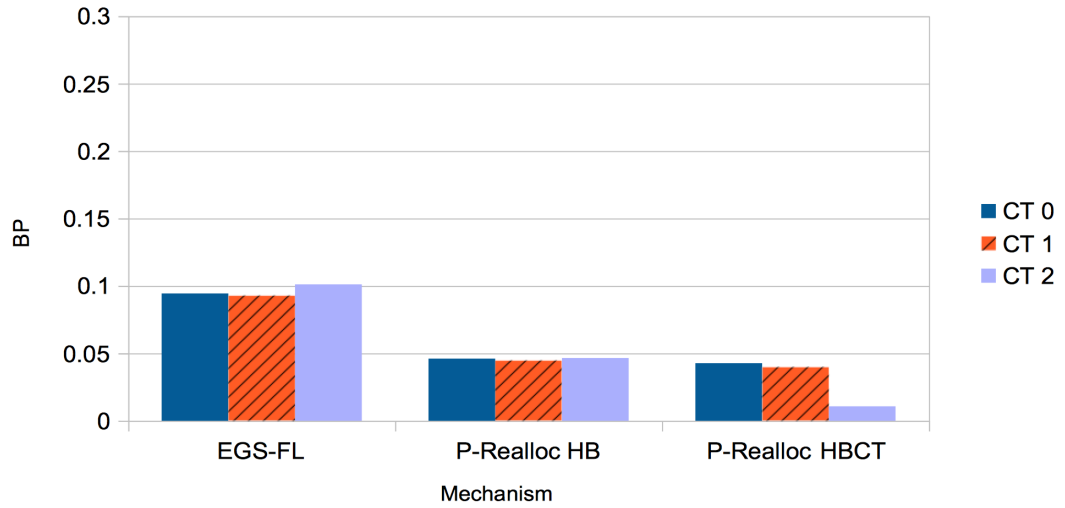


Figure 7.34: BP results per CT value for load 1,100 Erlang

due to the reallocation of resources from CT0 connections to prioritized demands.

As can be observed in Figure 7.35, for an offered traffic load of 1,100 Erlang, when Priority Realloc HB is implemented BBP of CT0 demands is 97% higher than CT1 demands and 120 % higher than CT2 demands, and when Priority Realloc HBCT is implemented CT0 demands BBP is 94% higher than CT1 and 221% higher than CT2 connections.

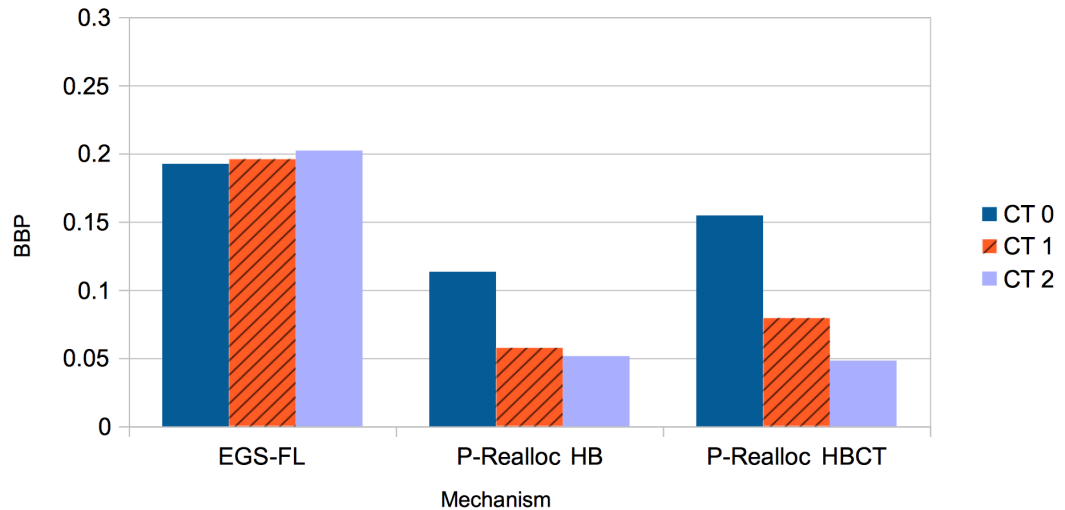


Figure 7.35: BBP results per CT value connections for load 1,100 Erlang

It is important to mention that when resources are reallocated from CT0 connections, these connections may have highest bandwidth requirement. This preemption of resources from highest BW requirement connections are accounted for and highest BW requirement connections BBP results reflect this deduction of resources.

7.2.2.8 Priority Realloc performance compared between different BW scenarios

In this Subsection we compare the results of Priority Realloc HB when implemented with BW requirement scenario 3 and with BW requirement scenario 4. Due to the highest spectrum fragmentation characteristic of scenario 3, the impact of Priority Realloc mechanism is higher in the network performance with this BW requirement scenario as can be observed by the performance metric results that are presented in this Subsection.

Figure 7.36 depicts the routes average external fragmentation level for BW requirement scenarios 3 and 4. It is possible to observe that even with the implementation of Priority Realloc HB, spectrum fragmentation with scenario 3 is still higher than the spectrum fragmentation with scenario 4.

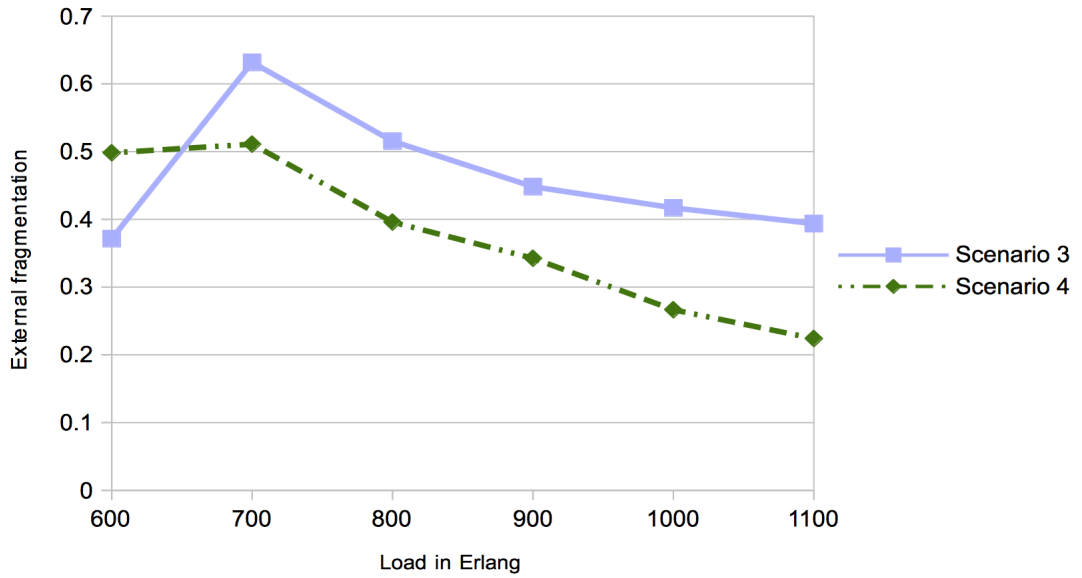


Figure 7.36: Average external fragmentation of routes for scenarios 3 and 4

As can be observed in Figure 7.37, in scenario 3 Priority Realloc is triggered a bit less often than in scenario 4 until the offered traffic load reach 900 Erlangs. For offered traffic load values above 900 Erlang, the mechanism is triggered as often in scenario 3 as it is in scenario 4.

In Figure 7.38 it is possible to observe that when Priority Realloc is implemented in scenario 3 the blocking probability results, presented in logarithmic scale, are lower than BP results in scenario 4. For an offered traffic load of 1,100 Erlang, for instance, BP for scenario 3 is 3% while BP for scenario 4 is 4.6%. Priority Realloc compensates the low spectrum assignment efficiency of scenario 3 resulted from its BW requirements characteristic. When this detriment

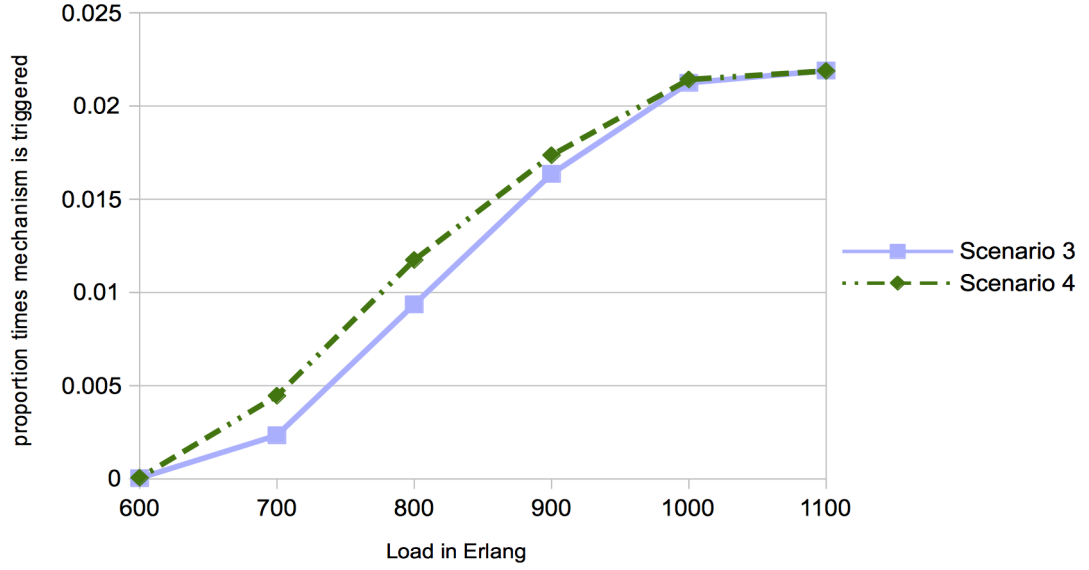


Figure 7.37: Proportion of times mechanism was triggered compared to the total number of demands for scenarios 3 and 4

characteristic is compensated, the number of connections established may increase due to the lower sum of FSs requirements of scenario 3 when compared to scenario 4.

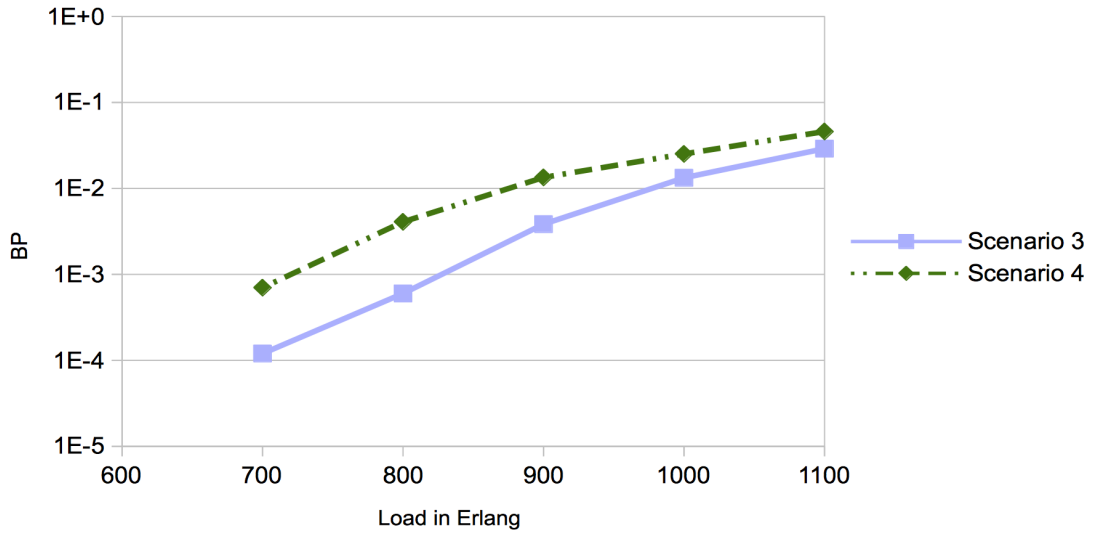


Figure 7.38: BP results for scenarios 3 and 4

Figure 7.39 presents results regarding the bandwidth blocking probability for scenarios 3 and 4. In this case the difference between the two scenarios is lower. Still, scenario 3 presents smaller values of BBP for any offered traffic load than scenario 4. By analyzing the BP and BBP results for the two scenarios it is possible to infer that in scenario 3 a smaller number of FSs from lowest BW requirement connections are preempted. Due to the higher level of spectrum

fragmentation of scenario 3 when a few FSs are preempted, the available FSs next to them can be assigned to a connection.

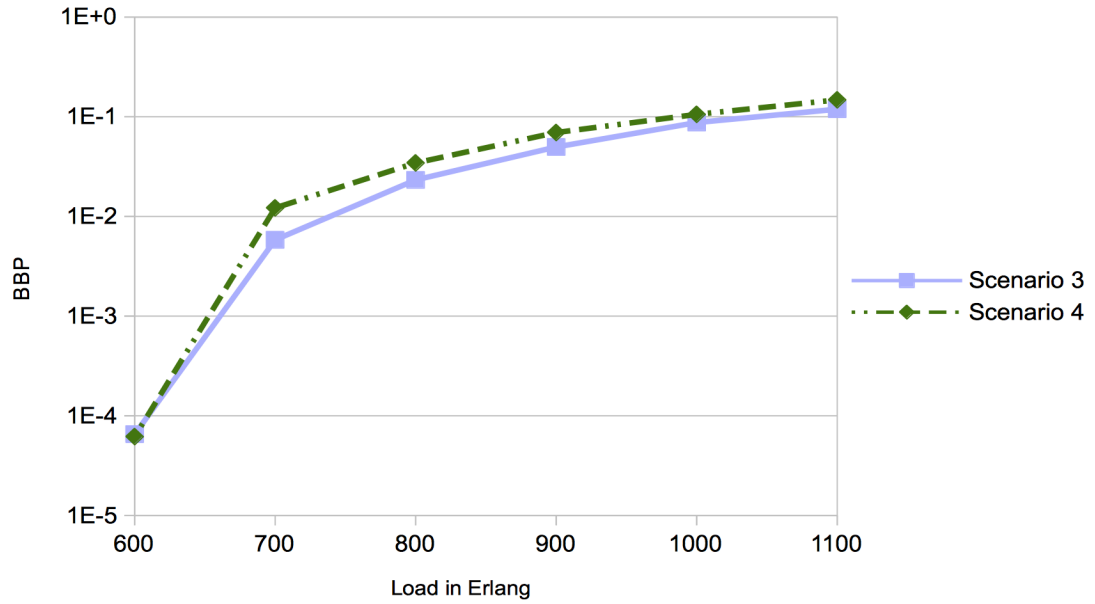


Figure 7.39: BBP results for scenarios 3 and 4

Figure 7.40 presents the BP ratio between BP resulted from scenario 3 and from scenario 4. Results indicate that the fairness level achieved in scenario 3 with Priority Realloc is higher than the fairness level achieved in scenario 4. In this case the fairness level enhancement was achieved by the increase of lowest BW requirement demands higher BP values that occurs in scenario 3. The combination of BW requirements in scenario 3 tends to result in 1 FS gaps which number of FSs does not accommodate 2 FSs requirement demands. The preemption of resources promoted by Priority Realloc HB may intensify the occurrence of this size gap throughout the network links, since reallocating 2 FSs from 3 FSs connections, results in 1 FS gaps.

The difference between BBP ratio results for scenario 3 and scenario 4 is smaller than the difference between BP ratio results for the two scenarios. Due to the higher spectrum fragmentation of scenario 3 a lower number of FSs has to be preempted in order to provide gap of minimum number of FSs to accommodate the demand. Therefore less FSs are preempted from lowest BW requirement connections, thus, this type of connections have a BBP value similar to scenario 4.

From the results, we conclude that BW requirements characteristics interfere on the impact of Priority Realloc mechanisms. As observed in scenario 3, the fairness level was promoted to a higher level than in scenario 4.

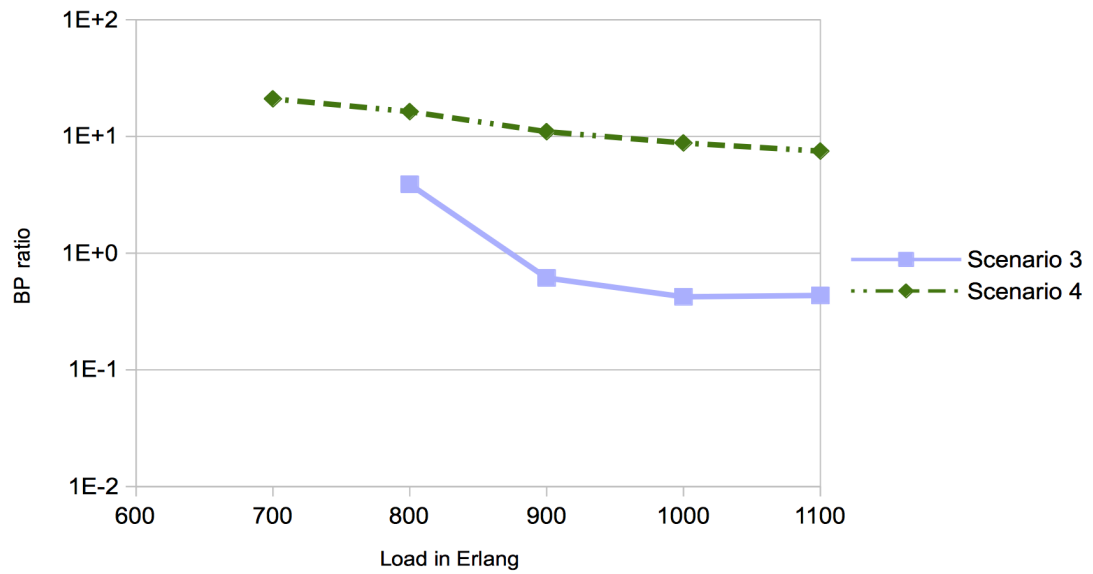


Figure 7.40: Ratio between highest and lowest BW requirement demands BP for scenarios 3 and 4

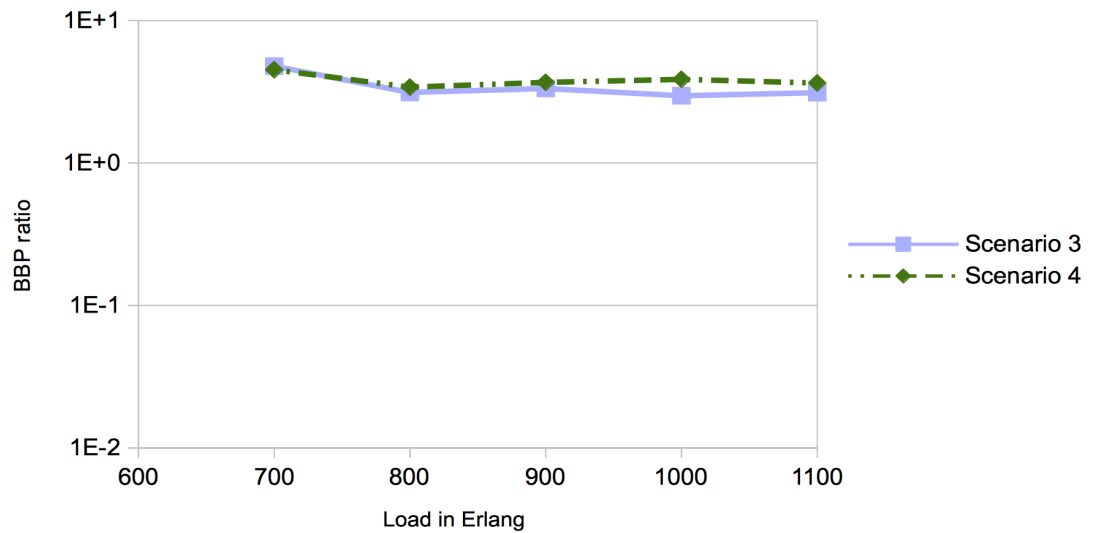


Figure 7.41: Ratio between highest and lowest BW requirement demands BBP for scenarios 3 and 4

8 Conclusion and future works

EON is a new paradigm, recently proposed, for transport optical network providing great resource capacity and flexibility in resources distribution. Due to these beneficial aspects, EONs are likely to replace WDM networks as the technology adopted by the industry for long haul data transport.

On the one hand, backbone network usually need to be able to provide differentiated service and, currently, there is only one limited differentiated service mechanism proposed for EONs in the literature while there is no differentiated resources allocation for WDM networks. On the other hand, due to its intrinsic characteristics EONs present two shortcomings, spectrum fragmentation and unfairness of service provisioning.

In scenarios where demands are dynamically provisioned, spectrum fragmentation is usually present throughout EONs links. Spectrum fragmentation tends to decrease resources distribution and efficient use. It also decreases service to higher BW requirement demands which become deeply deprived of service, resulting in unfairness on service provisioning. The fragmentation issue is extensively studied in the literature and many proposals are available. Studies and solutions on the fairness issue, however, are limited and seldom in the literature.

On the process of studying differentiated services for optical backbone networks we have developed and proposed a differentiated service mechanism for WDM networks, denominated RDM for WDM. RDM for WDM was tested in a WDM network simulator and results indicate it is capable of increasing WDM network performance when compared to benchmark algorithms.

This thesis objectives were impelled by the state of art regarding EONs evolution. Therefore, we proposed, developed and described Priority Realloc, a mechanism that dynamically solves the RSA problem in EONs whilst enabling service differentiation, decreasing spectrum fragmentation and service unfairness level. We developed the algorithms constituent of this mechanism which was

implemented in a network simulated scenario. Hence we have achieved this thesis main objective (**MO**).

The first part of our proposed mechanism for EONs, Priority Realloc, is a fragmentation-aware RSA algorithm denominated ESG-FL. ESG-FL tends to prevent future spectrum fragmentation in the network routes and links. Therefore this algorithm shall also increase resources distribution efficiency decreasing blocking probability. Simulations results comparing ESG-FL with other fragmentation-aware RSA algorithms, indicate that we achieve a modest decrease in blocking probability but also a decrease in spectrum fragmentation level.

Priority Realloc also understands and differentiates the service provided to diverse priorities connections. The second algorithm in Priority Realloc reallocates FSs from low priority connections to highest priority demands. This reallocation of resources adopts a similar procedure as path-triggered defragmentation.

Priority Realloc prioritizes service to highest bandwidth requirement demands. With this policy Priority Realloc aims at decreasing service unfairness that tends to deprive resources to highest BW requirement connections. When Priority Realloc only prioritizes service to highest bandwidth requirement demands it is denominated Priority Realloc HB. Another version of the mechanism also prioritizes service to highest CT value demands, this version of the mechanism is called Priority Realloc HBCT.

In order to assess Priority Realloc performance results and to study EON characteristics and their impact on network performance, we have developed an EON simulator called DSEON-Jsim. DSEON-Jsim is a Java based ad-hoc simulator with differentiated service capabilities and represents, by itself, a contribution to EONs research area which is scarce of network simulation tools for dynamic scenario.

One of the simulation performed in DSEON-Jsim concerns a study of the dynamic performance of an EON compared to a WDM network. The achieved results regarding the performance improvement promoted by EONs over WDM networks constitute an important contribution to the research area related to the level of benefit of adopting EON instead of WDM technology.

We have also simulated an EON in which we tested the relation between traffic bandwidth requirement values and spectrum fragmentation. Results presented

here prove that the bandwidth requirements characteristics do interfere on the networks spectrum fragmentation. This study is original and unique in this area of research and contributes to the development of resources allocation policies that aim at preventing further spectrum fragmentation.

In order to assess Priority Realloc performance we have simulated EONs implementing our proposed mechanism and benchmark algorithms.

In simulations results we observe that Priority Realloc enables the increase of prioritized demands establishment and resources assignment in detriment of lowest priority connection resources assigned. Thus, simulations results indicate that Priority Realloc promotes service differentiation, achieving the thesis objective 1 (**O1**).

Simulations results indicate that Priority Realloc promotes a decrease in spectrum fragmentation level and a substantial decrease in both blocking probability and bandwidth blocking probability. Based on the simulations results we observe that Priority Realloc achieves objective 2 (**O2**).

Simulation results also indicate that by implementing Priority Realloc, fairness level was substantially increased when compared to reference RSA algorithms, TTR. In addition, results indicate that Priority Realloc also presents lower blocking probability results for the same network conditions. Based on these results we conclude we have achieved thesis objective 3 (**O3**).

Due to limited descriptions or high computational complexity levels we could not reproduce all the RSA algorithms available in the literature. However we believe that Priority Realloc benefits in network performance are multifold since it provides service differentiation and mitigates two EON issues by implementing only one RSA mechanism. Currently there is no mechanism which description is available in the literature that provides the three benefits provided by Priority Realloc. We also believe that this unique capacity of Priority Realloc validates its superiority over the alternative algorithms available in the literature.

We have developed Priority Realloc to be established in a control plane where routing and spectrum allocation would be centralized and performed by one entity. Therefore we believe Priority Realloc would be adequate to rely on either the PCE with GMPLS or a software defined network (SDN). As future work we intend to study and propose network control plane extensions, for either the PCE with GMPLS protocol suite or Openflow for SDN. These extensions would guarantee these protocols would be able to implement Priority Realloc.

As future works we also intend to calculate the economic benefit provided by Priority Realloc, by accounting the profit promoted by prioritizing service to higher priority and higher BW requirement connections.

A future variation of Priority Realloc would constrain resources assigned to lower priority connections in order to spare resources for higher bandwidth requirement demands and to prevent horizontal spectrum fragmentation.

References

- [1] J. Armstrong, “OFDM for Pptical Communications,” *Journal of Lightwave Technology*, vol. 27, no. 3, pp. 189–204, 2009.
- [2] M. Jinno, H. Takara, B. Kozicki, Y. Tsukishima, Y. Sone, and S. Matsuoka, “Spectrum-efficient and scalable elastic optical path network: architecture, benefits, and enabling technologies,” *Communications Magazine, IEEE*, vol. 47, no. 11, pp. 66–73, 2009.
- [3] X. Yu, Y. Zhao, J. Zhang, Y. Yu, J. Zhang, X. Lin, and X. Cao, “Fragments-minimum spectrum allocation algorithm in flexible bandwidth multi-fiber optical networks,” in *Communications and Photonics Conference (ACP), 2012 Asia*. IEEE, 2012, pp. 1–3.
- [4] Y. Yin, H. Zhang, M. Zhang, M. Xia, Z. Zhu, S. Dahlfors, and S. Yoo, “Spectral and spatial 2d fragmentation-aware routing and spectrum assignment algorithms in elastic optical networks [invited],” *Journal of Optical Communications and Networking*, vol. 5, no. 10, pp. A100–A106, 2013.
- [5] R. Munoz, R. Casellas, and R. Martínez, “Dynamic distributed spectrum allocation in gmpls-controlled elastic optical networks,” in *European Conference and Exposition on Optical Communications*. Optical Society of America, 2011, pp. Tu–5.
- [6] K. Walkowiak, A. Kasprzak, and M. Klinkowski, “Dynamic routing of anycast and unicast traffic in elastic optical networks,” in *Communications (ICC), 2014 IEEE International Conference on*. IEEE, 2014, pp. 3313–3318.
- [7] X. Wang, J. Kim, S. Yan, M. Razo, M. Tacca, and A. Fumagalli, “Blocking probability and fairness in two-rate elastic optical networks,” in *Transparent Optical Networks (ICTON), 2014 16th International Conference on*. IEEE, 2014, pp. 1–4.
- [8] B. Mukherjee, *Optical communication networks*. McGraw-Hill New York, 1997.
- [9] I. Tomkos, E. Palkopoulou, and M. Angelou, “A survey of recent developments on flexible/elastic optical networking,” in *Transparent Optical Networks (ICTON), 2012 14th International Conference on*. IEEE, 2012, pp. 1–6.
- [10] R. Essiambre, G. Kramer, P. Winzer, G. Foschini, and B. Goebel, “Capacity limits of optical fiber networks,” *Lightwave Technology, Journal of*, vol. 28, no. 4, pp. 662–701, 2010.

- [11] A. Saleh and J. Simmons, "Technology and architecture to enable the explosive growth of the internet," *Communications Magazine, IEEE*, vol. 49, no. 1, pp. 126–132, 2011.
- [12] M. Jinno, H. Takara, and B. Kozicki, "Dynamic optical mesh networks: Drivers, challenges and solutions for the future," in *Optical Communication, 2009. ECOC'09. 35th European Conference on*. IEEE, 2009, pp. 1–4.
- [13] E. Palkopoulou, C. Merkle, D. A. Schupke, C. G. Gruber, and A. Kirstädter, "Traffic models for future backbone networks—a service-oriented approach," *European Transactions on Telecommunications*, vol. 22, no. 4, pp. 137–150, 2011.
- [14] M. Xia, M. Tornatore, C. U. Martel, and B. Mukherjee, "Risk-aware provisioning for optical wdm mesh networks," *IEEE/ACM Transactions on Networking (TON)*, vol. 19, no. 3, pp. 921–931, 2011.
- [15] A. Nafarieh, S. Sivakumar, W. Robertson, and W. Phillips, "Enhanced adaptive sla-aware algorithms for provisioning shared mesh optical networks," *Procedia Computer Science*, vol. 19, pp. 494–502, 2013.
- [16] J. Musacchio, G. Schwartz, and J. Walrand, "18 network economics: neutrality, competition, and service differentiation," *Next-Generation Internet: Architectures and Protocols*, p. 378, 2011.
- [17] S. Talebi, F. Alam, I. Katib, M. Khamis, R. Khalifah, and G. N. Rouskas, "Spectrum management techniques for elastic optical networks," *North Carolina State University Repository*, 2013.
- [18] O. Gerstel, M. Jinno, A. Lord, and S. B. Yoo, "Elastic optical networking: A new dawn for the optical layer?" *Communications Magazine, IEEE*, vol. 50, no. 2, pp. s12–s20, 2012.
- [19] A. Rosa, C. Cavdar, S. Carvalho, J. Costa, and L. Wosinska, "Spectrum allocation policy modeling for elastic optical networks," in *High Capacity Optical Networks and Enabling Technologies (HONET), 2012 9th International Conference on*. IEEE, 2012, pp. 242–246.
- [20] I. Tomkos, S. Azodolmolky, D. Careglio, E. Palkopoulou *et al.*, "A tutorial on the flexible optical networking paradigm: State of the art, trends, and research challenges," *Proceedings of the IEEE*, 2014.
- [21] R. Wang and B. Mukherjee, "Provisioning in elastic optical networks with non-disruptive defragmentation," *Journal of Lightwave Technology*, vol. 31, no. 15, pp. 2491–2500, 2013.
- [22] W. Richards, "Research Methodology in Software Engineering," in *Future directions in software engineering, summary of the Dagstuhl Workshop*. SIGSoft Software Engineering Notes, 1993, pp. 36–37.
- [23] B. Mukherjee, "Wdm optical communication networks: progress and challenges," *Selected Areas in Communications, IEEE Journal on*, vol. 18, no. 10, pp. 1810–1824, 2000.
- [24] I. Cisco Systems, "Introduction to dwdm technology," *technical reference*, 2001.

- [25] A. Gençata and B. Mukherjee, "Virtual-topology adaptation for wdm mesh networks under dynamic traffic," *Networking, IEEE/ACM Transactions on*, vol. 11, no. 2, pp. 236–247, 2003.
- [26] H. Zang, J. P. Jue, B. Mukherjee *et al.*, "A review of routing and wavelength assignment approaches for wavelength-routed optical wdm networks," *Optical Networks Magazine*, vol. 1, no. 1, pp. 47–60, 2000.
- [27] K. Zhu and B. Mukherjee, "A review of traffic grooming in WDM optical networks: Architectures and challenges," *Optical Networks Magazine*, vol. 4, no. 2, pp. 55–64, 2003.
- [28] X. Zhang and C. Qiao, "Wavelength assignment for dynamic traffic in multi-fiber wdm networks," in *Computer Communications and Networks, 1998. Proceedings. 7th International Conference on*. IEEE, 1998, pp. 479–485.
- [29] I. Recommendation, "G.694.1 Spectral grids for WDM applications: DWDM frequency grid," International Telecommunications Union, Tech. Rep., 2002.
- [30] —, "G.694.1 Spectral grids for WDM applications: DWDM frequency grid," International Telecommunications Union, Tech. Rep., 2012.
- [31] O. Dios, R. Casellas, F. Zhang, X. Fu, D. Ceccarelli, and I. Hussain, "Framework and Requirements for GMPLS based control of Flexi-grid DWDM networks," IETF, Tech. Rep., Feb 2014.
- [32] G. Zhang, M. De Leenheer, A. Morea, and B. Mukherjee, "A survey on OFDM-based elastic core optical networking," *Communications Surveys & Tutorials, IEEE*, vol. 15, no. 1, pp. 65–87, 2013.
- [33] D. M. Pataca, L. H. H. d. Carvalho, C. B. F. Adami, F. D. Simões, M. d. L. Rocha, and J. C. Oliveira, "Transmission of a 1.12 tb/s superchannel over 452 km fiber," *Journal of Microwaves, Optoelectronics and Electromagnetic Applications*, vol. 12, no. 2, pp. 524–532, 2013.
- [34] B. Kozicki, H. Takara, Y. Tsukishima, T. Yoshimatsu, T. Kobayashi, K. Yonenaga, and M. Jinno, "1 tb/s optical path aggregation with spectrum-sliced elastic optical path network slice," *ECOC 2009*, 2009.
- [35] P. Barreto da Silva, M. Abbade, and L. Bonani, "Performance of transparent optical networks with multiple bandwidth channels," in *Microwave & Optoelectronics Conference (IMOC), 2013 SBMO/IEEE MTT-S International*. IEEE, 2013, pp. 1–5.
- [36] G. Bosco, V. Curri, A. Carena, P. Poggiolini, and F. Forghieri, "On the performance of Nyquist-WDM terabit superchannels based on PM-BPSK, PM-QPSK, PM-8QAM or PM-16QAM subcarriers," *Journal of Lightwave Technology*, vol. 29, no. 1, pp. 53–61, 2011.
- [37] W. Shieh and I. Djordjevic, *Orthogonal frequency division multiplexing for optical communications*. Academic Press, 2010.
- [38] S. Kilmurray, T. Fehenberger, P. Bayvel, and R. I. Killey, "Comparison of the nonlinear transmission performance of quasi-nyquist wdm and reduced guard interval ofdm," *Optics express*, vol. 20, no. 4, pp. 4198–4205, 2012.

- [39] G. Bosco, A. Carena, V. Curri, P. Poggiolini, and F. Forghieri, "Performance Limits of Nyquist-WDM and CO-OFDM in High-Speed PM-QPSK Systems," *Photonics Technology Letters, IEEE*, vol. 22, no. 15, pp. 1129–1131, 2010.
- [40] G. Bosco, "Spectrally Efficient Transmission: a Comparison between Nyquist-WDM and CO-OFDM Approaches," in *Advanced Photonics Congress*. Optical Society of America, 2012, p. SpW3B.1.
- [41] B. Kozicki, H. Takara, Y. Sone, A. Watanabe, and M. Jinno, "Distance-adaptive spectrum allocation in elastic optical path network (slice) with bit per symbol adjustment," in *Optical Fiber Communication Conference*. Optical Society of America, 2010, p. OMU3.
- [42] Y. Li, L. Gao, G. Shen, and L. Peng, "Impact of ROADM colorless, directionless, and contentionless (CDC) features on optical network performance [invited]," *Journal of Optical Communications and Networking*, vol. 4, no. 11, pp. B58–B67, 2012.
- [43] M. Jinno, Y. Sone, and A. Hirano, "Management and control aspects of spectrum sliced elastic optical path network (SLICE)," in *ECOC 2010 Workshop, Sept*, 2010.
- [44] M. Jinno, H. Takara, B. Kozicki, Y. Tsukishima, T. Yoshimatsu, T. Kobayashi, Y. Miyamoto, K. Yonenaga, A. Takada, O. Ishida *et al.*, "Demonstration of novel spectrum-efficient elastic optical path network with per-channel variable capacity of 40 Gb/s to over 400 Gb/s," in *Optical Communication, 2008. ECOC 2008. 34th European Conference on*. IEEE, 2008, pp. 1–2.
- [45] K. Christodoulopoulos, I. Tomkos, and E. A. Varvarigos, "Routing and spectrum allocation in OFDM-based optical networks with elastic bandwidth allocation," in *Global Telecommunications Conference (GLOBECOM 2010), 2010 IEEE*. IEEE, 2010, pp. 1–6.
- [46] A. Patel, P. Ji, J. Jue, and T. Wang, "Survivable transparent Flexible optical WDM (FWDM) networks," in *Optical Fiber Communication Conference and Exposition (OFC/NFOEC), 2011 and the National Fiber Optic Engineers Conference*, march 2011, pp. 1–3.
- [47] X. Wan, L. Wang, N. Hua, H. Zhang, and X. Zheng, "Dynamic routing and spectrum assignment in flexible optical path networks," in *Optical Fiber Communication Conference*. Optical Society of America, 2011, p. JWA055.
- [48] Y. Yu, J. Zhang, Y. Zhao, X. Cao, X. Lin, and W. Gu, "The first single-link exact model for performance analysis of flexible grid wdm networks," in *Optical Fiber Communication Conference*. Optical Society of America, 2013, pp. JW2A–68.
- [49] J. Socrates-Dantas, R. M. Silveira, D. Careglio, J. R. Amazonas, J. Sole-Pareta, and W. V. Ruggiero, "Novel differentiated allocation of resources methodology based on russian dolls model for revenue optimization in transparent wdm backbone networks," in *Under revision*, 2014, pp. 1–20.

- [50] T. Takagi, H. Hasegawa, K. Sato, Y. Sone, B. Kozicki, A. Hirano, and M. Jinno, "Dynamic routing and frequency slot assignment for elastic optical path networks that adopt distance adaptive modulation," in *Optical Fiber Communication Conference*. Optical Society of America, 2011.
- [51] P. R. Wilson, M. S. Johnstone, M. Neely, and D. Boles, "Dynamic storage allocation: A survey and critical review," in *Memory Management*. Springer, 1995, pp. 1–116.
- [52] Y. Li, M. J. Francisco, I. Lambadaris, and C. Huang, "Traffic classification and service in wavelength routed all-optical networks," in *Communications, 2003. ICC'03. IEEE International Conference on*, vol. 2. IEEE, 2003, pp. 1375–1380.
- [53] F. Le Faucheur, W. Lai *et al.*, "Requirements for support of differentiated services-aware MPLS traffic engineering," IETF RFC 3564, July, Tech. Rep., 2003.
- [54] D. Awduche, L. Berger, V. Srinivasan, T. Li, and D. Gan, "Rsvp-te: extensions to rsvp for lsp tunnels," IETF RFC 3209, Tech. Rep., Dec 2001.
- [55] J. de Oliveira, J. Vasseur, L. Chen, and C. Scoglio, "Label switched path (LSP) preemption policies for MPLS traffic engineering," IETF RFC 4655, August, Tech. Rep., 2007.
- [56] J. de Oliveira, C. Scoglio, I. Akyildiz, and G. Uhl, "New preemption policies for DiffServ-aware traffic engineering to minimize rerouting in MPLS networks," *IEEE/ACM Transactions on Networking (TON)*, vol. 12, no. 4, pp. 733–745, 2004.
- [57] M. Meyer and J. Vasseur, "MPLS traffic engineering soft preemption," IETF RFC 5712, January, Tech. Rep., 2010.
- [58] B. Chen, W.-D. Zhong, and S. K. Bose, "Providing differentiated services for multi-class traffic in IP/MPLS over WDM networks," *Photonic Network Communications*, vol. 15, no. 2, pp. 101–110, 2008.
- [59] F. Le Faucheur, "Russian dolls bandwidth constraints model for DiffServ-aware MPLS traffic engineering," IETF RFC 4127, Tech. Rep., Jun 2005.
- [60] J. Segovia, P. Vilà, E. Calle, and J. L. Marzo, "Improving the resilience of transport networks to large-scale failures," *Journal of Networks*, vol. 7, no. 1, pp. 63–72, 2012.
- [61] M. Tornatore, D. Lucerna, B. Mukherjee, and A. Pattavina, "Multilayer protection with availability guarantees in optical WDM networks," *Journal of Network and Systems Management*, vol. 20, no. 1, pp. 34–55, 2012.
- [62] L. Song, J. Zhang, and B. Mukherjee, "Dynamic provisioning with availability guarantee for differentiated services in survivable mesh networks," *Selected Areas in Communications, IEEE Journal on*, vol. 25, no. 3, pp. 35–43, 2007.

- [63] T. E. El-Gorashi and J. M. Elmirghani, "Differentiated resilience with dynamic traffic grooming for WDM mesh networks," in *Transparent Optical Networks, 2009. ICTON'09. 11th International Conference on*. IEEE, 2009, pp. 1–6.
- [64] J. Dantas, D. Careglio, R. Silveira, W. Ruggiero, and J. Sole-Pareta, "PCE QoS tools and related scalability in WDM networks," in *Transparent Optical Networks (ICTON), 2012 14th International Conference on*. IEEE, 2012, pp. 1–7.
- [65] J. Ash, J. Le Roux *et al.*, "Path computation element (PCE) communication protocol generic requirements," RFC 4657, Tech. Rep., September 2006.
- [66] A. Farrel, J.-P. Vasseur, and J. Ash, "A path computation element (PCE)-based architecture," IETF RFC 4655, August, Tech. Rep., 2006.
- [67] J. Dantas, D. Careglio, R. Silveira, W. Ruggiero, and J. Sole-Pareta, "PCE algorithm for traffic grooming and QoS in multi-layer/multi-domain IP over WDM networks," in *Transparent Optical Networks (ICTON), 2011 13th International Conference on*. IEEE, 2011, pp. 1–5.
- [68] Y. Sone, A. Watanabe, W. Imajuku, Y. Tsukishima, B. Kozicki, H. Takara, and M. Jinno, "Bandwidth squeezed restoration in spectrum-sliced elastic optical path networks (SLICE)," *Journal of Optical Communications and Networking*, vol. 3, no. 3, pp. 223–233, 2011.
- [69] P. M. Moura, N. L. S. Fonseca, and R. A. Scaraficci, "Fragmentation Aware Routing and Spectrum Assignment Algorithm," Instituto de Computação, Universidade Estadual de Campinas, Tech. Rep., October 2013.
- [70] A. K. Horota, G. B. Figueiredo, and N. L. da Fonseca, "Algoritmo de roteamento e atribuição de espectro com minimização de fragmentação em redes Ópticas elásticas," in *Simpósio Brasileiro de Redes de Computadores e Sistemas Distribuídos (SBRC)*. Sociedade Brasileira de Computação, 2014, pp. 895–908.
- [71] R. Wang and B. Mukherjee, "Spectrum management in heterogeneous bandwidth optical networks," *Optical Switching and Networking*, vol. 11, pp. 83–91, 2014.
- [72] R. Yumer, N. Akar, and E. Karasan, "Class-based first-fit spectrum allocation with fragmentation avoidance for dynamic flexgrid optical networks," *Optical Switching and Networking*, vol. 15, pp. 44–52, 2015.
- [73] K. Christodoulopoulos, I. Tomkos, and E. Varvarigos, "Dynamic bandwidth allocation in flexible ofdm-based networks," in *Optical Fiber Communication Conference*. Optical Society of America, 2011.
- [74] A. Castro, L. Velasco, M. Ruiz, M. Klinkowski, J. P. Fernández-Palacios, and D. Careglio, "Dynamic routing and spectrum (re) allocation in future flexgrid optical networks," *Computer Networks*, vol. 56, no. 12, pp. 2869–2883, 2012.
- [75] A. Patel, P. Ji, J. Jue, and T. Wang, "Defragmentation of transparent flexible optical WDM (FWDM) networks," in *Optical Fiber Communication Conference and Exposition (OFC/NFOEC), 2011 and the National Fiber Optic Engineers Conference*, march 2011, pp. 1–3.

- [76] K. Wen, Y. Yin, D. J. Geisler, S. Chang, and S. Yoo, "Dynamic on-demand lightpath provisioning using spectral defragmentation in flexible bandwidth networks," in *European Conference and Exposition on Optical Communications*. Optical Society of America, 2011, pp. Mo-2.
- [77] E. Mannie, "Generalized multi-protocol label switching (GMPLS) architecture," IETF RFC 3945, Tech. Rep., Oct 2004.
- [78] F. Le Faucheur, T. Nadeau, J. Boyle, K. Kompella, W. Townsend, and D. Skalecki, "Protocol Extensions for Support of Diffserv-aware MPLS Traffic Engineering," RFC 4124, Tech. Rep., June 2005.
- [79] J. Vasseur, J. Le Roux, A. Ayyangar, E. Oki, A. Ikejiri, A. Atlas, and A. Dolganow, "Path computation element (pce) communication protocol (pcep)," RFC 5440, March, Tech. Rep., 2009.
- [80] W. S. Lai, "Bandwidth constraints models for differentiated services (DiffServ)-aware MPLS traffic engineering: performance evaluation," IETF RFC 4128, June, Tech. Rep., 2005.
- [81] C. Systems, "Cisco crs 16-slot line-card chassis route processor," *technical reference*, 2014.
- [82] S. Orłowski, R. Wessäly, M. Pióro, and A. Tomaszewski, "Sndlib 1.0 survivable network design library," *Networks*, vol. 55, no. 3, pp. 276–286, 2010.
- [83] O. Pedrola, A. Castro, L. Velasco, M. Ruiz, J. Fernández-Palacios, and D. Careglio, "CAPEX Study for a multilayer IP/MPLS-over-flexgrid optical network," *Journal of Optical Communications and Networking*, vol. 4, no. 8, pp. 639–650, 2012.
- [84] R. Ghimire and S. Mohan, "A token-based routing mechanism for GMPLS-controlled WDM networks," *Optical Switching and Networking*, vol. 9, no. 2, pp. 170–178, 2012.
- [85] J. Socrates-Dantas, R. M. Silveira, D. Careglio, J. R. Amazonas, J. Sole-Pareta, and W. V. Ruggiero, "A study in current dynamic fragmentation-aware rsa algorithms," in *Transparent Optical Networks (ICTON), 2014 16th International Conference on*. IEEE, 2014, pp. 1–4.
- [86] F. Palmieri, U. Fiore, and S. Ricciardi, "Simulnet: a wavelength-routed optical network simulation framework," in *Computers and Communications, 2009. ISCC 2009. IEEE Symposium on*. IEEE, 2009, pp. 281–286.
- [87] P. C. B. Silva, "Novos algoritmos para alocação eficiente de canais em redes ópticas elásticas," Ph.D. dissertation, Pontifícia Universidade Católica de Campinas, Fev 2014.
- [88] P. C. B. d. Silva and M. L. F. Abbade. (2014) Simulador EONSim - ElasticOptical Networks Simulator . [Online]. Available: <http://sourceforge.net/p/eonsim/wiki/Home/>
- [89] J. S. dantas. (2015) DSEON-Jsim - Java based simulator for EONs with differentiated service . [Online]. Available: <https://sourceforge.net/projects/dseonjsim/>

- [90] G. M. Duraes, A. Soares, J. R. Amazonas, and W. Giazza, "The choice of the best among the shortest routes in transparent optical networks," *Computer Networks*, vol. 54, no. 14, pp. 2400–2409, 2010.
- [91] I. de telecomunicacoes. (2015) Simulador EONSim - ElasticOptical Networks Simulator . [Online]. Available: <http://www.av.it.pt/anp/on/refnet2.html>
- [92] R. A. Scaraficci and N. L. da Fonseca, "Alternative routing and zone-based spectrum assignment algorithm for flexgrid optical networks," in *Communications (ICC), 2014 IEEE International Conference on*. IEEE, 2014, pp. 3295–3300.
- [93] M. Xia, M. Tornatore, C. U. Martel, and B. Mukherjee, "Service-centric provisioning in WDM backbone networks for the future internet," *Journal of Lightwave Technology*, vol. 27, no. 12, pp. 1856–1865, 2009.
- [94] R. Garg, H. Saran, R. S. Randhawa, and M. Singh, "A sla framework for qos provisioning and dynamic capacity allocation," in *Quality of Service, 2002. Tenth IEEE International Workshop on*. IEEE, 2002, pp. 129–137.

Appendix A – RDM mechanism for WDM networks economic impact analysis

Economical network performance analysis is a complex area of research and is out of the scope of this thesis. However, we did a brief analysis of the economic impact of the RDM mechanism for WDM network dynamic scenario which results we present in this Appendix.

By enabling differentiated service implementation the RDM mechanism for WDM network has a direct impact on a Service Provider's (SP) revenue. Actual economic models adopted by SPs are confidential and, therefore, are not available for the research community. The various economic studies available in the literature contain diverse economic revenue models. In this study we adopted the model presented in [93]. According to [93], the sales revenue (R_{sales}) represents the total income for selling services, depending, mainly, on the number of established connections and the service fee collected from each service level. Thus, the sales revenue is calculated as

$$R_{sales} = \sum_{i=1}^n F_i \quad (\text{A.1})$$

F_i being the fee for established connection i , and n is the total number of established connections [93].

Authors in [93] have studied the impact of implementing differentiated service based on availability time. In order to perform an analysis on economic revenue benefit, they propose the use of service fee values according to four different service levels. In order to analyze the economical benefit of our proposed mechanism we adopted the differentiated fee values presented in the article. To avoid using nominal values we consider the proportional service fee values according to a service fee value of reference, in this case the value of the Silver

Table A.1: Nominal service fee values and corresponding proportional values

Service level	Service fee (typical value)	Proportional value
Bronze	24,979.00	0.65
Silver	38,400.00	1.00
Gold	57,600.00	1.50
Premium	76,800.00	2.00

service level. Table A.1 presents the nominal service fee values proposed by [93] and the corresponding proportional values.

Considering established connections may comprise different levels of service it is possible to infer Eq. (A.2)

$$n = n_{bronze} + n_{silver} + n_{gold} + n_{premium} \quad (\text{A.2})$$

Substituting the proportional fee values from Table A.1 into Eq. (A.1), results in

$$\sum_{i=1}^n F_i = n_{bronze} * 0.65F + n_{silver} * 1F + n_{gold} * 1.5F + n_{premium} * 2F \quad (\text{A.3})$$

n_x (x = service level) being the number of connections belonging to a given class of service and F the fee for Silver service level.

The sales revenue, however, is not the total final amount an SP would receive for the service offered. In reality, when an SLA is not met a penalty is applied to the SP. This penalty decreases the total sales revenue. As stated in [93] the net-revenue is the revenue minus the total amount paid on penalty and is calculated as

$$R_{netsales} = \sum_{i=1}^n F_i - \sum_{i=1}^m P_i \quad (\text{A.4})$$

P_i being the penalty in case the service provided violates an SLA and m the total number of connections which have violated an SLA [93].

Considering connections which have violated an SLA may comprise different levels of service it is possible to infer Eq. (A.5)

Table A.2: Nominal penalty values and corresponding proportional values

Service level	Penalty fee (typical value)	Proportional value
Bronze	0.00	0.00
Silver	11,250.00	0.29
Gold	20,160.00	0.53
Premium	38,400.00	1.00

$$m = m_{bronze} + m_{silver} + m_{gold} + m_{premium} \quad (\text{A.5})$$

We adopted the penalty fee values used in [93] and calculated the proportional values according to the service level, in which the reference value is the Silver service level fee. Table A.2 presents the nominal penalty values proposed by [93] and their corresponding proportional values.

Using the proportional values given in Table A.2, the expression for the total penalty results in:

$$\sum_{i=1}^m P_i = m_{bronze} * 0F + m_{silver} * 0.29F + m_{gold} * 0.53F + m_{premium} * 1F \quad (\text{A.6})$$

m being the number of connections belonging to a given class of service that have violated SLA and F the fee for the Silver service level.

Substituting Eqs. (A.3) and (A.6) into (A.4) results:

$$\begin{aligned} R_{netsales} = & (n_{bronze} * 0.65F + n_{silver} * 1F + \\ & n_{gold} * 1.5F + n_{premium} * 2F) \\ & - (m_{bronze} * 0F + m_{silver} * 0.29F + \\ & m_{gold} * 0.53F + m_{premium} * 1F) \end{aligned} \quad (\text{A.7})$$

Using the simulations' final results and Eq. (A.7) we can calculate the revenue gain of implementing differentiated services for the proposed BC models. We consider a blocked demand as a connection that has violated a SLA and. By evaluating Eq. (A.7) with data resulted from the simulations we observe that, by implementing both the RDM-full and the RDM-less mechanisms, the net-revenue is increased when compared to grooming scenario. Figure A.1 presents the

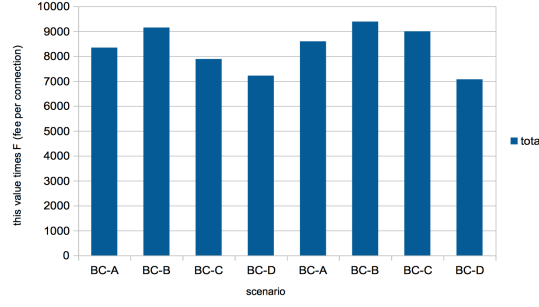


Figure A.1: Proportional net-revenue for each RDM scenario minus the proportional net-revenue for grooming according to fee per connection assigned

results of revenue gain by implementing each of the RDM mechanisms model, RDM-less and RDM-full, in comparison to not implementing either mechanism, i.e., implementing only the grooming scheme. Each bar in Figure A.1 is the difference between the RDM's (full or less) and the grooming's net revenue. As all results are positive, this means that the RDM mechanisms have always performed better than the grooming scenario. The results in Figure A.1 also show the gain variation according to the BC model adopted.

With a pricing policy based on the number of established connections, the highest gain is provided by the BC model B for both RDM-less and RDM-full. Due to the increase on the number of higher classes connections being established, with this configuration the revenue is 9,000 times the reference fee charged for established connections. For instance, if the average fee for an established connection is US\$ 100, in the period of time comprising 500 thousand demand arrivals, the total extra gain provided by implementing the mechanism would be equivalent to approximately US\$ 900,000.

The least positive impact occurred in the scenario in which the RDM-full algorithm was implemented and in which the BC model adopted was the BC model D. With this configuration the revenue is 7,000 times the reference fee charged for established connections, which represents a US\$ 700,000 gain if the average fee for a established connection is US\$ 100, in the period of time comprising 500,000 demand arrivals.

An alternative pricing methodology may be based on the amount of resources assigned to a connection. A complete model presented by [94] considers a SLA signed for a period between T_1 and T_2 , with a provisioned capacity C . Let $u(t)$ be the current capacity allocated to the user at time t . In the absence of penalties, the net amount the user has to pay at the end of the period (T_1, T_2) would be:

$$\begin{aligned}
& rC(T_2 - T_1) + p \int_{T_i}^{T_2} \max(O, u(t) - C) dt \\
& - d \int_{T_i}^{T_2} \max(O, C - u(t)) dt
\end{aligned} \tag{A.8}$$

C is the user's provisioned link capacity, r the charging rate per capacity and unit of time, d a discount rate and p a premium rate. Discount rate refers to the amount of capacity the user has not used from its agreed provisioned capacity. Premium rate refers to extra capacity used over the agreed provisioned capacity [94].

As we have not considered any SLA specification, we have not taken into account neither the premium nor the discount rates that are used in Eq. (A.8). In addition, since penalty fees relate to the amount of resources that have been established in the SLA to be provisioned but have not been allocated, we also do not consider them in this economic analysis. Due to the aforementioned reasons, Eq. (A.8) can be greatly simplified and the total revenue is given by

$$TotalRevenue = fU \tag{A.9}$$

U being the total actual capacity allocated to all SP's clients, f is service fee per capacity unit. We evaluate Eq. (A.9) when the simulation terminates and all resources allocated to connections are registered. By substituting the proportional service fee values from Table A.1 in Eq. (A.9) results the following expression for the total revenue for differentiated services according to allocated resources:

$$\begin{aligned}
TotalRevenue = & 0.65 * rU_{bronze} + rU_{silver} + \\
& 1.5 * rU_{gold} + 2 * rU_{premium}
\end{aligned} \tag{A.10}$$

From the total revenue provided by Eq. (A.10) we subtracted the revenue provided by the grooming scenario, so that the actual gain or loss in revenue can be assessed. Figure A.2 presents the results of revenue per assigned bandwidth (in Gbps) for the two RDM mechanisms and each of the BC models. We can observe that when the charging policy is based on the amount of assigned resources, the RDM-full mechanism tends to decrease an SP's total revenue, while by

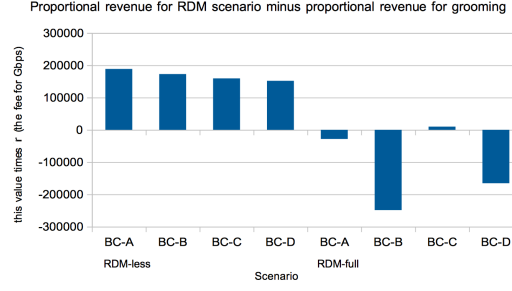


Figure A.2: Proportional revenue for each RDM scenario minus the proportional revenue for grooming according to fee per BW served

Table A.3: CT value distributions

Probability distribution	CT 0	CT 1	CT 2	CT3
Uniform	0.25	0.25	0.25	0.25
Probability distribution 1	0.60	0.25	0.10	0.05
Probability distribution 2	0.05	0.10	0.25	0.60
Probability distribution 3	0.30	0.05	0.55	0.10

implementing the RDM-less mechanism the revenue is increased.

Figure A.2 also shows that the profitability of RDM-less mechanism varies according to the chosen BC model and the highest gain is provided by BC model A. By implementing RDM-less and adopting the BC model A in a time interval comprising 500 thousand demand arrivals, the mechanism may promote an increase of $200,000 \times r$ the fee for 1 Gbps allocation. If this fee value is, for instance, US\$ 1 the gain would reach US\$ 200,000 dollars for the time interval comprising the 500 thousand demand arrivals. However, by implementing the RDM-full mechanism and adopting the BC model B the total revenue would be decreased in approximately US\$ 250,000 dollars. In the RDM-full scenario the best result was obtained by adopting BC model C, however the revenue gain over the grooming revenue in this case is negligible.

The revenue results show that the best RDM mechanism configuration solution depends on the SP's pricing policy. The RDM-full mechanism is not adequate for an SP that adopts a pricing policy based on the amount of resources allocated to its clients, while the same model may be highly beneficial for an SP with a pricing policy based on number of established connections. The selected BC model also impacts on the total revenue achieved.

In order to assess the variation of economic results according to the distribution of the CT values, we have performed simulations with traffic matrices that follow different CT value distributions. The four CT value distributions simulated are shown in Table A.3.

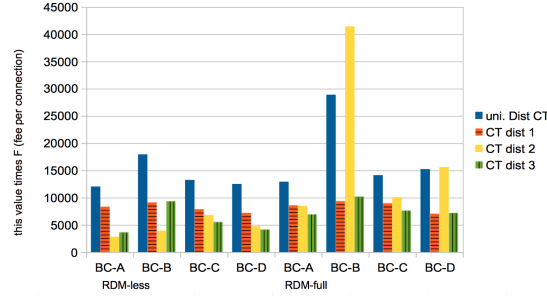


Figure A.3: Proportional net-revenue for each RDM scenario minus the proportional net-revenue for grooming according to fee per established connection for different CT distributions

Figure A.3 and summarizes the results according to the number of established connections to the CT distribution the demand matrix follows.

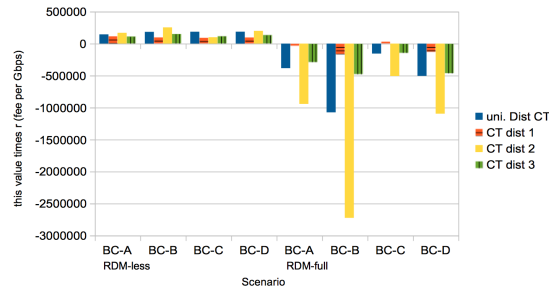
As shown in FigureA.3, the RDM-full mechanism presented a good performance providing higher increase on net-revenue than most of the RDM-less configurations. The BC model B adopted together with the RDM-full mechanism was the configuration that presented the best performance in terms of net-revenue increase. This configuration presented the highest net-revenue increase for all CT value distributions. For CT value distribution 2 the increase on revenue reached $40,000 \times r$, whereas the second best and third best configurations increased net-revenue in approximately $30,000 \times r$ and $10,000 \times r$ respectively.

Table A.4 shows the scenario configurations, in terms of RDM type and BC model, organized according to their level of profitability. It is possible to observe that, for the pricing policy based on established connections, RDM-full with the BC model B is the configuration that presented the highest net revenue increase for all CT value distributions. It is also possible to observe that for the less beneficial configuration scenarios, the CT value distribution does impact on the choice of configuration. For example, for the 4th best configuration the possibilities vary according to the CT value distribution and can be optimized by the adoption of the BC models A, C or D.

According to Figure A.4, when the pricing policy is based on the amount of resources allocated to connections the best configurations are very different from the pricing policy based on established connections. In this case, implementing the RDM-full mechanism decreases the revenues when compared to grooming, for all configuration scenarios but one. In a scenario with CT value distribution 1 the BC model C along the RDM full mechanism guarantees a very small increase on the revenue when compared to a scenario in which only grooming is implemented, while the BC model B decreases revenue in approximately $200,000 \times r$ the fee

Table A.4: Mechanism configurations in order of level of benefit for a pricing policy based on established connection

RDM type	CT value distribution				
	BC model	Uniform	Dist. 1	Dist. 2	Dist. 3
1 st	full/B	full/B	full/B	full/B	full/B
2 nd	less/B	less/B	full/D	less/B	less/B
3 rd	full/D	full/C	full/C	full/C	full/C
4 th	full/C	full/A	full/A	full/D	full/D
5 th	less/C	less/A	less/C	full/A	full/A
6 th	less/D	less/C	less/D	less/C	less/C
7 th	full/A	less/D	less/B	less/D	less/D
8 th	less/A	less/D	less/A	less/A	less/A

**Figure A.4:** Proportional revenue for each RDM scenario minus the proportional revenue for grooming according to fee per BW served for different CT distributions

per Gbps allocated. It is also possible to observe that the RDM-less mechanism increases the revenue for all CT value distribution scenarios with the adoption of any of the BC models.

Figure A.5 shows the results only for the RDM-less mechanism so that the variation on revenue increase may be better appreciated. Each CT distribution scenario results in a different amount of revenue increase, and the election of a BC model also increases or decreases revenues according to the CT value distribution scenario. For example, for scenario with CT value distribution 2 adopting the BC model B guarantees the highest increase on the revenue, while for scenario with uniform distribution of CT values there is small difference in revenue increase between the three best BC models: B, C and D.

As can be observed in Table A.5, when the pricing policy is based on the amount of allocated resources, the best RDM mechanism is always the RDM-less, but the BC model adopted varies with the CT value distribution. For example, the BC model A provides the smallest revenue increase for the scenario with uniform distribution of CT value, but it guarantees the largest revenue increase for CT value distribution 1. It is also possible to observe that for the four worst configurations in terms of revenue, the configurations of RDM-full and

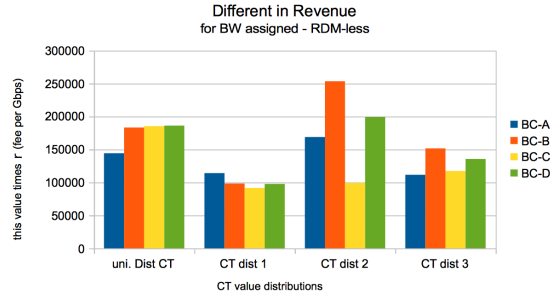


Figure A.5: Proportional revenue for RDM-less scenario minus the proportional revenue for grooming according to fee per BW served for different CT distributions and BC models adopted

Table A.5: Mechanism configurations in order of level of benefit for a pricing policy based on resources allocation

RDM type	CT value distribution			
BC model	Uniform	Dist. 1	Dist. 2	Dist. 3
1 st	less/D	less/A	less/B	less/B
2 nd	less/C	less/B	less/D	less/D
3 rd	less/B	less/D	less/A	less/C
4 th	less/A	less/C	less/C	less/A
5 th	full/C	full/C	full/C	full/C
6 th	full/A	full/A	full/A	full/A
7 th	full/D	full/D	full/D	full/D
8 th	full/B	full/B	full/B	full/B

the BC model adopted do not have their classification changed according to CT value distribution. For example, the worst revenue results are originated by the adoption of the BC model B for all CT value distribution scenarios.

The study of the economic impact of our proposed model shows that the best RDM mechanism's configuration depends on the pricing policy and the traffic matrix characteristics of the WDM network. The selected pricing policy of an SP determines if either the RDM-less or the RDM-full mechanism is the best solution to increase the revenue. As far as the traffic matrix is concerned, the best BC model to be adopted as a solution to increase revenue depends on the CT value distribution of the demands when the pricing policy is based on resources allocation and once RDM-less type is implemented.

As already mentioned, the SP's pricing policies are confidential information and the hypotheses adopted in this study do not have any general numerical validity. However, the study does show that the RDM mechanism may be a powerful tool to increase revenue in a WDM network and is flexible enough to be adjusted to different SLA criteria.